January 2016

Low-cost and Energy-efficient Solutions for Multicomponent Distillation

Gautham Madenoor Ramapriya
Purdue University

Graduate School Form
30 Updated 12/26/2015

PURDUE UNIVERSITY
GRADUATE SCHOOL
Thesis/Dissertation Acceptance

This is to certify that the thesis/dissertation prepared

By Gautham Madenoor Ramapriya

Entitled
LOW-COST AND ENERGY-EFFICIENT SOLUTIONS FOR MULTICOMPONENT DISTILLATION

For the degree of Doctor of Philosophy

Is approved by the final examining committee:

Rakesh Agrawal
Chair

Gintaras V. Reklaitis

Mohit Tawarmalani

Phillip C. Wankat

To the best of my knowledge and as understood by the student in the Thesis/Dissertation Agreement, Publication Delay, and Certification Disclaimer (Graduate School Form 32), this thesis/dissertation adheres to the provisions of Purdue University's "Policy of Integrity in Research" and the use of copyright material.

Approved by Major Professor(s): Rakesh Agrawal

Approved by: John A. Morgan 7/27/2016
Head of the Departmental Graduate Program Date

LOW-COST AND ENERGY-EFFICIENT SOLUTIONS FOR MULTICOMPONENT DISTILLATION

A Dissertation
Submitted to the Faculty
of
Purdue University
by
Gautham Madenoor Ramapriya

In Partial Fulfillment of the
Requirements for the Degree
of
Doctor of Philosophy

August 2016
Purdue University
West Lafayette, Indiana

I dedicate this thesis to my parents, sister and grandparents for their unconditional love

ACKNOWLEDGEMENTS

I am deeply grateful to my adviser, Professor Rakesh Agrawal, for choosing to have me as his student, and for guiding me for the past five years. This thesis would not have been possible without his continued ideas, inputs and guidance. There have been many occasions when he has been a source of encouragement to me when I did not believe in myself. I have valued his mentorship, and would like to convey my sincere thanks for his efforts to educate/advise me on matters apart from research as well. His enthusiasm to do great research, work habits and relentless pursuit of excellence have inspired me. I greatly admire his research contributions, and hope I can contribute to research in the future at least a fraction of what he has.

I would like to thank Professor Mohit Tawarmalani for co-advising me on this project, and for teaching me so much about optimization. His acuteness and incisive questions have been useful to the research work in this thesis. I have been very fortunate to have been a part of a number of enlightening discussions with him. Without his support, this research would have been incomplete.

I would like to thank Professor Gintaras Reklaitis and Professor Phillip Wankat for agreeing to be on my doctoral committee, for their inputs during my presentations, and for their time. I am also thankful to the US Department of Energy for funding this research.

I would like to express my sincere thanks to Professor Shankar Narasimhan who inspired me to take up research after my undergraduate studies.

I am thankful to Melissa Laguire and Katherine Henke for being there whenever we needed them.

I would also like to thank all past and current group members (Dr. Arun Giridhar, Dr. Vishesh Shah, Dr Ullaganathan Nallasivam, Dr. Haibo Zhang, Dr. Anirudh Shenvi, Dr. Joshua Huff, Dr. Dharik Mallapragada, Dr. Easah Musleh, Emre Gencer, Zheyu Jiang, Radhakrishna Tumbalam Gooty, Luis Jiminez, Ajiththaa Selvarajah, Taufik Ridha, Yiru Li) with whom I have had discussions on a number of related topics. I would not have been able to do a lot of things I did towards this thesis if it was not for their involvement and individual contributions.

I would like to thank Piyush Dak, Punyashloka, Ankit, Anuj, Biswajit and Ramakrishna for bearing my presence for at least a year at home. I cherish the time I spent with them. I would like to express my sincere thanks to Gururaj and Maanitraj for the wonderful times we had. I am grateful to Sumeet Thete for his willingness to extend help whenever I needed. I am thankful to Suman Debnath, Astitva Tripathi, Vikranth Karra, Raghuvamsi Chavali, Ankit Jain, Anuradha Bhat, Chinmay Joglekar, Krishna Singhal, Anand Venkatesan, Karthikeyan Marimuthu, Harshavardhan Choudhari, Dhairya Mehta, Jayachandran Devaraj, Aniruddha Kelkar, Anshu Gupta, Vinod Venkatakrishnan, Kaiwalya Sabnis, Atish Parekh, Ashish Vora, Meenesh Singh, Vishrut Garg, Saurabh Dongaonkar, Sambit Palit, Pritish Kamat, Tej Choksi, Rohit Jaini, Agnes Mendonca, Ranjita Ghose, Mayank Shekhar and Ravi Joshi for making my stay at West Lafayette pleasant.

Finally, I would like to thank my parents, sister and grandparents who have been my constant pillars of support during all my good and bad times. I dedicate this thesis to them for their unconditional love.

TABLE OF CONTENTS

Page

Page

LIST OF TABLES

Table Page

LIST OF FIGURES

Figure Page

Figure Page

Figure Page

Figure Page

Figure Page

ABSTRACT

Madenoor Ramapriya, Gautham. Ph.D., ChE, Purdue University, August 2016.
Low-cost and Energy-efficient Solutions for Multicomponent Distillation.
Major Professor: Rakesh Agrawal.

Distillation accounts for 90-95% of all the separations on a chemical plant, and for about 3% of the world energy consumption. Even modest improvements to the process of distillation can have tremendous impact on the chemical economy world over. The goal of a major part of this thesis is to use process intensification methods to present, thoroughly investigate and systematically synthesize new processes for multicomponent separations which can serve as attractive candidates for distillation technology of tomorrow.

Industrial application of dividing wall columns (DWCs) for multicomponent separation has gained significance in recent years. We realize that only a small fraction of possible DWCs have been so far presented and considered for implementation to separate mixtures containing three and four components. In this work, we present a multitude of hitherto unknown DWCs for n-component distillation. A reason for this drastic expansion in available DWCs is the identification that a strategy called the ‘conversion of a thermal coupling to a liquid-only transfer stream’ could be applied to DWCs. For the example of four- and five-component FTC distillation alone, while only one DWC was known so far

for over fifty years, 35 and 575 new DWCs, respectively, have been discovered as a result of this work. Further, among the new DWCs, we have identified a subset of DWCs in which the vapor flow in every section of the DWC can be regulated during operation by means external to the column. This feature makes it possible to build and operate the DWCs near optimality and ensure purity of product streams. Such an outcome could potentially lead to over 30% saving on operating and capital costs in comparison to processes currently in operation.

Further, we propose and study general methods to consolidate distillation columns of a distillation configuration using heat and mass integration with an additional section. The proposed method encompasses all heat and mass integrations known till date, and includes many more. Each heat and mass integration eliminates a distillation column, a condenser, a reboiler and the heat duty associated with a reboiler. Thus, heat and mass integration can potentially offer significant capital and operating cost benefits. Furthermore, we make a comprehensive comparison between the conventional column-consolidation and the proposed column-consolidation to understand when the conventional strategy is inefficient due to pronounced remixing losses. Finally, we present a preliminary formulation to synthesize thermodynamically equivalent versions of thermally coupled configurations.

CHAPTER 1. INTRODUCTION

1.1 Background

The earliest application of distillation as a batch process to separate mixtures has been traced to around 3500 BCE.[1] However, continuous distillation is believed to have found application for the first time in the 19th century.[1] Over the years, the process has evolved, and is considered a “mature” chemical technology as the knowledge about the process know-how has increased considerably.[2] Today, distillation has become an important separation technique, and is used extensively in the chemical and petrochemical industry.

The distillation process, with the application of heat to a mixture, exploits the differing tendencies of the various components in a mixture to distribute into the vapor and liquid phases, to eventually separate out each component from the mixture. A component which has a higher tendency to leave the liquid phase and enter the vapor phase is considered to be more volatile than a component which has a higher tendency to leave the vapor phase and enter the liquid phase. In continuous distillation, streams enriched in the more volatile components are withdrawn from a distillation column above streams enriched in the less volatile components. For example, the sequence shown in Figure 1.1, which is popularly called the indirect split sequence, is used to separate a non-azeotropic mixture *ABC.* Only non-azeotropic mixtures are considered in this thesis. However, if the

concepts presented in the thesis have to be extended to azeotropic mixtures, then, the components forming the azeotropes and causing the non-ideality are lumped together. Each lump is to be treated as an independent pseudo-component, and the concepts presented in the thesis, then applied. As a final step in the separation process to produce pure component products from the lumps/pseudo-components, azeotrpic distillation techniques could be used.

In Figure 1.1, and in the remainder of the thesis, *A*, *B*, *C*, *D*, etc. denote pure components with volatilities decreasing in alphabetical order. Streams in the

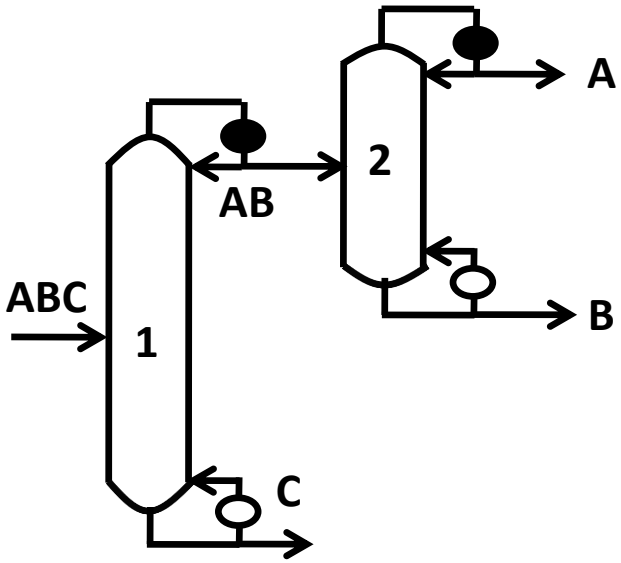

Figure 1.1 Three-component indirect split configuration

chapter are named according to the components they predominantly contain. *AB* in Figure 1.1, for example, is assumed to predominantly contain components *A* and *B*, and such streams containing more than one component is termed a submixture. However, in real operation, as also will be seen in some of the simulations presented in this work, the extent of contamination in any

submixture/product stream may be significant depending on the operational and design specifications of the distillation column. Further, in all the figures of the thesis, unfilled circles denote reboilers, while filled circles denote condensers.

As can be observed from the first distillation column in Figure 1.1, stream *C*, enriched in the less volatile component is withdrawn from the bottom of the column, while stream *AB* enriched in the more volatile components is withdrawn from the top of the column. The top product (here *AB*) of a column is called the distillate, while the product associated with the reboiler (here *C*) is termed the bottoms. Between the distillate and the feed, the column comprises of separation stages which make up the rectifying section, while that between the feed and the bottoms is the stripping section. More generally, along a column, the net mass flow is in the upward direction in a rectifying section, and in the downward direction in a stripping section. In the second column, *AB* is further separated into pure *A* and *B*. Such a sequence of distillation columns, with unique separation-tasks assigned to each distillation column is termed a distillation configuration. Typically, a multi-column distillation configuration is used to recover streams enriched in desired chemicals on an industrial plant.

1.2 Motivation

The distillation process is ubiquitous in chemical, petrochemical and biochemical plants. Typically, distillation accounts for 90-95% of all the separations on a chemical plant.[3] In the U.S. alone, there are 40,000 massive distillation towers in operation, consuming an energy equivalent of 1.2 million

barrels of crude oil per day.[2] Approximately 33% of this energy is used for petroleum crude distillation to produce naphtha, kerosene, diesel, gas oil, and heavies.[4] At the world scale, a study suggests that distillation accounts for approximately 3% of the total world energy consumption.[5]

The utility of distillation in the chemical industry is expected to increase further in the future. With renewable economy receiving much focus, and efforts to renewably produce liquid fuels and chemicals, for example, from biomass, the number of distillation plants is going to increase. Furthermore, with extensive findings of shale gas reserves, for the associated fractionation of natural gas liquids to recover various branched and unbranched alkanes, new distillation plants would be needed. In light of the above discussed ubiquitous nature of distillation, even modest improvements to the distillation technology can have far-reaching effects on the world chemical economy. The research work in this thesis addresses this possibility by serving to improve and invent new processes for distillation.

1.3 Research objective

Process intensification is an area of process engineering which concurrently reduces process equipment alongside energy consumption. The goal of this research is to apply process intensification concepts to distillation, leading to new processes, and their systematic performance investigation and synthesis. It is hoped that some of the new processes presented would be useful for industrial application. The industrial application of these new processes for

multi-component distillation is expected to not only reduce energy consumption and capital cost for many applications by approximately 30%, but also mitigate the CO_2 emission from such distillation plants significantly.

1.4 Overview of thesis

This thesis is organized into the following chapters:

Chapter 2: New, Ternary Dividing Wall Structures: This chapter presents novel DWCs for ternary distillations and discusses the operational benefits they offer over the conventional DWC. Most portions of this chapter have been borrowed from Madenoor Ramapriya et al.[6]

Chapter 3: Enumeration of New Fully Thermally Coupled Dividing Wall Columns: This chapter enumerates all possible FTC DWCs for any *n*-component distillation, and then, from the enumerated set, identifies the subset of easy-to-operate DWCs. Most portions of this chapter have been borrowed from Madenoor Ramapriya et al.[7]

Chapter 4: Method to Draw Dividing Wall Columns of Any Distillation Flowsheet: This chapter presents a general method to draw the DWC of any given distillation flowsheet/sequence of splits.

Chapter 5: Heat and Mass Integration of Distillation Columns: This chapter introduces a method to heat and mass integrate distillation columns with the incorporation of an additional section between the consolidated columns. Application of this method leads to reduction in equipment and energy

consumption simultaneously for multi-component distillation. Most portions of this chapter have been borrowed from Madenoor Ramapriya et al.[8]

Chapter 6: Remixing Loses Due to Consolidation of Distillation Columns: This chapter investigates and compares the efficacy of conventional column-consolidation methodology with alternate column-consolidations which have been proposed in the literature to eliminate losses due to remixing.

Chapter 7: Short-cut Methods Versus Rigorous Methods for Performance Evaluation of Distillation Configurations: This chapter investigates the feasibility of using short-cut methods (which have some inherent assumptions) to evaluate the heat duty requirements of distillation configurations.

Chapter 8: A Formulation for Thermodynamically Equivalent Thermally Coupled Configurations: This chapter presents a preliminary mathematical formulation to identify thermodynamically equivalent versions of thermally coupled configurations.

Chapter 9: Summary: This chapter summarizes the new findings of the research work performed towards this dissertation.

References

1. Wankat PC. Separations: A Short History and a Cloudy Crystal Ball. Chem Eng Education. 2009;43(4):286–295.
2. Humphrey JL, Keller, GE. Introduction. In Separation Process Technology. McGraw-Hill, New York, 1997.
3. Humphrey JL, Siebert AF. Separation Technologies: An Opportunity for Energy Savings. Chem Eng Prog. 1992;88(6):32–41.
4. Bagajewicz M, Ji S. Rigorous Procedure for the Design of Conventional Atmospheric Crude Fractionation Units. Part I: Targeting. Ind Eng Chem Res. 2001;40(2):617–626.
5. Hewitt G, Quarini J, Morell M. More efficient distillation. Chem Eng. 1999;21:16-19.
6. Madenoor Ramapriya G, Tawarmalani M, Agrawal R. Thermal Coupling Links to Liquid-only Transfer Streams: A Path for New Dividing Wall Columns. AIChE J. 2014;60(8):2949-2961.
7. Madenoor Ramapriya G, Tawarmalani M, Agrawal R. Thermal Coupling Links to Liquid-only Transfer Streams: An Enumeration Method for New FTC Dividing Wall Columns. AIChE J. 2016;62(4):1200–1211.
8. Madenoor Ramapriya G, Tawarmalani M, Agrawal R. A new framework for combining a condenser and reboiler in a configuration to consolidate distillation columns. Ind Eng Chem Res. 2015;54(42):10449-10464.

CHAPTER 2. NEW, TERNARY DIVIDING WALL STRUCTURES

In this chapter, we propose new Dividing Wall Columns (DWCs) that are equivalent to the ternary Fully Thermally Coupled (FTC) Petlyuk configuration. A special feature of all the new DWCs is that during operation, they allow independent control of the vapor flowrate in each partitioned zone of the DWC by means that are external to the column. Because of this feature, we believe that the new arrangements presented in this work will enable and accelerate the FTC configuration to be successfully implemented and optimally operated as a DWC in an industrial setting for ternary mixtures. Also, interesting column arrangements result when a new DWC drawn for a *3*-component mixture is adapted for the distillation of a mixture containing more than three components.

2.1 Introduction

Thermal coupling links in distillation are known to reduce the overall costs of a configuration on a plant, owing to simultaneous reduction in capital and operating costs.[1-3] Figure 2.1 shows the fully thermally coupled three-component Petlyuk configuration with thermal coupling links at submixtures *AB* and *BC*. Furthermore, we refer to the configuration of Figure 2.1 in this chapter as the TC-TC configuration. The first and second 'TC' respectively denote the thermal coupling links at submixtures *AB* and *BC*.

Despite its potential to significantly reduce the overall costs, the TC-TC configuration, as sketched in Figure 2.1, has seen limited industrial application. One reason for this is the operability issue that accompanies this TC-TC

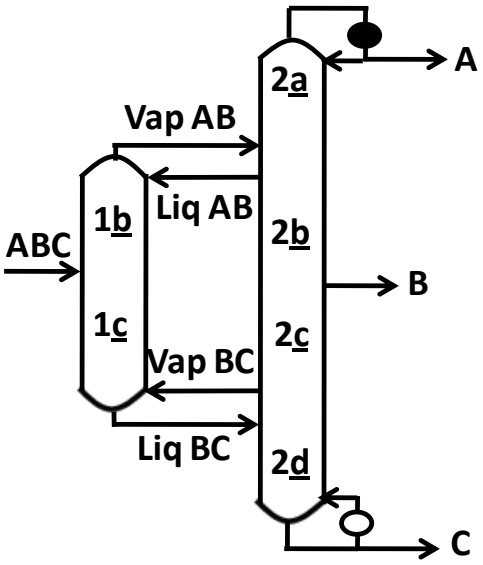

Figure 2.1 Three-component fully thermally coupled Petlyuk configuration: the TC-TC configuration.

configuration. In Figure 2.1, vapor *AB* is withdrawn from the top of column 1, and fed to column 2. This requires the pressure at the top of section 1b to be greater than that at the bottom of section 2a (assuming compressors are not used in the transfer line). Further, vapor *BC* is withdrawn from the top of section 2d, and fed to the bottom of column 1. This requires the pressure at the top of section 2d to be greater than that at the bottom of section 1c. Such conflicting pressure requirements in the two distillation columns bring in operational complications to this TC-TC configuration. To overcome these operability issues, Agrawal and Fidkowski[4] proposed the configurations of Figure 2.2, which are thermodynamically equivalent to the TC-TC configuration of Figure 2.1. In the configurations of Figure 2.2, the pressure in one column can be uniformly maintained greater than the other column, which simplifies some of the major operational complications of the TC-TC configuration.

For further savings in plant space and capital costs, the TC-TC configuration can be incorporated into a single shell, popularly called the DWC,

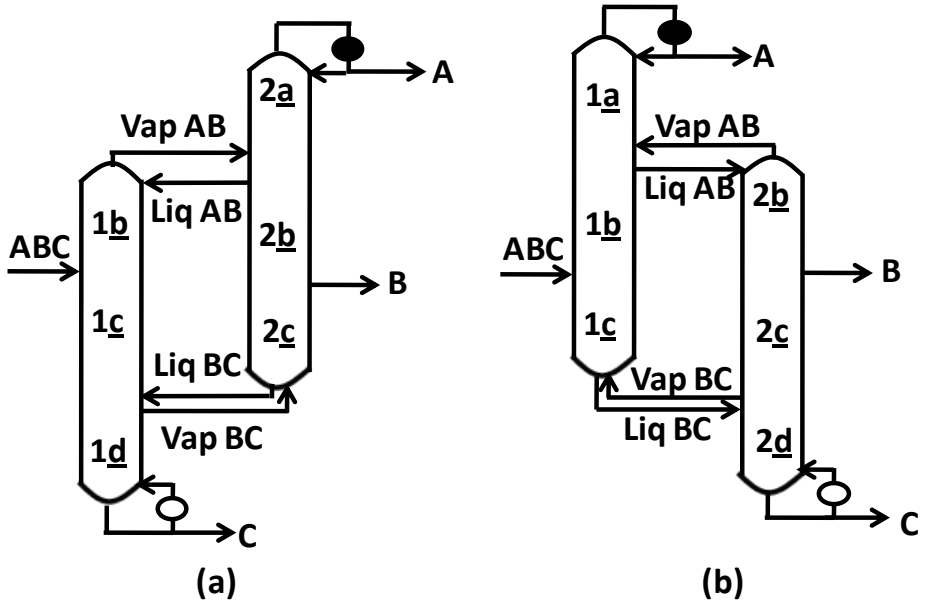

Figure 2.2 Operable versions of the TC-TC configuration.[4]

as shown in Figure 2.3.[5] In this chapter, we will refer to this configuration as the TC-TC column. We have adopted a naming system where TC-TC configuration refers to the two-column configuration shown in Figure 2.1, and TC-TC column refers to the one column system with a vertical partition as shown in Figure 2.3. Also, note that, later in the chapter, we refer to the skeleton partitioning arrangement/structure of Figure 2.3 by the same name (TC-TC column), even when it is used for separating four or higher component feeds. In the case of multicomponent separations using TC-TC column, the submixtures transferred at the thermal couplings will differ from what is shown in Figure 2.3. Further, for convenience, the different parts of DWCs in the chapter are shaded and named

distinctly to represent different zones. For example, the TC-TC column of Figure 2.3 is divided into four zones, namely Z_T, Z_1, Z_2 and Z_B.

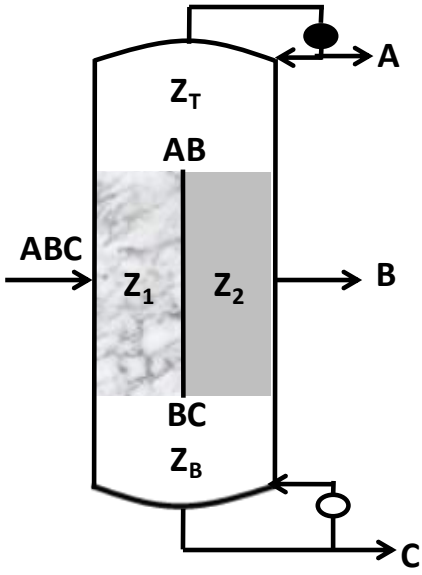

Figure 2.3 DWC version of the TC-TC configuration: TC-TC column.

Although the TC-TC column was introduced by Wright[5] as early as 1949, the first industrial application of this column did not happen until the late 1980s.[6] Since then, the use of multicomponent DWCs has seen a rapid increase in several industrial applications.[7,8] Updates on the recent developments in DWCs can be found in the works of Aspiron and Kaibel[9], Dejanovic et al.[10] and Yildirim et al.[8]

Though the TC-TC column of Figure 2.3 offers ample opportunity to reduce overall costs, it suffers from somewhat similar operability issues (related to pressure) as the TC-TC configuration of Figure 2.1. The pressure drop in the TC-TC column is an important consideration for its onsite operation.[11] In the TC-TC column, the pressure drop in the two parallel zones, Z_1 and Z_2, on either side of the vertical partition, are constrained to be equal. Subject to this constraint and

the mechanical resistances in the Z_1 and Z_2 zones, there is a natural uncontrolled split of the vapor ascending from the zone Z_B into the zones Z_1 and Z_2. This uncontrolled split implies that the relative vapor flowrates in zones Z_1 and Z_2 cannot be manipulated during operation. Though methods to address the control of the vapor split issue during the design and dimensioning phase of the TC-TC column have been proposed,[12,13] none exists for application during online operation that we are aware of, except for an experimental study which uses valves for this vapor split control in an experimental distillation setup that is thermodynamically equivalent to a DWC.[14] This vapor split can significantly affect the product purities, total annualized costs, and has implications on how far the TC-TC column is away from its optimal operation.[2,15,16] Though the liquid split at the top of the vertical partition also can have similar effects, it is generally well-controlled during operation, using collectors and distributors. Further, the operable versions of the TC-TC configuration shown in Figure 2.2 also simplify to the same DWC arrangement of Figure 2.3. Hence, the operational advantages in the configurations of Figure 2.2 over the TC-TC configuration are not translated to their dividing wall versions.

In this chapter, we present new DWCs that are more operable than the TC-TC column for a three-component feed mixture. Further, through modeling, we show that all the new DWCs are equivalent to the TC-TC column (or configuration). Finally, we make some interesting observations when a DWC designed for a three-component feed is used to distill a feed mixture containing more than three components. We first show how a thermal coupling link can

always be converted to an equivalent liquid-only transfer stream, and then, the resulting configurations can be easily used to generate new DWCs.

2.2 Conversion of thermal coupling to liquid-only transfer stream

Distillation configurations with liquid transfers between distillation columns are easier to operate and control than configurations with vapor transfers between distillation columns. Based on this fact, for the distillation of a ternary mixture, Agrawal[17] proposed the three configurations of Figure 2.4, which are

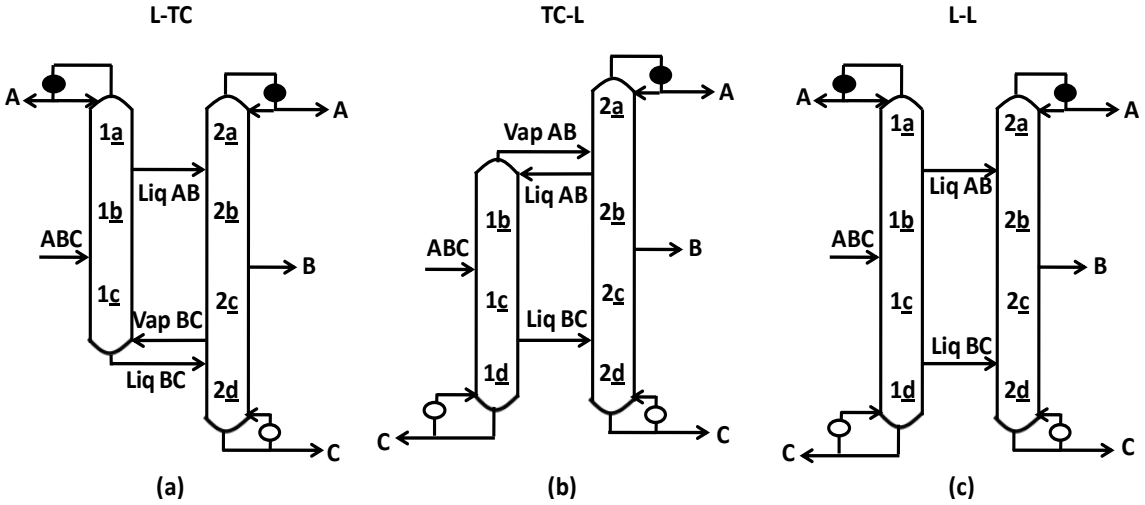

Figure 2.4 Configurations with reduced number of vapor transfers proposed by Agrawal[17] (a) L-TC configuration; (b) TC-L configuration; (c) L-L configuration.

more operable than the TC-TC configuration of Figure 2.1. To obtain the configurations in Figure 2.4 from that in Figure 2.1, the thermal coupling links at submixture AB or/and CD have been converted to liquid-only transfer streams with the addition of new sections 1a or/and 1d. We respectively refer to the configurations of Figures 2.4(a), 2.4(b) and 2.4(c) as the L-TC, TC-L and L-L

configurations. For example, the L-TC configuration is named so because of the liquid transfer at submixture *AB* and thermal coupling link at submixture *BC*.

Based on physical reasoning, Agrawal[17] proposed that the configurations of Figure 2.4 have the same overall minimum vapor requirement as the TC-TC configuration, and hence, are equivalent to the TC-TC configuration. Here, we show this mathematically by proving that whenever a thermal coupling link in a configuration (for e.g. TC-TC configuration) is replaced with a liquid-only transfer stream (for e.g. L-TC, TC-L or L-L configuration), the resulting configuration is always equivalent to the original configuration with the thermal coupling link. To show this proof, we use the arrangements shown in Figure 2.5. The thermal coupling at the top of section S2 in Figure 2.5(a) is converted to a liquid-only transfer stream in Figure 2.5(b) with the addition of a new section S1. The notation for the symbols used in the figure is provided at the top of the figure. The lettered quantities shown along any section in the figure indicate the respective liquid and vapor flows in the section, after accounting for the relevant mass balances. While the quantities shown adjacent to the left of each section in the figure denote the respective vapor flows, the quantities shown adjacent to the right denote the respective liquid flows in the section. The liquid and vapor flows in section S2 as well as in section S4 of both the Figures 2.5(a) and 2.5(b) are retained to be the same. Further,

$$\frac{\mathrm{L}}{\mathrm{V}} \text{ ratio in section S3 of Figure 2.5(a)} = \frac{\mathrm{L_{S3}}}{\mathrm{L_{S3}} + \mathrm{M_{S3}}} \tag{2.1}$$

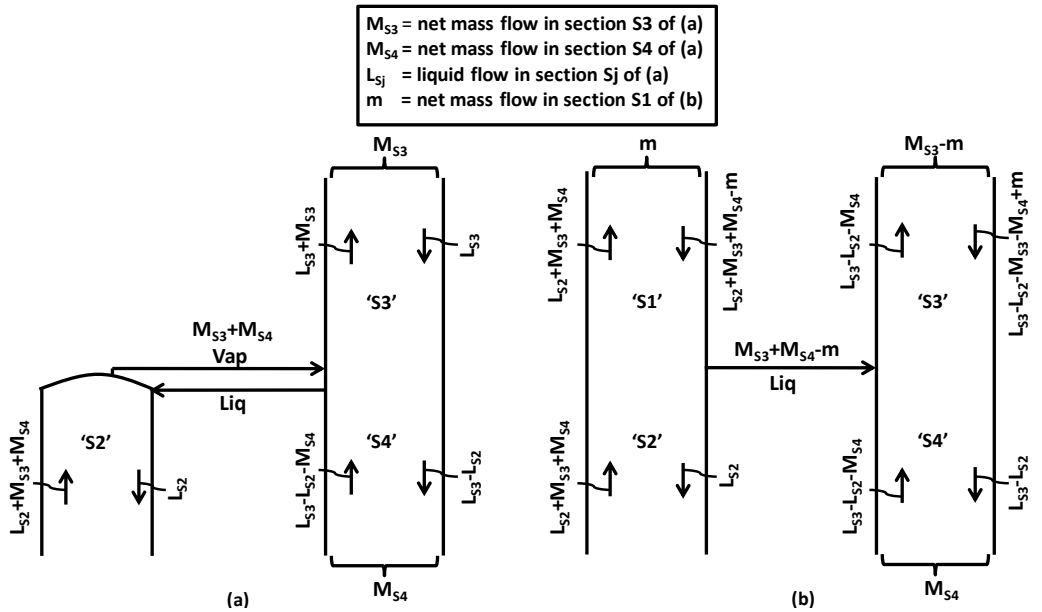

Figure 2.5 (a) Any thermally coupled arrangement; (b) Thermally coupled arrangement of (a) replaced with a liquid-only transfer stream and a new section S1.

In Figure 2.5(b), to constrain that section S1 be equivalent to section S3, the number of stages and the L/V ratios in the two sections must be equal. To achieve the equality in L/V ratios, one degree of freedom is available in the form of the variable 'm', the net mass flow in section S1. Determining the value of 'm' that ensures this constraint,

$$\frac{L}{V}\ \text{ratio in section S1 of Figure 2.5(b)} = \frac{L}{V}\ \text{ratio in section S3 of Figure 2.5(b)}$$

$$\Rightarrow \frac{L_{S2} + M_{S3} + M_{S4} - m}{L_{S2} + M_{S3} + M_{S4}} = \frac{L_{S3} - L_{S2} - M_{S3} - M_{S4} + m}{L_{S3} - L_{S2} - M_{S4}}$$

$$\Rightarrow m = \frac{M_{S3}(L_{S2} + M_{S3} + M_{S4})}{L_{S3} + M_{S3}} \qquad (2.2)$$

We now substitute 'm' to determine the mass flow in the liquid transfer from the first column to the second, and the L/V ratio in sections S1 and S3 of Figure 2.5(b). It follows that:

$$\text{Mass flow in liquid transfer} = M_{S3} + M_{S4} - m = \frac{M_{S4}L_{S3} + M_{S3}(L_{S3} - L_{S2})}{L_{S3} + M_{S3}} \quad (2.3)$$

which is clearly non-negative because $L_{S3} \geq L_{S2}$. Therefore, the liquid transfer is guaranteed to be in the direction shown in Figure 2.5(b). Further,

$$\frac{L}{V} \text{ ratio in sections S1 and S3 of Figure 2.5(b)} = \frac{L_{S3}}{L_{S3} + M_{S3}} \quad (2.4)$$

which, interestingly from Equation 2.1, is the same L/V ratio in section S3 of Figure 2.5(a). This means that, for the value of 'm' given by Equation 2.2, the two sections S1 and S3 in Figure 2.5(b) are equivalent to the section S3 in Figure 2.5(a). The above discussion implies that the mass M_{S3} that is distilled in one section S3 of Figure 2.5(a) is divided between similar, two sections, S1 and S3, in Figure 2.5(b), which respectively distill a mass of 'm' and 'M_{S3}-m' of the same composition. So, any liquid-vapor traffic in the thermally coupled arrangement of Figure 2.5(a) can be identically duplicated in the liquid-only transfer arrangement of Figure 2.5(b). Thus, the two arrangements in Figure 2.5 are only topologically different, but equivalent in all other aspects, irrespective of the number of components or vapor-liquid equilibrium associated with the distillation sections. A similar proof can be easily derived when a thermal coupling at the bottom of a column is converted to a liquid-only transfer stream.

2.3 New, operable three-component DWCs

We present the new, more operable DWC versions of the L-TC, TC-L and L-L configurations: the L-TC, TC-L and L-L columns in Figure 2.6. Note that

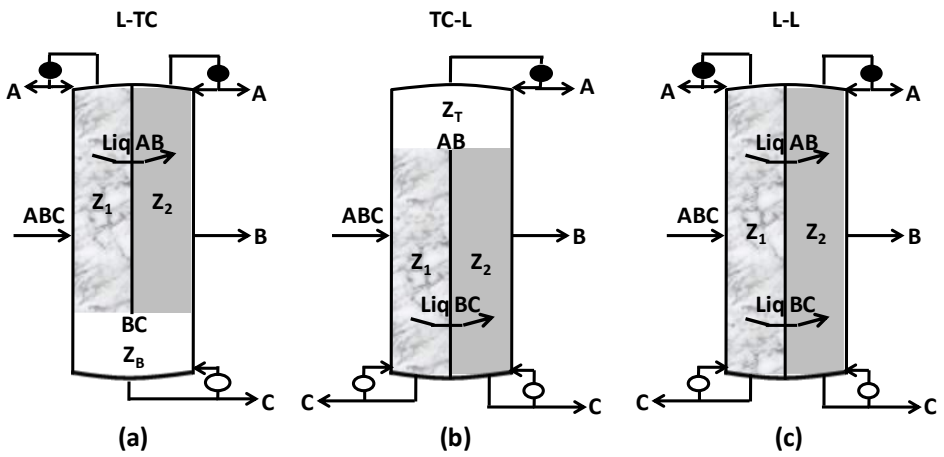

Figure 2.6 New more operable DWCs derived from Figure 2.4 (a) L-TC column; (b) TC-L column; (c) L-L column.

the same names will be used later when the same structures are used for higher component separations. A distinct feature of all the DWCs of Figure 2.6 is that the liquid transfers associated with the submixtures *AB* and *BC* that are explicitly shown, are made around (or across) the vertical partition. This is achieved by collecting the liquid of desired quantity from an intermediate location of one zone (Z_1), and then feeding it to an intermediate location of the other zone (Z_2), on the other side of the vertical partition. An example of such a liquid transfer is shown for the L-TC column in Figure 2.7. The liquid flows can be managed either through a gravitational head or by the use of pumps. Valves in the liquid lines (not shown in the figure) could be used to manipulate the liquid split from collection pot 1. There is no vapor exchange between the two intermediate locations of the two parallel zones. Thus, the vertical partitions are continuous. Such a construction in all the new DWCs eliminates the constraint that the pressure drop in the two parallel zones, on either side of the vertical partition, be

equal. This feature of the new DWCs, as will be seen, makes them more operable than the conventional TC-TC column.

The L-TC column in Figure 2.6(a), like the TC-TC column in Figure 2.3,

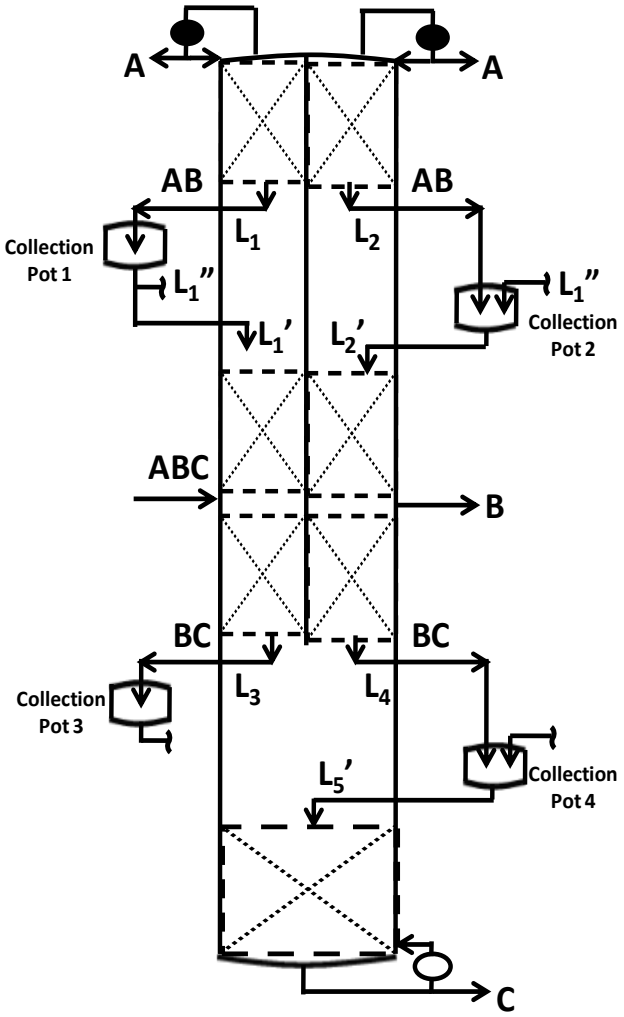

Figure 2.7 An example depiction of liquid transfers in the L-TC column. Some of the collection pots shown, in certain cases, could be eliminated or combined into one pot.

has one vapor split at the bottom of the vertical partition. However, the two condensers at *A* in the L-TC column can be manipulated to create the desired pressure drop in zones Z_1 and/or Z_2. This can be achieved by either placing a

valve in the piping before the condenser, or, by controlling the inlet temperature of the cooling medium within each of the condensing heat exchangers.[18] Alternatively, the heat exchanger may be designed to be a submersible heat exchanger, whereby, submergence of the passage for the condensing fluid can be controlled to tailor the active area through which most of the heat transfer takes place. This will control the condensing temperature, and hence the pressure of the condensing fluid. The control of the pressure at the top of either of the zones Z_1 or Z_2 will tailor the pressure drop across that zone, and hence the vapor flowrate through that zone. Thus, the L-TC column offers a control mechanism for the vapor split at the bottom of the vertical partition that is external to the column.

Interestingly, the TC-L and L-L columns have no vapor splits. The two reboilers at *C* can be used to operate each section in the two parallel zones, on either side of the vertical partition, at the desired L/V ratios. It is worth noting that, in the case of the L-L column, the two parallel zones can be operated like two independent distillation columns, which may give the configuration more flexibility and freedom to operate.

The L-TC and TC-L columns use one more heat exchanger, and the L-L column uses two more than the TC-TC column. Arrangements can be made to each DWC of Figure 2.6 to reduce the total number of heat exchangers to two. One possible arrangement of the L-TC, TC-L and L-L columns using one reboiler and one condenser is shown in Figure 2.8. In the L-TC column of Figure 2.8(a), cooling utility of sufficiently low temperature is used as a common condensing

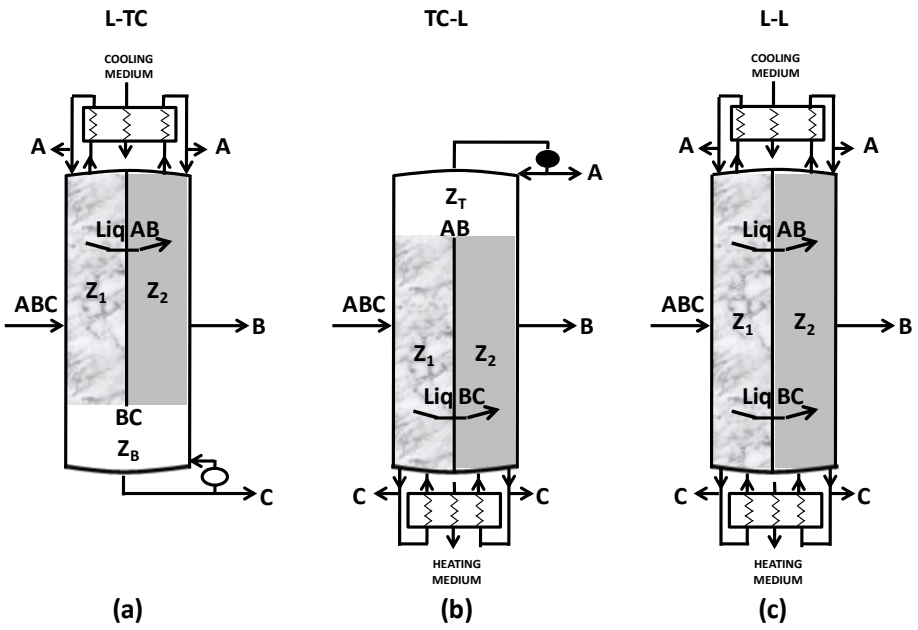

Figure 2.8 Arrangement of the (a) L-TC; (b) TC-L; (c) L-L columns with one reboiler and condenser.

medium to simultaneously condense *A* vapor streams collected from both the parallel zones, Z_1 and Z_2. To achieve this, the heat exchanger has two separate passages for the vapor collected from the two zones. To control the vapor flowrates in the two parallel zones, the condenser heat exchanger may be designed so that the condensing fluid in each of the passages can achieve its own desired approach temperature to the cooling medium temperature. This can be implemented in several possible ways. Each passage can be designed with a different active surface area to tailor the approach temperature. Alternatively, the passage for the cooling medium can also be divided into two. The flowrate and inlet temperature of the cooling medium for each of the passages may be independently controlled to allow for differences in the temperature of the

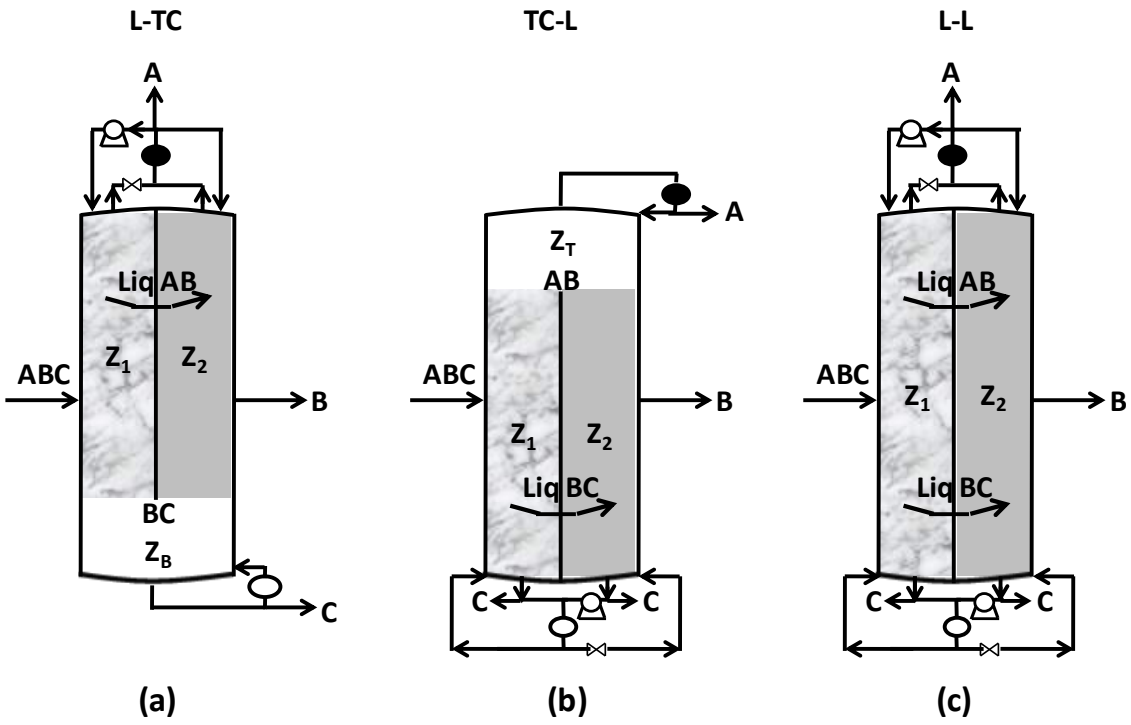

Figure 2.9 An alternate arrangement of the (a) L-TC; (b) TC-L; (c) L-L columns with one reboiler and condenser, that uses pumps and throttling valves.

condensing fluids. Likewise, in the TC-L column of Figure 2.8(b), *C* liquid streams collected from the two parallel zones, Z_1 and Z_2, are fed to two separate passages in the reboiler. A common heating medium of sufficiently high temperature is used to simultaneously vaporize the liquids in the two passages. Similar to the condenser heat exchanger for L-TC column, the vapor boilup rate in each of the passages of the reboiler can be controlled to provide the desired split of vapor flow between zones Z_1 and Z_2. In the L-L column of Figure 2.8(c), the condenser and reboiler arrangements of Figures 2.8(a) and 2.8(b) respectively, are used together.

Figure 2.9 shows an alternate arrangement for the L-TC, TC-L and L-L columns with one reboiler and condenser. In the L-TC column of Figure 2.9(a), a

throttling valve is provided in the vapor line leaving zone Z_1 (assuming that the top of zone Z_1 is at a higher pressure than the top of zone Z_2) to reduce the pressure of the vapor to that leaving zone Z_2. The combined vapor is condensed in a single heat exchanger. A part of the condensed pure liquid *A* is withdrawn as product, while the rest is used as reflux to the two zones. The reflux to zone Z_1 is pumped. Alternatively, the condenser heat exchanger could be located at such a height that liquid reflux to zone Z_1 could be fed under gravitational head, and if needed, a valve may be used in the liquid feed line to zone Z_2 to reduce the pressure build-up. In the TC-L column of Figure 2.9(b), a pump is provided in the liquid line leaving zone Z_2 (assuming that the bottom of zone Z_2 is at a lower pressure than the bottom of zone Z_1) to increase the pressure of the liquid to that leaving zone Z_1. The combined liquid is boiled in the reboiler and used for boil-up to the two zones. A throttling valve is used in the vapor line entering zone Z_2 for reducing the pressure. Alternatively, the bottom of the column with respect to the reboiler inlet could be located at such a height so as to allow liquid drain from zone Z_2 via gravitational head without the use of a pump. In this case, pressure of the liquid from the bottom of zone Z_1 to the mixing point is appropriately manipulated. The L-L column of Figure 2.9(c) uses the condenser and reboiler arrangements of Figures 2.9(a) and 2.9(b) respectively. In Figure 2.9, for the purpose of illustration, the throttling valves and pumps are shown before/after streams that enter/leave one of the two parallel zones. In general, depending on the pressure in the two parallel zones of the DWC, the pump and the throttling valves may be switched between either zones; or additional valves or pumps

may be used in additional lines to manipulate pressure drops in various lines external to the column.

With the TC-TC, L-TC, TC-L and L-L columns being equivalent to each other, we also expect the height of these columns for any given application to be not significantly different from each other. The additional capital cost in the new DWCs of Figure 2.6 (or 2.8 or 2.9 or their variants) is therefore expected to be only due to the use of additional heat exchangers/pumps/valves and a longer vertical partition. The additional equipments account for better operability in the new DWCs.

2.4 Operational flexibility of the L-TC, TC-L and L-L columns

For the TC-TC configuration of Figure 2.1, Fidkowski and Krolikowski[2] identified, for ideal saturated liquid feed mixtures, under constant molar overflow conditions, a range of vapor splits from section 2d to sections 1c and 2c, over which the total minimum vapor requirement of the configuration remains optimal. Since the TC-TC column in Figure 2.3 is equivalent to the TC-TC configuration, a wide window of optimal vapor splits can be useful for the operation of the TC-TC column. For example, in the TC-TC column of Figure 2.3, if there is a wide range of vapor flow from zone Z_B to zone Z_1 (and consequently Z_2) that allows for optimal operation, then there is more leeway/flexibility in the vapor split at the bottom of the vertical partition for close to optimal operation, and vice-versa.

Fidkowski and Krolikowski[2] studied the optimal operation range of the TC-TC configuration for the first four ternary feed compositions listed in Table 2.1. In

order to span the spectrum of possible representative compositions for ternary feeds, we extend our study to include three more feed compositions, added at the bottom of Table 2.1. Their[2] optimization model is solved using BARON[19] within GAMS[20] with a tolerance of 0.001. The BARON solver ensures global optimality of the obtained solutions. The results for all the feed compositions, and two sets of relative volatilities are shown in Table 2.2. Table 2.2 lists the optimal range of vapor flow in section 1c for the TC-TC configuration, as percent of its total minimum vapor requirement. Thus, for the TC-TC configuration in Figure 2.1, for a given feed, if the calculated range for the vapor flowrate in section 1c is from V_1 to V_2 over which the total minimum vapor flowrate remains at V_{min}, then $\Delta V=V_2-V_1$, and the value $100*\Delta V/V_{min}$ is listed in Table 2.2. Since the vapor and liquid traffic in section 1c of the TC-TC configuration can be identically retained in the same section of the L-TC, TC-L and L-L configurations without raising the overall heat duty, these configurations also have the same optimal range of vapor flow in this section as the TC-TC configuration. Thus, the results in Table 2.2 also apply to the L-TC, TC-L and L-L configurations.

From Table 2.2, we note that there are a number of feed conditions, especially when the relative volatilities are low, where the split of the vapor between two zones Z_1 and Z_2 in Figures 2.3 and 2.5 must be controlled within a narrow range for avoiding the suboptimal operation. For example, for case AbC with both the relative volatility sets, and cases aBc and ABC with $[\alpha_{AB},\alpha_{BC}]=[1.1,1.1]$, the allowed variations in the optimal vapor flowrate for section 1c are substantially small. For these cases, the vapor split across zones Z_1 and

Z_2 must be controlled carefully. Otherwise, the heat duty will increase. The greatest advantage of the new L-TC, TC-L and L-L columns is that it allows for such tight control of vapor flow on each side of the vertical partition. This preserves the lower heat duty requirement, and ensures the purity of the intermediate product B.

Table 2.1 List of representative ternary feed compositions used for simulation results in Table 2.2.

Feed composition (f)	A	B	C
abC	0.1	0.1	0.8
aBc	0.1	0.8	0.1
Abc	0.8	0.1	0.1
ABC	0.33	0.33	0.34
ABc	0.45	0.45	0.1
AbC	0.45	0.1	0.45
aBC	0.1	0.45	0.45

There is yet another flexibility of the L-TC, TC-L and L-L columns of Figure 2.6, which is missing from the TC-TC column of Figure 2.3. Once physically built, they also allow operation in the side rectifier and side stripper modes. For example, in the L-L column, if no liquid *BC* is transferred across the vertical partition, with only the liquid *AB* transfer, the column could produce *B* from the bottom of zone Z_2. In this case, no *B* may be produced from an intermediate

Table 2.2 Optimal vapor flowrate range for section 1c in the TC-TC, L-TC, TC-L and L-L configurations, as percent of the total minimum vapor requirement. Description of feed composition f (abC, aBc, etc.) is provided in Table 2.1.

$[\alpha_{AB},\alpha_{BC}]$	f	$\Delta V/V_{min}$ (%)
[2.5,2.5]	abC	46.9
	aBc	38.1
	Abc	16.3
	ABC	20.4
	ABc	14.8
	AbC	0.9
	aBC	40.6
[1.1,1.1]	abC	36
	aBc	4.2
	Abc	32.4
	ABC	2.6
	ABc	9.3
	AbC	0.2
	aBC	15.4

location of zone Z_2. This will be analogous to the operation of a side stripper. In an alternate case, where liquid *BC* is transferred but no liquid *AB* is transferred, *B* could be produced from the top of zone Z_2 of the L-L column, leading to the operation similar to a side rectifier. Thus, a L-L column, once built, can be operated as a fully thermally coupled column/side rectifier/side stripper. Similarly,

without any liquid transfer across the vertical partition, L-TC and TC-L columns could be operated in the side rectifier and side stripper modes respectively. This added flexibility can be quite advantageous, as, for certain feed conditions, a side rectifier or a side stripper may be thermodynamically more efficient than the fully thermally coupled TC-TC configuration.[21] Conversely, a DWC already built on a plant to operate in the side rectifier/side stripper mode can be suitably modified to operate as a L-TC/TC-L column respectively.

2.5 Three-component DWC structures for distilling *n*-component mixtures

Our new *n*-component skeleton dividing wall structures presented earlier can be easily adapted to separate a multicomponent feed containing more than *n* components. In such cases, product streams enriched in different components will be produced. However, the possible product streams and the number of operating modes increase rapidly with the number of components in the feed. Any of these operating modes can be included within a larger flowsheet that separates multicomponent mixtures into component product streams. We will first illustrate the adaptation of the various operating modes of the L-TC, TC-L and L-L columns, originally drawn for the distillation of a ternary feed, to a quaternary feed mixture, *ABCD*. Then, as a generalization of our approach, we will distill a quinary mixture using one of our ternary skeleton dividing wall structures.

The L-TC, TC-L and L-L columns have two submixture transfers from intermediate locations, one above the feed and the other below the feed (*AB* and *BC* in the earlier studied three-component case). When a quaternary feed

mixture *ABCD* is distilled in these columns, there are two possible submixtures, *ABC* or *AB*, which could be transferred from an intermediate location above the feed. Similarly, from an intermediate location below the feed, the two possible submixture transfers are *BCD* or *BC*. This implies that, for each of the three vertical partitioned columns shown in Figure 2.6, we have four possible combinations of the two submixtures. Figure 2.10 shows these combinations.

Some interesting observations can be made from Figure 2.10. When compared to the TC-TC column for separating *ABCD* (not shown), the L-TC, TC-L and L-L columns of Figure 2.10, apart from better vapor split control, offer an additional flexibility to produce two different products from the top or/and bottom of the column. For example, in the L-TC and L-L columns of Figures 2.10(a) and 2.10(c), stream *A* can be produced as a product from the top of one zone, while stream *AB* may be produced as a product from the top of the other. Similarly, in TC-L and L-L columns of Figures 2.10(b) and 2.10(c), one has an option to produce stream *D* from the bottom of one zone, and *CD* from the bottom of the other zone. Furthermore, in some of the DWCs of Figure 2.10, one sidedraw stream may be withdrawn from zone Z_2, if desirable, instead of two. For example, from zone Z_2 of Figure 2.10(f), instead of withdrawing two sidestreams, *BC* and *C*, a single sidestream *C* may be withdrawn. In such a case, the two separations taking place in zone Z_2 are *ABC->AB\C* and *CD->C\D*.

An interesting case emerges in Figures 2.10(j) through 2.10(l), where all the products may be produced with high purity. The sequence of component splits/separations shown in Figures 2.10(j), 2.10(k) and 2.10(l), using the TC-TC

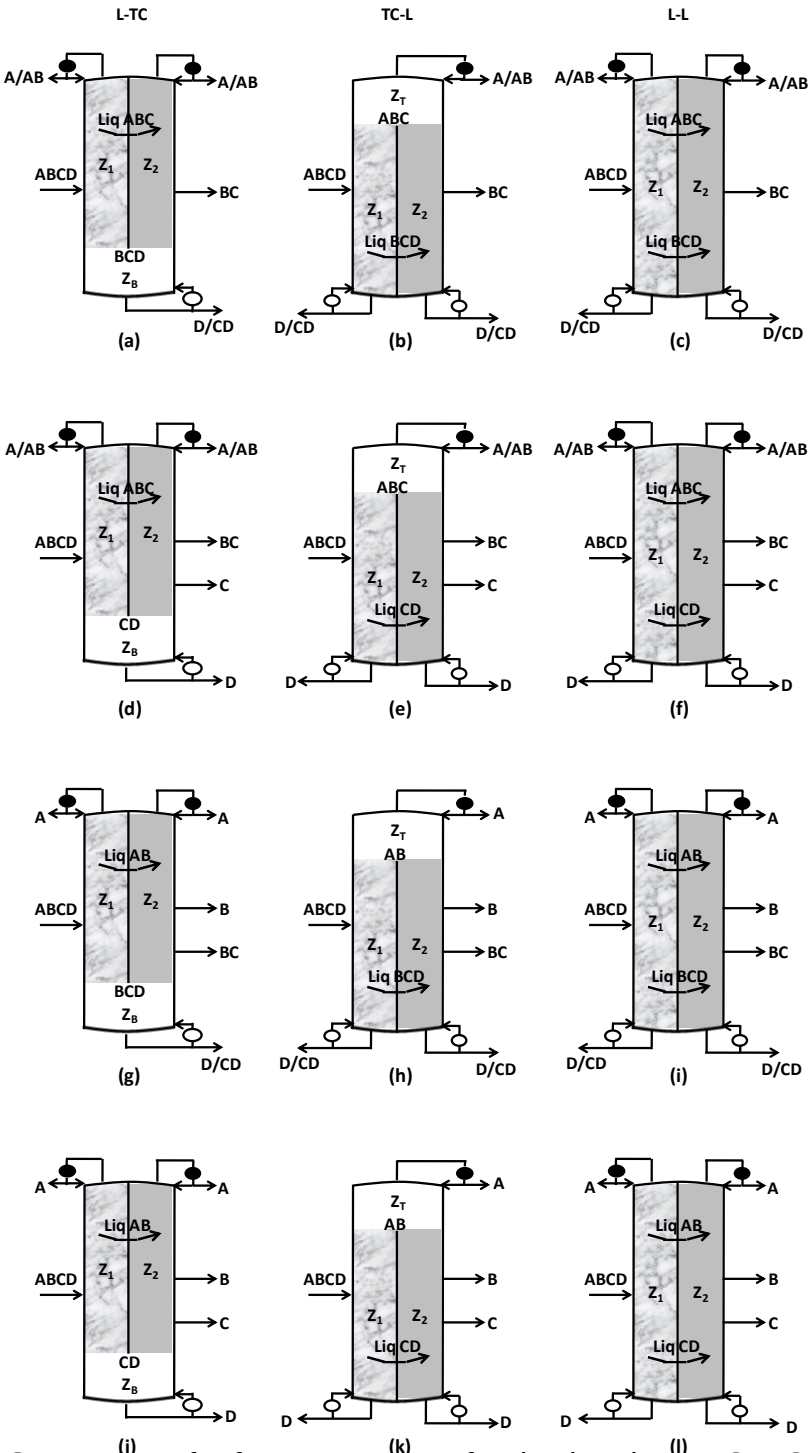

Figure 2.10 Separation of a four-component feed using the L-TC, TC-L and L-L column structures.

column, has been known in the past.[6,22,23] The use of our new L-TC, TC-L and L-L columns instead, allows for a better control of vapor flow on each side of the

vertical partition. This makes it easy to control the production of pure *B* and *C* product streams from an operating plant, and also allows the column to be operated closer to its designed optimal heat duty.

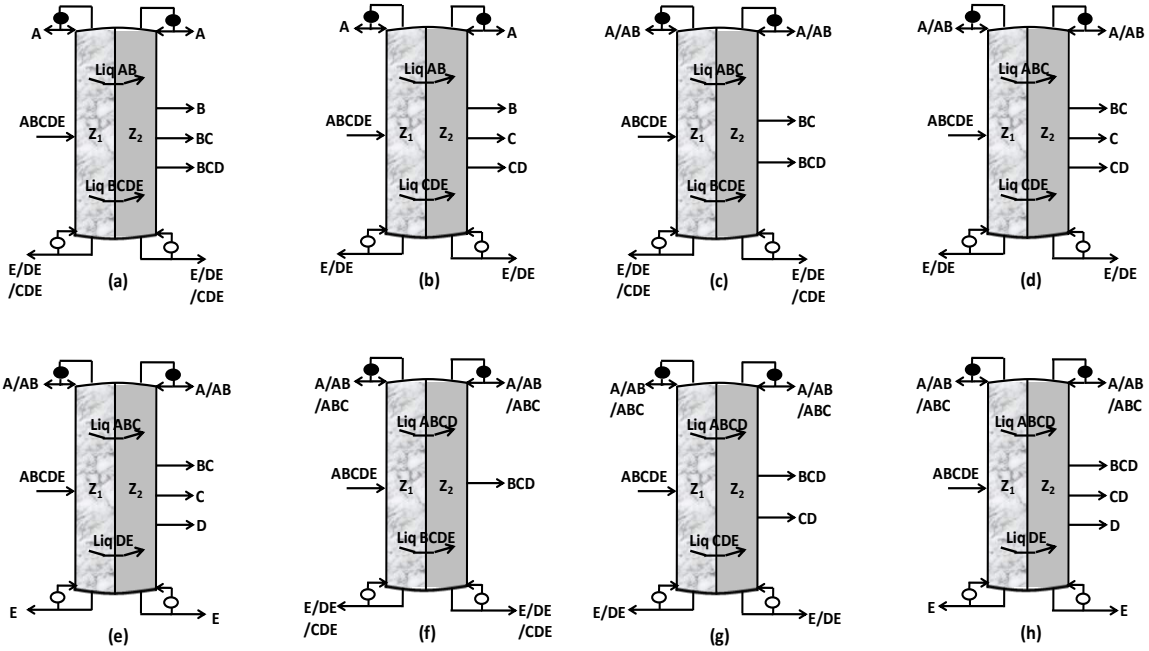

Figure 2.11 Separation of a five-component feed using the L-L column structure.

Based on the observations made for quaternary mixtures, the various operating modes from the use of the L-L column to separate a quinary mixture are shown in Figure 2.11. Some of the intermediate withdrawal streams from zone Z_2 of these distillation columns may be eliminated, if desired. It is clear that the concept can also be applied to L-TC and TC-L columns.

2.6 Conclusions

DWCs are finding increasing prominence industrially for multicomponent separations. The DWCs, derived from the fully thermally coupled configurations,

are of special interest because of their low heat duty requirements. However, the heat duty and cost benefits from such DWCs are susceptible to the vapor split at the bottom of any of its vertical partitions, which is unregulated during operation. This susceptibility increases as the number of components in the feed increase because of the increase in the number of vapor splits in the DWC.

To reduce the operational difficulties from the dividing wall derivative of the three-component fully thermally coupled Petlyuk column (called TC-TC column), we introduced new more operable DWCs, the L-TC, TC-L and L-L columns in this chapter. The new DWCs are derived from distillation configurations by transforming a thermal coupling link to a liquid-only transfer stream. We show that such transformations are equivalent to the originally thermally coupled configuration. The new DWCs are characterized by longer continuous vertical partitions and liquid transfers of submixtures around the vertical partitions, which makes them more operable. While the L-TC column has one vapor split, the TC-L and L-L columns have no vapor splits. Moreover, the vapor split in the L-TC column can be easily controlled during online operation.

Any thermal coupling link in a distillation configuration can be converted to a liquid-only transfer, as proposed by Agrawal,[17] and incorporated into a DWC as presented in this chapter. We believe this concept will, for the first time, enable the industrial practitioners to successfully implement and optimally operate the *3*-component fully thermally coupled configuration in a DWC.

We demonstrate an interesting extension whereby a new dividing wall configuration drawn for a *3*-component mixture can be easily adapted to distil a

mixture containing more than *n*-components. Thus, we show the use of ternary DWCs such as the L-TC, TC-L and L-L columns for the distillation of a four-component and a five-component mixture.

The findings in the chapter indicate that the new DWCs are attractive and promising candidates for industrial application. An extensive design and control study, as has been devoted to the conventional TC-TC column, will increase the rate of industrial implementation.

References

1. Petlyuk FB, Platonov VM, Slavinskii DM. Thermodynamically Optimal Method for Separating Multicomponent Mixtures. Int Chem Eng. 1965;5(3):555-561.
2. Fidkowski ZT, Krolikowski L. Thermally coupled system of distillation columns: optimization procedure. AIChE J. 1986;32:537–546.
3. Triantafyllou C, Smith R. The Design and Optimization of Fully Thermally Coupled Distillation Columns. Trans Inst Chem Eng. 1992;70:Part A, 118.
4. Agrawal R, Fidkowski ZT. More operable arrangements of fully thermally coupled distillation columns. AIChE J. 1998;44(11):2565-2568.
5. Wright RO. Fractionation Apparatus. 1949. US Patent 2,471,134.
6. Kaibel G. Distillation Columns with Vertical Partitions. Chem Eng Tech. 1987;10(1):92-98.
7. Kaibel B, Jansen H, Zich E, Olujic Z. Unfixed Dividing Wall Technology For Packed And Tray Distillation Columns. Distill Absorpt. 2006;152:252-266.
8. Yildirim O, Kiss AA, Kenig EY. Dividing wall columns in chemical process industry: A review on current activities. Sep Pur Tech. 2011;80:403-417.
9. Asprion N, Kaibel G. Dividing wall columns: Fundamentals and recent advances. Chem Eng Process. 2010;49:139-146.
10. Dejanovic I, Matijasevic L, Olujic Z. Dividing wall column—A breakthrough towards sustainable distilling. Chem Eng Process. 2010;49:559-580.
11. Sangal VK, Bichalu L, Kumar V and Mishra IM. Importance of pressure drop in divided wall distillation column. Asia-Pac J Chem Eng. 2013;8:85–92.
12. Lestak F, Collins C. Advanced distillation saves energy & capital. Chem Eng. 1997;104(7):72-76.
13. Dejanovic I, Matijasevic L, Jansen H, Olujic Z. Designing a Packed dividing wall column for an Aromatics Processing Plant. Ind Eng Chem Res. 2011;50:5680–5692.
14. Dwivedi D, Strandberg JP, Halvorsen IJ, Preisig HA, Skogestad S. Active Vapor Split Control for Dividing-Wall Columns. Ind Eng Chem Res. 2012;51(46): 15176–15183.
15. Mutalib MIA, Smith R. Operation And Control Of Dividing Wall Distillation Columns. Part 1: Degrees of Freedom and Dynamic Simulation. Trans Inst Chem Eng. 1998;76:Part A:308-318.

16. Maralani LT, Xigang Y, Yiqing L, Chao G, Guocong Y. Numerical Investigation on Effect of Vapor Split Ratio to Performance and Operability for Dividing Wall Column. Chin J Chem Eng. 2013;21(1):72–78.
17. Agrawal R. Thermally Coupled Distillation with Reduced Number of Intercolumn Vapor Transfers. AIChE J. 2000;46(11):2198- 2210.
18. Agrawal R. Multicomponent Columns with Partitions and Multiple Reboilers and Condensers. Ind Eng Chem Res. 2001;40(20):4258-4266.
19. Tawarmalani M, Sahinidis NV. A polyhedral branch-and-cut approach to global optimization. Mathematical Programming. 2005;103(2):225-249.
20. McCarl B, Meeraus A, Van der Eijk P, Bussieck M, Dirkse S, Steacy P, Nelissen F, McCarl GAMS user guide, GAMS Development Corporation, 2012.
21. Agrawal R, Fidkowski ZT. Are Thermally Coupled Distillation Columns Always Thermodynamically More Efficient for Ternary Distillations? Ind Eng Chem Res. 1998;37(8): 3444-3454.
22. Brugma AJ. Process and Device for Fractional Distillation of Liquid Mixtures, More Particularly Petroleum. US Patent 2,295,256, 1942.
23. Cahn RP, Di Miceli AG. Separation of multicomponent mixture in single tower. US Patent 3,058,893, 1962.

CHAPTER 3. ENUMERATION OF NEW FULLY THERMALLY COUPLED DIVIDING WALL COLUMNS

As studied in the previous chapter, novel DWCs can be obtained by converting thermal couplings to liquid-only transfer streams. Here, we develop a simple four-step method to generate a complete set of DWCs containing *n*-2 dividing walls, for a given *n*-component fully thermally coupled (FTC) distillation. Among the novel DWCs, some easy-to-operate DWCs possess the property that the vapor flow in every section of the DWC can be controlled during operation by means that are external to the column. We develop a simple method to enumerate all such easy-to-operate DWCs. We expect that the easy-to-operate DWCs can be operated close-to-optimality; leading to a successful industrial implementation of the *n*-component ($n \geq 3$) FTC distillation in the form of a DWC. As an illustration, we show figures of all easy-to-operate DWCs with two dividing walls for the four-component FTC distillation.

3.1 Introduction

The heat duty and cost benefits from fully thermally coupled (FTC) distillation have been well established.[1-3] *FTC distillation uses reboiler only at the least volatile component and condenser only at the most volatile component*. *Also, all feasible submixtures are produced and transferred between distillation sections to achieve the separation of the given feed mixture into product streams*. The distillation configurations which achieve FTC distillation for three and four-component separations are shown in Figures 3.1(a) and 3.2(a), respectively.

These are the *classic-FTC configurations*, the very first ones to be invented for FTC distillation,[1] with $n(n\text{-}1)$ sections for distilling an n-component mixture.

More FTC configurations, as operable alternatives to the classic-FTC configuration were suggested by Agrawal.[4] A feature of these FTC configurations is that, for n-component FTC distillation, they retain the $n(n\text{-}1)$ sections of the classic-FTC configuration, but introduce copies of some of the sections, so that thermal couplings are converted to liquid-only transfers. Examples of FTC

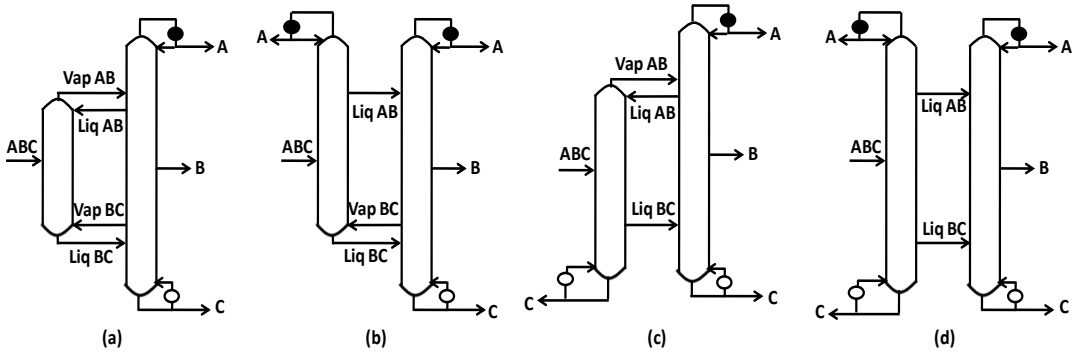

Figure 3.1 Three-component FTC configurations. Classic-FTC configuration with six sections is shown in (a).

configurations resulting from this conversion strategy for three-component separations are shown in Figures 3.1(b)-(d).[4] The configurations in Figures 3.1(b), 3.1(c) and 3.1(d) are obtained from that in Figure 3.1(a) by converting thermal couplings respectively at *AB*, *BC* and, *AB* & *BC* to liquid-only transfers. A formal proof of why all the four FTC configurations in Figure 3.1 are *thermodynamically equivalent* to each other is provided in Reference 5. An alternate proof, is provided in Appendix A.

To reduce the capital costs of distillation configurations, multiple distillation columns can be implemented inside a single shell along with the use of vertical

partitions.[6] Such arrangements, popularly known as dividing wall columns (DWCs), are promising candidates for widespread industrial applications.[7,8] Recently, we studied the DWC versions of the FTC configurations, which we shall refer to as *FTC DWCs*.[5,9,10] The FTC DWCs corresponding to the FTC configurations of Figures 3.1(a)-(d) are respectively shown in Figures 3.3(a)-(d).

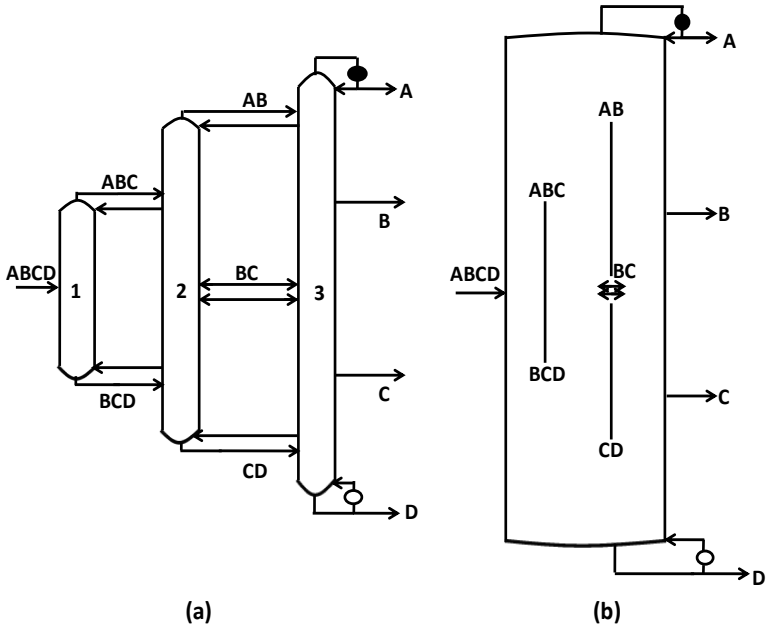

Figure 3.2 (a) Four-component classic-FTC configuration and (b) its DWC version.

To derive maximum operating cost benefits from a FTC DWC, it has to be operated at or close to optimality. This means that each section of a FTC DWC, with the designated number of stages, has to operate at specific L/V ratios, otherwise, the heat duty requirement of the DWC may increase from the minimum possible value (for e.g., see Reference 2 or Figure 13-70 in Reference 11). In the FTC DWC of Figure 3.3(a) (DWC version of the classic-FTC

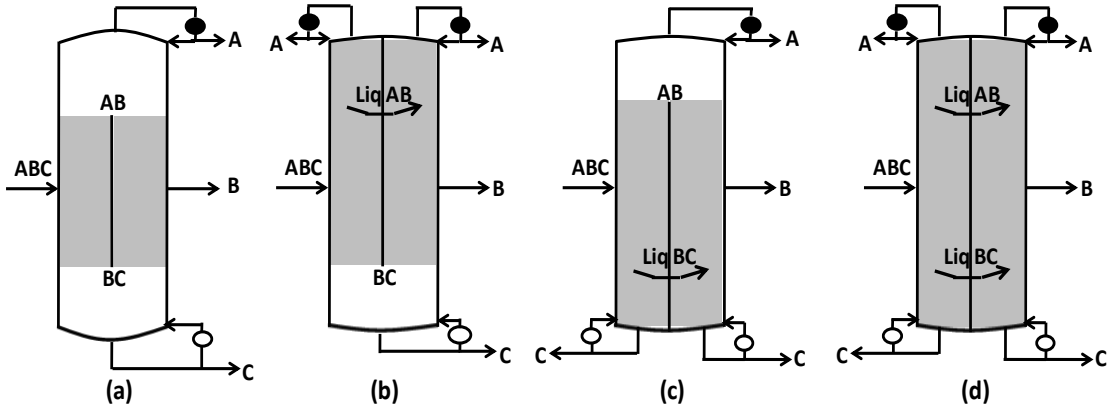

Figure 3.3 FTC DWCs of the FTC configurations in Figure 3.1.

configuration), for certain mixtures, optimal operation could be quite challenging.[5] This is because the vapor split at the bottom of the vertical partition cannot be conveniently controlled during operation by means that are external to the column. Thus, the vapor split at the bottom of the vertical partition can dynamically change depending upon the disturbances and mechanical resistances in each parallel zone of the FTC DWC. Further, the operational complication increases with the number of components because the number of vapor splits in the corresponding FTC DWC of the classic-FTC configuration (For e.g., see Figure 3.2(b)), also increases. Thus, in such an FTC DWC implementation of a classic-FTC configuration, there is a high probability of operation far away from optimality, and hence considerably reduced benefits.

Unlike the FTC DWC of Figure 3.3(a), the FTC DWCs of Figures 3.3(b)-(c) have a favorable operability feature associated with them. The vapor flow in all their sections can be regulated during operation by means that are external to the column.[5,9,10] This regulatory control is achieved by the use of valves/reboilers/condensers.[12] Thus, we expect such FTC DWCs to be easier to

operate compared to the FTC DWC of Figure 3.3(a). In general, not all FTC DWCs have the above feature.

The first objective of this chapter is to enumerate all the FTC DWCs that can be derived from the classic-FTC configuration by converting one or more thermal couplings to liquid-only transfers. For an *n*-component mixture, the classic-FTC configuration contains several thermal couplings and any combination of one or more of these thermal couplings can be converted to liquid-only transfers. We first enumerate all possible combinations of such conversions, and then draw their corresponding DWC versions to obtain all the FTC DWCs. This is achieved by first enumerating all the FTC configurations containing *n*-1 distillation columns, and then drawing their corresponding DWC versions. The FTC DWCs provide us with a complete set of DWCs for implementing FTC distillation that uses *n*-1 distillation columns. However, all the FTC DWCs are not amenable to the control of vapor flow in all the sections by means external to the column. As our second objective, we identify DWCs and operating modes from the set of FTC DWCs that are attractive from an operating perspective.

3.2 A complete set of *n*-component FTC DWCs

Our strategy for the generation of *n*-component FTC DWCs is depicted by the flowchart shown in Figure 3.4. We start with the classic-FTC configuration. In Step 2, we draw all equivalent FTC configurations by systematically converting each thermal coupling to liquid-only transfer. In Step 3, we draw the

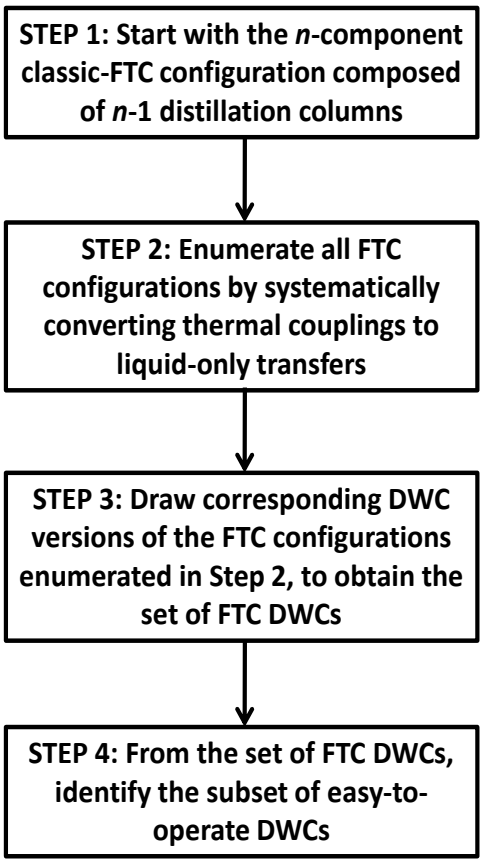

Figure 3.4 A flowchart of the steps followed to create easy-to-operate DWCs.

corresponding DWC version for each FTC configuration. Finally in Step 4, we identify from this set of FTC DWCs, the subset of DWCs in which, during operation, the vapor flow, in every section, can be regulated by means external to the column.

Following Agrawal's method of converting a thermal coupling to a liquid-only transfer,[4] we first calculate the number of *all* feasible FTC configurations. For this purpose, in Step 1, we use the *n*-component classic-FTC configuration with *n*-1 distillation columns (for e.g., shown in Figures 3.1(a) and 3.2(a) for three and four components) as the starting point. Then, in Step 2, we consider a

distillation column from the classic-FTC configuration, and count the number of possible unique submixtures/products at which each of the *top and bottom* ends can terminate, when the strategy to convert thermal coupling to liquid-only transfer has been adopted. Since the top and bottom terminations of a modified column are independent of each other, a multiplicative product of these two numbers gives the number of unique modifications that are possible for the distillation column under consideration, of the classic-FTC configuration. Finally, since the modifications to one column of the classic-FTC configuration is independent of the modifications to another, the multiplicative product of the number of possible unique modifications, evaluated for each and every distillation column within the *n*-component classic-FTC configuration, gives the total number of FTC configurations.

We illustrate Step 2 of the procedure by starting with the four-component classic-FTC configuration of Figure 3.2(a). In Figure 3.5, thermal coupling at *ABC* of the feed column is converted to liquid-only transfer by first extending it to *AB* (Figure 3.5(a)), and then all the way to product *A* (Figure 3.5(b)). In Figure 3.5(c), thermal coupling at *AB* of Column 2 is converted to liquid-only transfer. In Figures 3.5(d) and 3.5(e), after converting the thermal coupling at *AB* of Column 2 to liquid-only transfer, the thermal coupling at *ABC* of Column 1 is also converted to liquid-only transfer stream. Thus, *ABC* can be extended to *AB* (Figure 3.5(d)) or *A* (Figure 3.5(e)), giving us a total of three termination possibilities (*ABC, AB* or *A*) at the top end of the feed column. Similarly, the thermal coupling *AB* at the top of Column 2 in Figure 3.2(a) can be extended to *A*, giving us two termination

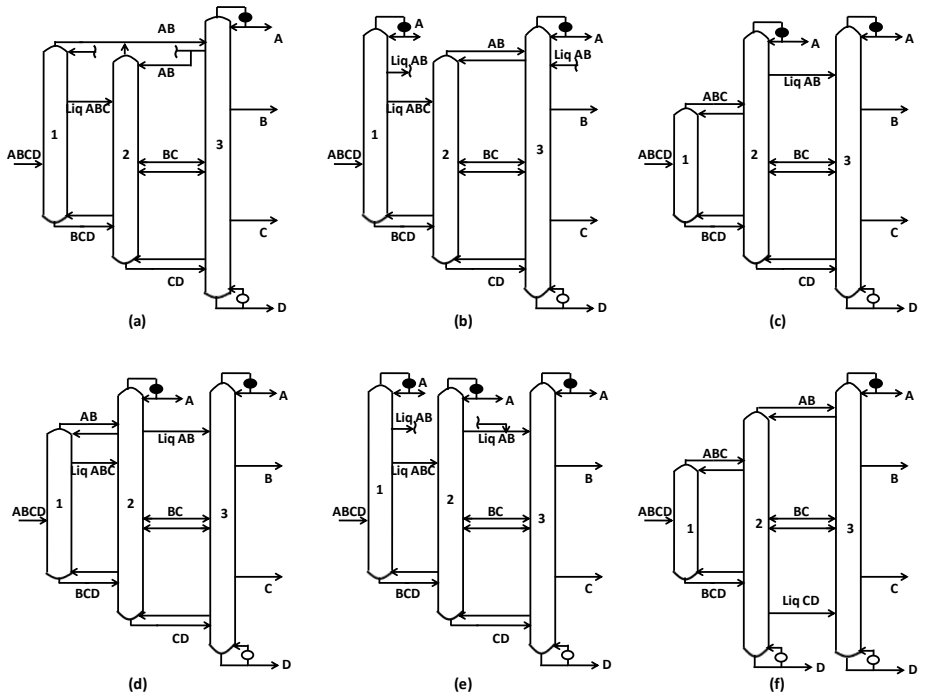

Figure 3.5 Examples of 4-component FTC configurations. (a)-(e) show possible ways of converting thermal coupling at the top of a column to liquid-only transfer. (f) converting thermal coupling at bottom end of column, to liquid-only transfer.

possibilities (*AB* or *A*). Figure 3.5(f) shows a FTC configuration where the bottom thermal coupling at *CD* of Column 2 has been converted to liquid-only transfer stream. Additional insights and interesting observations about these FTC configurations are further provided in Appendix B.

Before deriving an expression to calculate the total number of FTC configurations, we introduce a naming methodology to name the different distillation columns of the classic-FTC configuration. We name a distillation column based on its feeds and products. In the *n*-component classic-FTC configuration (shown in Figures 3.1(a), 3.2(a) for n=3, 4), for a distillation column which has all feeds comprising of k components ($n \geq k \geq 2$), each product stream

exiting the column has k-1 components. So, we name this the k:k-1th column of the classic-FTC configuration. For example, the distillation columns in the four-component classic-FTC configuration shown in Figure 3.2(a) are, sequentially, from the feed side to the product side, Column 4:3, Column 3:2 and Column 2:1.

Now, consider any c:(c-1)th distillation column of the n-component classic-FTC configuration. We first count the possible number of unique terminating top products of this distillation column after modification. Observe that every j-component submixture/product ($j \leq c$-1) containing the most volatile component is a candidate top product for the modified distillation column. In general, for the c:c-1 column, there is one (c-1)-component submixture containing the most volatile component, one (c-2)-component submixture containing the most volatile component, …, and one 1-component product containing the most volatile component. Thus, there are (c-1) candidate termination points at the top for Column c:c-1. By symmetry, this column also has (c-1) candidate termination points at the bottom for modification. Thus, combining the scenarios for the top and bottom of the column, a total of (c-1)^2 modifications are possible for Column c:c-1. Therefore, N_{FTC}, the total number of FTC configurations is given by

$$N_{FTC} = \{\prod_{c=3}^{c=n}(c-1)^2\} \text{ for } n \geq 3 \qquad (3.1)$$

The multiplicative product starts from c=3 and not c=2 because the Column 2:1 cannot be modified any further. This total number has been computed for up to ten components in the first column of Table 3.1. Finally, N_{FTC}, given by Equation 3.1, is also the number of FTC configurations that can be derived starting from a classic-FTC configuration with a satellite column.[13]

Table 3.1 Number of DWCs derived from Equations 3.1, 3.2, 3.3 and 3.4.

n	*Total # of DWCs for FTC distillation with n-2 dividing walls (N_{FTC}-Eq. 1)*	*Easy-to-operate DWCs with only liquid transfers at all intermediate submixtures ($N_{FTC\ T/B}$-Eq. 2)*	*Subset of $N_{FTC\ T/B}$ with no vapor splits (N_{Bot}-Eq. 3)*	*Subset of $N_{FTC\ T/B}$ with more than one easy-to-operate operating mode ($N_{FTC\ T/B\ subset}$-Eq. D1)*
3	4	3	2	
4	36	15	6	5
5	576	105	24	49
6	14,400	945	120	513
7	518,400	10,395	720	6,171
8	25,401,600	135,135	5,040	85,215
9	1,625,702,400	2,027,025	40,320	1,335,825
10	1.31682E+11	34,459,425	362,880	23,492,385

In Step 3, a DWC version of each FTC configuration can be drawn in a manner analogous to how DWCs in Figure 3.3 are drawn from FTC configurations in Figure 3.1. Figure 3.6 demonstrates the construction by drawing DWCs for the FTC configurations in Figure 3.5. We find that each three-column FTC configuration results in a new, unique FTC DWC. For an *n*-component mixture separation, the FTC DWCs given by N_{FTC} provide us a complete set of DWCs for implementing *n*-1 column FTC distillation. For those interested, the N_{FTC} FTC DWCs could have also been derived starting directly from the FTC DWC of the classic-FTC configuration, and a depiction of the counting method starting from this DWC for the four-component case is shown in Appendix C. Furthermore, observe that the FTC DWCs shown in Figure 3.6 are still challenging to operate as described in the context of the FTC DWC in Figure 3.3(a). Therefore, in the next Step 4, we identify from the set of FTC DWCs, DWCs which are amenable to better controllability of vapor splits.

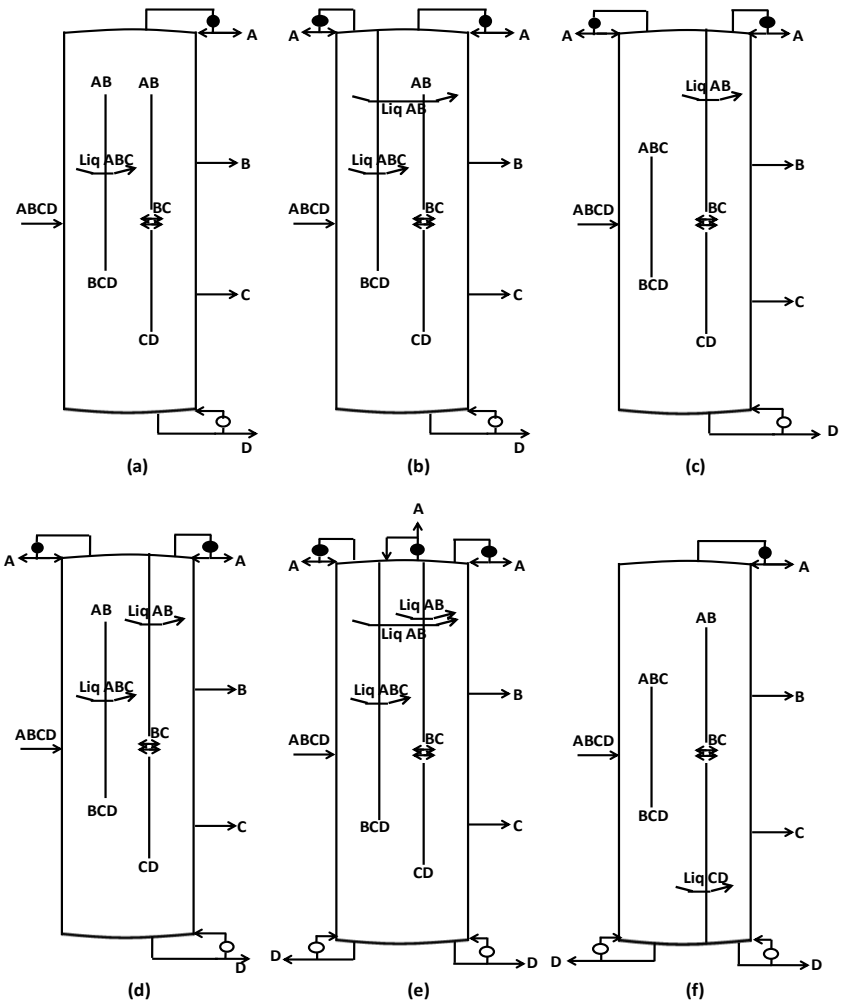

Figure 3.6 (a)-(f) FTC DWCs of the FTC configurations in Figure 3.5(a)-(f).

3.3 Identification of easy-to-operate DWCs

In this section, we identify the subclass of FTC DWCs in which the vapor flow in every section of the DWC can be regulated during operation by external means. For *convenience*, we term all the DWCs which have this controllability of vapor flow feature in every zone of the DWC, as *easy-to-operate* DWCs. For example, the FTC DWCs of Figures 3.3(b)-(d) are easy-to-operate. *Importantly, observe that the shaded zones in Figures 3.3(b)-(d) have the controllability of*

vapor flow feature associated with them because these zones are adjacent to a vertical partition that extends either to the top or bottom of the DWC. In other words, to identify the easy-to-operate DWCs from the set of all FTC DWCs, we look for DWCs which have each vertical partition extended at least to one end (top or bottom) of the DWC, and this is sufficient for each partitioned zone of such DWCs to be amenable for external vapor flow control. This comment can be translated to the FTC configurations to obtain such easy-to-operate DWC implementations. Each distillation column of such an FTC configuration must either have the most volatile component as its top product or the least volatile component as its bottom product. Note that the column that produces both the most volatile and least volatile components is admissible. The FTC configurations in Figures 3.1(b)-(d), for example, exhibit this property. In the following paragraphs, we introduce Step 4 to enumerate such configurations.

Again, consider Column *c*:*c*-1 of the *n*-component classic-FTC configuration. After modifying this column by converting thermal couplings to liquid-only transfer streams, either the top product of the column must be the most volatile component or the bottom product of the column must be the least volatile component. Assume that the top product of the column is the most volatile component, *A*. With the top product fixed, as explained earlier, there are *c*-1 candidate terminating bottom products. Likewise, when the bottom product of the column is fixed to be the least volatile component, there are *c*-1 candidate terminating top products. Thus, there are a total of (*c*-1)+(*c*-1)-1=(2*c*-3) modifications of the Column *c*:*c*-1 which have the earlier cited property. One is

subtracted from the sum (c-1)+(c-1) because the case when the column is modified to simultaneously have the most volatile component as the top product, and the least volatile component as the bottom product, is counted twice. Therefore,

$$N_{FTC\,T/B} = \prod_{c=3}^{c=n}(2c-3) = \frac{2^{n-1}}{\sqrt{\pi}}\Gamma\left(n-\frac{1}{2}\right) \text{ for } n \geq 3 \qquad (3.2)$$

These numbers have been computed for up to ten components in Table 3.1. *Here, we note that while the remaining FTC DWCs that were not counted in $N_{FTC\,T/B}$ are never easy-to-operate, those that have been counted are easy-to-operate only under certain conditions.* We now elaborate on these requirements.

FTC distillation contains transfer of *intermediate submixtures*, i.e., submixtures which don't contain both the most volatile and the least volatile components (like *BC* in Figure 3.2(a)). The mass transfer at these intermediate submixtures is generally denoted using bi-directional arrows, as shown for *BC* in Figure 3.2(a).[14] This is a representation of five possible distinct scenarios of liquid-vapor flow at the intermediate submixture, which are shown in Figure 3.7 (the net mass flow is from left to right). When the scenarios of Figure 3.7(a)-(d), each of which includes a vapor transfer, are implemented in an FTC DWC at the intermediate submixtures, they are generally implemented as shown in Figure 3.2(b) for the four-component case, with two vertical partitions, and a gap in between, which allows for the vapor transfer. However, when this mass transfer is implemented only as a liquid transfer (Figure 3.7(e)) in an FTC DWC, it is generally implemented as shown in Figure 3.8. (Note that this liquid transfer

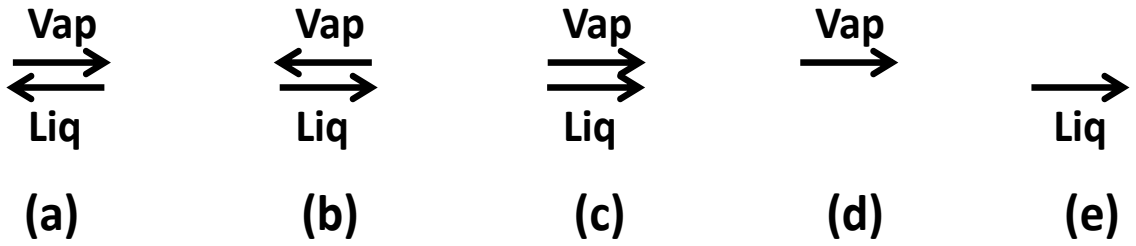

Figure 3.7 (a)-(e) Possible simplifications of the two bi-directional-arrow representation for mass transfer at any intermediate submixture. 'Vap' stands for vapor, and 'Liq' for liquid.

implementation is a direct substitution/constraint at an intermediate submixture for its mass transfer, and is *not* related to the strategy of converting a thermal coupling to liquid-only transfer, that was described earlier in the chapter and in Appendix A; that conversion strategy adds new sections, retains thermodynamic equivalence on conversion, and is applicable for thermal couplings, not for intermediate submixtures). In place of the earlier two vertical partitions, there is a single vertical partition running from *AB* to *CD*, and a portion of the liquid *BC* collected from one side of the wall is transferred to the other side. In this work, we regard Figures 3.2(b) and 3.8 as two distinct *operating-modes* of the same FTC DWC, one with an associated vapor transfer at *BC* allowing for any of the scenarios in Figures 3.7(a)-(d) to be implemented, and the other with no associated vapor transfer, but only a liquid transfer. Constraining the mass transfer at *BC* to only a liquid transfer (Figure 3.7(e)) could possibly rise the DWC's overall vapor duty as against when the mass transfer at *BC* is flexible to take any of the scenarios of Figures 3.7(a)-(d). However, note that the operating

mode of the FTC DWC with a vapor transfer at *BC* comes with the operational challenge of a vapor split internal to the DWC.

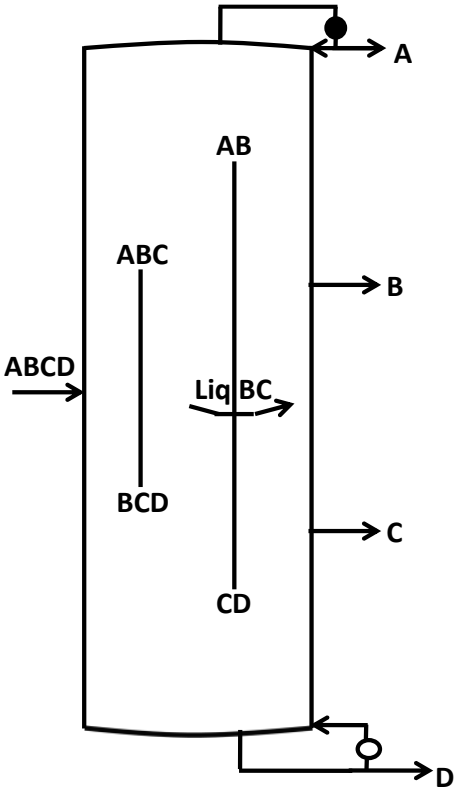

Figure 3.8 The operating mode of a four-component FTC DWC characterized by only liquid transfer at *BC*.

At this point, we make the distinction between a *dividing wall* and a *vertical partition*, as proposed by Christiansen et al.[15] While the operating-mode of Figure 3.2(b) has two dividing walls and three vertical partitions, the operating-mode of Figure 3.8 has two dividing walls and two vertical partitions. Thus, there are two distinct operating-modes for any FTC DWC associated with each intermediate submixture (with-gap and no-gap). So, if there are X intermediate submixtures produced, then there are 2^X distinct operating-modes for each FTC DWC. Note that, for the same FTC DWC, the operating-modes are not thermodynamically

equivalent to one another, and hence, may have different minimum heat duty requirements.

As the situation dictates, in order to distil a given mixture, any of the five scenarios of Figure 3.7 may be used at an intermediate submixture, and the appropriate operating-mode of an FTC DWC is used. Our goal here is ease of operation. In this context, we have observed that, while the presence of a vapor transfer/split at an intermediate submixture (allowing for Figures 3.7(a)-(d), implying with-gap between partitions) does not guarantee that all the $N_{FTC\ T/B}$ DWCs are easy-to-operate, using only a liquid transfer (Figure 3.7(e), implying no-gap between partitions) at all intermediate submixtures ensures all $N_{FTC\ T/B}$ DWCs remain easy-to-operate. As an example, we show all the fifteen easy-to-operate DWCs given by Equation 3.2 for the four-component case in Figure 3.9. In the figure, for convenience, the fifteen DWCs are arranged in the form of a 5×3 matrix such that, along any row, the parallel zone to which *ABCD* is fed, is the same, and along any column, the parallel zone from which the intermediate products *B* and *C* are withdrawn, is the same. Among the easy-to-operate $N_{FTC\ T/B}$ DWCs, that only transfer liquid for all the intermediate submixtures (implying no-gap between partitions), consider the DWCs in which every vertical partition is attached to the bottom of the DWC. For example, in the four-component case, see the six DWCs in Figures 3.9(a), (c), (d), (f), (g) and (i). Such DWCs have no vapor splits at the bottom of any vertical partition. So, the vapor flow control in each partitioned zone of these DWCs is achieved prior to entry of the vapor into the DWC. Using the logic that the number of candidate terminating

submixtures/product needs to be counted for each vertical partition at the top, the number of such DWCs can be derived to be (see Table 3.1 for numbers):

$$N_{Bot} = \prod_{c=3}^{c=n}(c-1) = (n-1)! \tag{3.3}$$

By symmetry, this is also the number of DWCs in which every vertical partition is attached to the top of the DWC.

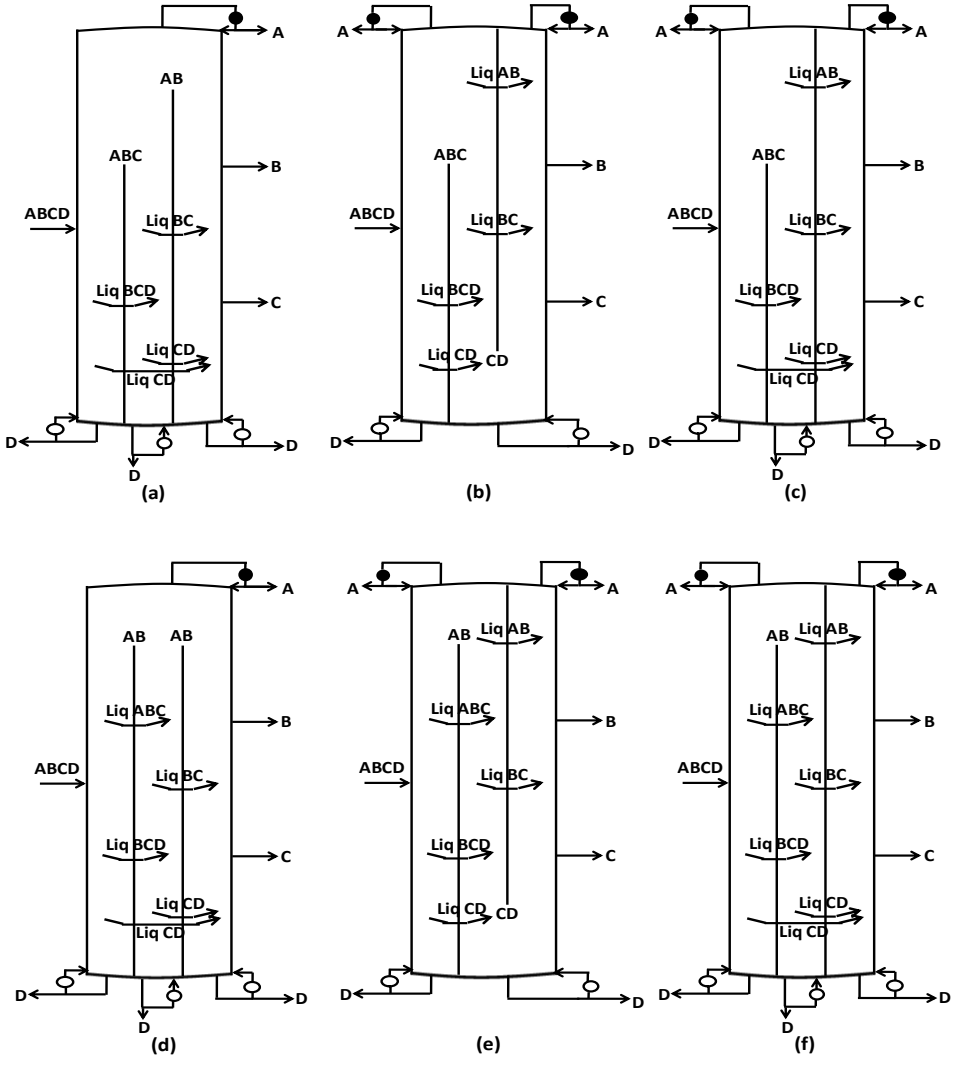

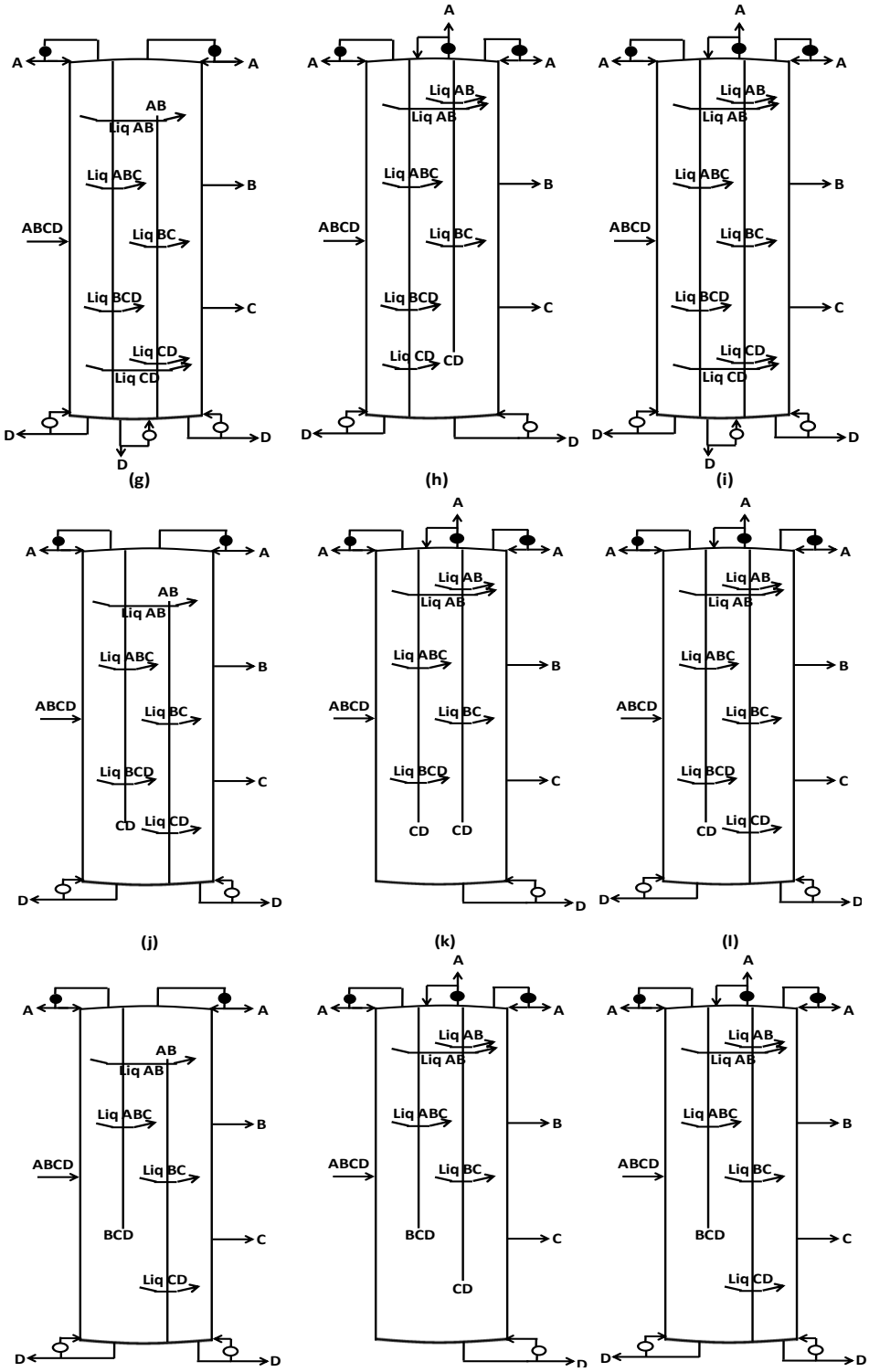

Figure 3.9 (a)-(o) All the four-component, unique $N_{FTC\ T/B}$ easy-to-operate FTC DWCs with only liquid transfers at all the intermediate submixtures.

3.4 Heat duty of easy-to-operate DWCs with only liquid transfers for intermediate submixtures

The transition split solution to the FTC configuration is known to always have the least vapor duty requirement.[16] While determining the transition split solution for minimum vapor duty, each intermediate submixture is free to take any of the scenarios shown in Figure 3.7. However, if any intermediate submixture is constrained in this system to take the scenario of Figure 3.7(e) (liquid transfer), there exists a possibility that the total vapor duty could rise. In this section, we attempt to understand the impact on overall vapor duty of using only the scenario of Figure 3.7(e) (liquid transfer) at all intermediate submixtures. Such an understanding is necessary because the N_{FTC} DWCs described in the previous section (including the ones in Figure 3.9) use the scenario of Figure 3.7(e) (liquid transfer) at all intermediate submixtures to retain the easy-to-operate feature. Here, we use the four-component system, which has only one intermediate submixture, *BC*, as a case study. We simulated the FTC DWC shown in Figure 3.8 in which the transfer at the intermediate submixture *BC* is all liquid (recall that the heat duty of this DWC is identical to any of the DWCs in Figure 3.9), and compared it with the FTC DWC shown in Figure 3.2(b), which additionally allows a vapor transfer at the intermediate submixture *BC*. We compared the overall minimum vapor requirement of these two operating-modes of the FTC DWC for 120 ideal saturated liquid feed mixtures[17]; given by 8 unique relative volatility combinations of easy/difficult separation between any two components (Table 3.2), along with 15 representative feed compositions (Table

Table 3.2 Different combinations of relative volatilities for a four-component mixture in the feed stream.

Separability (α)	α_{AB}	α_{BC}	α_{CD}
eee	2.5	2.5	2.5
eed	2.5	2.5	1.1
ede	2.5	1.1	2.5
edd	2.5	1.1	1.1
dee	1.1	2.5	2.5
ded	1.1	2.5	1.1
dde	1.1	1.1	2.5
ddd	1.1	1.1	1.1

3.3) that were chosen to span the composition space. For each of these ideal feed mixtures, the two operating-modes (Figures 3.2(b) and 3.8) are optimized (with a tolerance of 0.001 for convergence using BARON[18]) using the Global Minimization Algorithm[19], an approach that determines the globally minimum total vapor requirement of a distillation configuration based on the Underwood's equations[20], under assumptions of infinite trays and constant relative volatilities between components. The pure products are assumed to be withdrawn as saturated liquids.

The results of this comparative evaluation reveal that the operating-modes of Figures 3.2(b) and 3.8 have exactly equal overall minimum vapor requirements for 113 out of the 120 feed mixtures (≈94% of the mixtures)! Halvorsen et al.[21]

Table 3.3 Different combinations of feed compositions for a four-component mixture in the feed stream.

Feed composition (f)	A	B	C	D
Abcd	85	5	5	5
a**B**cd	5	85	5	5
ab**C**d	5	5	85	5
abc**D**	5	5	5	85
a**BCD**	5	31.7	31.7	31.7
Ab**CD**	31.7	5	31.7	31.7
ABc**D**	31.7	31.7	5	31.7
ABCd	31.7	31.7	31.7	5
ab**CD**	5	5	45	45
a**B**c**D**	5	45	5	45
a**BC**d	5	45	45	5
Abc**D**	45	5	5	45
Ab**C**d	45	5	45	5
ABcd	45	45	5	5
ABCD	25	25	25	25

also observed that for the distillation of a feed mixture of aromatic compounds under their consideration, only liquid transfer at the *BC* intermediate submixture was adequate in providing the lowest heat duty for the FTC configuration. Based on our findings and intuition, we expect using the liquid transfers (Figure 3.7(e)) at all the intermediate submixtures in a FTC configuration to have no adverse impact on heat duty for most feed conditions. In the case study, there is only one feed condition for which the heat duty penalty of not allowing the vapor transfer at the intermediate submixture *BC* (Figure 3.2(b) versus Figure 3.8) is more than 10%

(Table 3.4). Interestingly, from the table, the observed instances of different minimum heat duty requirement between the two operating-modes occur only

Table 3.4 Seven feed conditions for which the total minimum heat duty requirement with only liquid transfer (Figure 3.8) is higher than the corresponding operating-mode with an associated vapor transfer (Figure 3.2b).

Separability	Feed Composition	Vapor Duty Penalty (%)
eee	**AB**cd	6.3
eee	a**B**c**D**	8.2
eee	**ABcD**	9.0
eee	a**B**cd	0.8
ddd	**A**b**C**d	3.3
ddd	a**B**c**D**	17.6
ddd	a**B**cd	1.3

when the separability between all the consecutive component pairs is the same, i.e, when the separability is either ‘eee’ or ‘ddd’. For the cases listed in Table 3.4, we suggest exploring two liquid one-way transfer streams containing predominantly *B* and *C* components, but in different proportions, separated by a few stages[22], as shown in Figure 3.10. Such configurations may help reduce the penalty of using only liquid transfers at intermediate submixtures.

3.5 Easy-to-operate DWCs with vapor transfers at intermediate submixtures

In the previous sections, we studied FTC DWCs with only liquid transfers at all the intermediate submixtures (for e.g., see Figure 3.9). Alternatively, in the

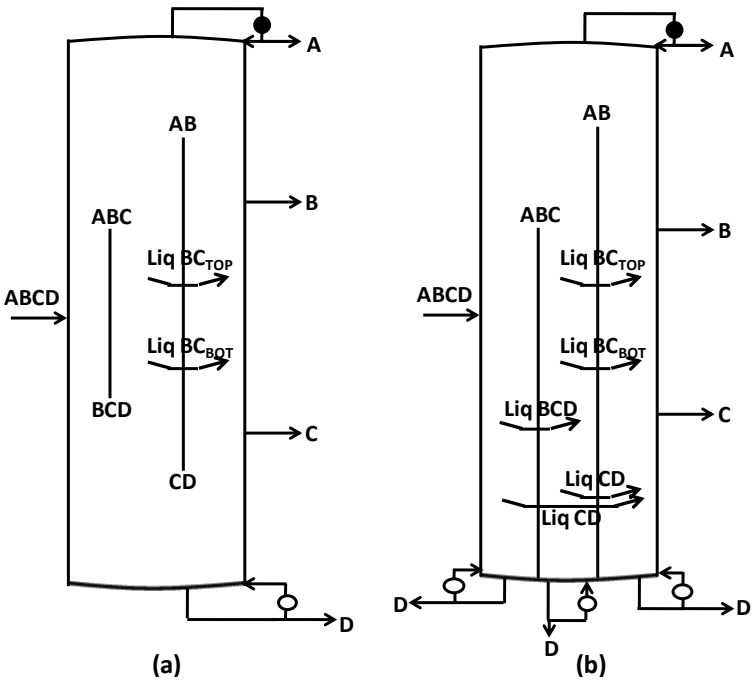

Figure 3.10 DWCs obtained from (a) the FTC DWC in Figure 3.8; (b) the FTC DWC in Figure 3.9(a); by replacing a single *BC* liquid transfer stream with two liquid transfer streams, BC_{TOP} and BC_{BOT}, separated by a few stages.

DWCs of Figure 3.9, the liquid transfer at the *BC* intermediate submixture may be replaced by a liquid-vapor flow arrangement of Figure 3.7(a)-(d). However, a question that remains unanswered is whether it is possible to allow for vapor transfers at the intermediate submixtures in the $N_{FTC\ T/B}$ FTC DWCs given by Equation 3.2, and still preserve the easy-to-operate feature. To answer this question, consider the FTC DWCs shown in the third column of the 5×3 matrix of Figure 3.9. In Figure 3.11, we show each of their second operating-mode with a vapor transfer/split at *BC*. Note that the vapor transfer/split is at an intermediate location of an earlier continuous partition. This vapor split can be controlled by the condensers and reboilers at *A* and *D* respectively. Thus, out of the $N_{FTC\ T/B}$ DWCs given by Equation 3.2, there is a subset of FTC DWCs which remain

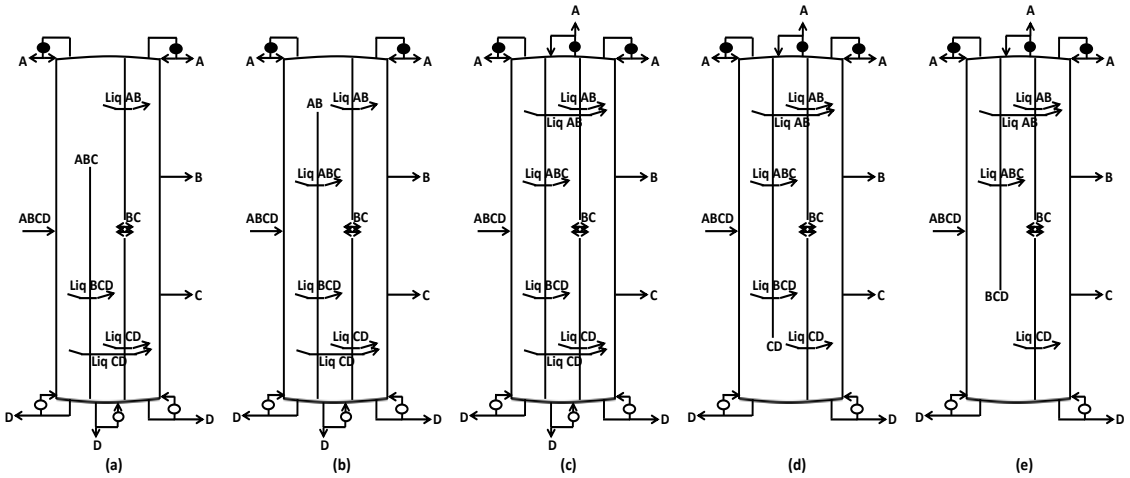

Figure 3.11 Easy-to-operate, alternate operating-mode of the FTC DWCs shown in (a) Figure 3.9c; (b) Figure 3.9f; (c) Figure 3.9i; (d) Figure 3.9l; (e) Figure 3.9o; with a vapor and liquid transfer at intermediate submixture *BC*.

easy-to-operate even though a vapor transfer is used at an intermediate submixture. Such DWCs have multiple operating-modes (with and without the vapor transfer, at least at one intermediate submixture) that are easy-to-operate. For the four-component case, we have identified all such DWCs in Figure 3.11 (or Figures 3.9(c),(f),(i),(l),(o)).

It is easy to identify the FTC DWCs which have more than one easy-to-operate operating-mode by closely examining the $N_{FTC\ T/B}$ DWCs (given by Equation 3.2) with liquid transfers at all the intermediate submixtures. In these FTC DWCs, only if a vertical partition runs continuously from the bottom to the top of the DWC, a vapor transfer can be introduced at *any one* intermediate submixture of this vertical partition, and still be easy-to-operate. This is how the DWCs in the third column of the 5×3 matrix in Figure 3.9 were easily selected for implementing a vapor split at *BC*. Therefore, among the $N_{FTC\ T/B}$ DWCs (given by

Equation 3.2) with liquid transfers at all the intermediate submixtures, we must look for DWCs which have at least one dividing wall running continuously from the bottom of the DWC to the top (except the first dividing wall which has no associated intermediate submixture). To calculate this number, we deduct from $N_{FTC\ T/B}$, the number of DWCs, $N_{No\ Top\ to\ Bottom}$, which have no dividing wall running continuously from the bottom of the DWC to the top (the first dividing wall is an exception as it has no associated intermediate submixture). To determine $N_{No\ Top\ to\ Bottom}$, translating the above information to the *n*-component FTC configuration: (i) Column *n*:*n*-1 must be modified to either have the top product as the most volatile component or the bottom product as the least volatile component. The number of such possible modifications for this column has already been observed in the chapter to be 2*n*-3 (ii) If the Column *c*:*c*-1 (3≤*c*≤ *n*-1) is modified to have the most volatile component as the top product, then the bottom product cannot be the least volatile component, and vice versa. So, if Column *c*:*c*-1 is modified to have the most volatile component as the top product, the number of possible terminating bottom products excluding the least volatile component is *c*-2, and likewise for the case when the column is modified to have the least volatile component as the bottom product. Thus, (*c*-2)+(*c*-2) = 2*c*-4 modifications are possible for Column *c*:*c*-1. Thus, $N_{No\ Top\ to\ Bottom} = (2n-3) * \prod_{c=3}^{c=n-1}(2c-4)$ for *n*≥4. So, $N_{FTC\ T/B\ subset}$, the subset of $N_{FTC\ T/B}$ DWCs which has more than one easy-to-operate operating mode is given by:

$$N_{FTC\ T/B\ Subset} = N_{FTC\ T/B} - N_{No\ Top\ to\ Bottom} \text{ for } n \geq 4$$

$$N_{FTC\ T/B\ Subset} = (2n-3)\{\prod_{c=3}^{c=n-1}(2c-3) - \prod_{c=3}^{c=n-1}(2c-4)\} \text{ for } n \geq 4 \quad (3.4)$$

The number of easy-to-operate operating modes itself for each DWC of the $N_{FTC\ T/B\ subset}$ DWCs depends on the number of dividing walls in the DWC amenable for introducing a vapor transfer at an intermediate submixture (i.e, the dividing walls attached simultaneously to the top and bottom of the DWC), and the number of intermediate submixtures associated with each of these dividing walls. When there are choices of intermediate submixtures at which a vapor split can be introduced, the choice of the submixture may be made to minimize the heat duty requirement.

3.6 Conclusions

FTC distillation has been known to be very useful for multicomponent separations due to its low heat duty requirements. Agrawal[4] suggested the conversion of a classical thermal coupling to a liquid-only transfer stream without compromising on the heat duty requirement. Employing such a strategy on the classic-FTC configuration leads to alternate FTC configurations. In this chapter, we have developed a simple method to enumerate the FTC configurations with *n*-1 distillation columns that can be derived by converting a thermal coupling to a liquid-only transfer or vice-versa.

For an *n*-component mixture, from the FTC configurations, we have enumerated all feasible corresponding DWCs. This allows us to specify for the first time the complete set of FTC DWCs with *n*-2 dividing walls for FTC distillation. It is observed from Table 3.1 that the number of DWCs representing

FTC distillation increases rapidly as the number of components in the feed mixture increases.

Interestingly, unlike the FTC DWC of the classic-FTC configuration, *some* of the other enumerated FTC DWCs allow the operator to regulate the vapor flow in every section of the DWC by means that are external to the column. We call such DWCs as easy-to-operate DWCs. We identified a first subset of easy-to-operate DWCs with only liquid transfers at all the intermediate submixtures, and another which also allows for vapor transfer/split at the intermediate submixtures. Further, we enumerated the two subsets using simple methods, and drew them explicitly for a four-component mixture. We expect that such DWCs can be operated at or near optimality, and hence the heat duty benefits of FTC distillation can be realized during operation. For this reason, we believe such DWCs will be very lucrative to consider for industrial implementation.

For FTC distillation, our DWCs offer a multitude of options for an industrial practitioner. These DWCs are attractive candidates to be evaluated for controllability and other design features. Our enumeration techniques will thus allow the practitioner to consider a comprehensive set of DWC implementations for a given application, thereby making it possible to achieve operational practicality without compromising on energy consumption.

References

1. Petlyuk FB, Platonov VM, Slavinskii DM. Thermodynamically Optimal Method for Separating Multicomponent Mixtures. Int Chem Eng. 1965;5(3):555-561.
2. Fidkowski ZT, Krolikowski L. Thermally coupled system of distillation columns: optimization procedure. AIChE J. 1986;32:537–546.
3. Triantafyllou C, Smith R. The design and optimisation of fully thermally coupled distillation columns. Trans Inst Chem Eng. 1992;70:118-132.
4. Agrawal R. Thermally Coupled Distillation with Reduced Number of Intercolumn Vapor Transfers. AIChE J. 2000;46(11):2198-2210.
5. Madenoor Ramapriya G, Tawarmalani M, Agrawal R. Thermal Coupling Links to Liquid-only Transfer Streams: A Path for New Dividing Wall Columns. AIChE J. 2014;60(8):2949-2961.
6. Wright RO. Fractionation Apparatus. 1949. US Patent 2,471,134.
7. Yildirim O, Kiss AA, Kenig EY. Dividing wall columns in chemical process industry: A review on current activities. Sep Pur Tech. 2011;80:403-417.
8. Dejanovic I, Matijasevic L, Olujic Z. Dividing wall column—A breakthrough towards sustainable distilling. Chem Eng Process. 2010;49:559-580.
9. Agrawal R, Madenoor Ramapriya G. Multicomponent Dividing Wall Columns. U.S. Patent Application 14/525205, 2014.
10. Madenoor Ramapriya G, Tawarmalani M, Agrawal R. New, useful dividing wall columns for sustainable distillation. Proceedings of the 10th International Conference on Distillation & Absorption 2014, Pg. 76-81.
11. Doherty MF, Fidkowski ZT, Malone MF, Taylor R. Distillation (chapter 13). In: Perry's Chemical Engineers Handbook, 8th Edition, Green DW (editor), McGraw-Hill, NY, 2007.
12. Agrawal R. Multicomponent Distillation Columns with Partitions and Multiple Reboilers and Condensers. Ind Eng Chem Res. 2001;40(20):4258-4266.
13. Agrawal R. Synthesis of Distillation Column Configurations for a Multicomponent Separation. Ind Eng Chem Res. 1996;35(4):1059-1071.
14. Sargent RWH, Gaminibandara K. Optimum Design of Plate Distillation Columns. In: Optimization in Action. Dixon LCW, Ed., New York: Academic Press, 1976:267-314.
15. Christiansen AC, Skogestad S, Lien K. Complex distillation arrangements: Extending the petlyuk ideas. Comp Chem Eng. 1997;21:S237–S242.

16. Fidkowski ZT, Agrawal R. Multicomponent thermally coupled systems of distillation columns at minimum reflux. AIChE J. 2001;47:2713-2724.

17. Giridhar AV, Agrawal R. Synthesis of Distillation Configurations: I. Characteristics of a Good Search Space. Comput Chem Eng. 2010;34(1):73-83.

18. Tawarmalani M, Sahinidis NV. A polyhedral branch-and-cut approach to global optimization. Math Program. 2005;103(2):225–249.

19. Nallasivam U, Shah VH, Shenvi AA, Tawarmalani M, Agrawal R. Global Optimization of Multicomponent Distillation Configurations: 1. Need for a Global Minimization Algorithm. AIChE J. 2013;59(3):971-981.

20. Underwood AJV. Fractional Distillation of Multicomponent Mixtures. Chem Eng Prog. 1948;44(8):603-614.

21. Halvorsen IJ, Dejanović I, Skogestad S, Olujić Z. Internal configurations for a multi-product dividing wall column. Chem Eng Res Des. 2013;91(10):1954–1965.

22. Madenoor Ramapriya G, Tawarmalani M, Agrawal R. Modified basic distillation configurations with intermediate sections for energy savings. AIChE J. 2014;60(3):1091-1097.

23. Agrawal R. More operable fully thermally coupled distribution column configurations for multicomponent distillation. Chem Eng Res Des. 1999;77:543–553.Fractionation Apparatus. 1949. US Patent 2,471,134.

CHAPTER 4. METHOD TO DRAW DIVIDING WALL COLUMNS OF ANY DISTILLATION FLOWSHEET

We present a very easy-to-follow procedure to draw all possible DWCs for any given distillation flowsheet. We identify that, to keep the partitioning inside a DWC simple, one common method of synthesizing DWCs cannot be used for all distillation configurations in the search space. So, two independent methods are presented, and the method of choice for a particular configuration to be redrawn as a DWC is dependent on the particular category the given distillation configuration belongs to. The methods comprise of an intuitive, comprehensive set of rules to draw a DWC from any given distillation flowsheet. Thus, a systematic procedure for synthesizing DWCs for multi-component distillation was achieved. It is noteworthy that, even for a ternary distillation, a number of attractive DWCs that had been missing from the literature have now been identified as a result of the method. Thus, a multitude of options are now available for distilling any given mixture in a DWC.

4.1 Introduction

A DWC was first conceived in 1949, and first implemented industrially in the 1980s.[1,2] Since these major developments in DWC technology, DWC has become a topic of keen interest for industry and academia alike, especially for ternary distillations, as the DWCs implemented so far have been mostly for three-component separations. In the prior literature on DWCs so far, three ternary DWCs have been conventionally considered and extensively studied[1,3-5] (apart from some novel ternary DWCs introduced in References 6 and 7). The three

DWCs are shown in Figure 4.1(a). The two-column thermally coupled configurations that are equivalent to these DWCs are shown below them in the same figure. In the figure, (i), (ii) and (iii) are respectively the FTC, side-rectifier (SR) and side-stripper (SS) systems.

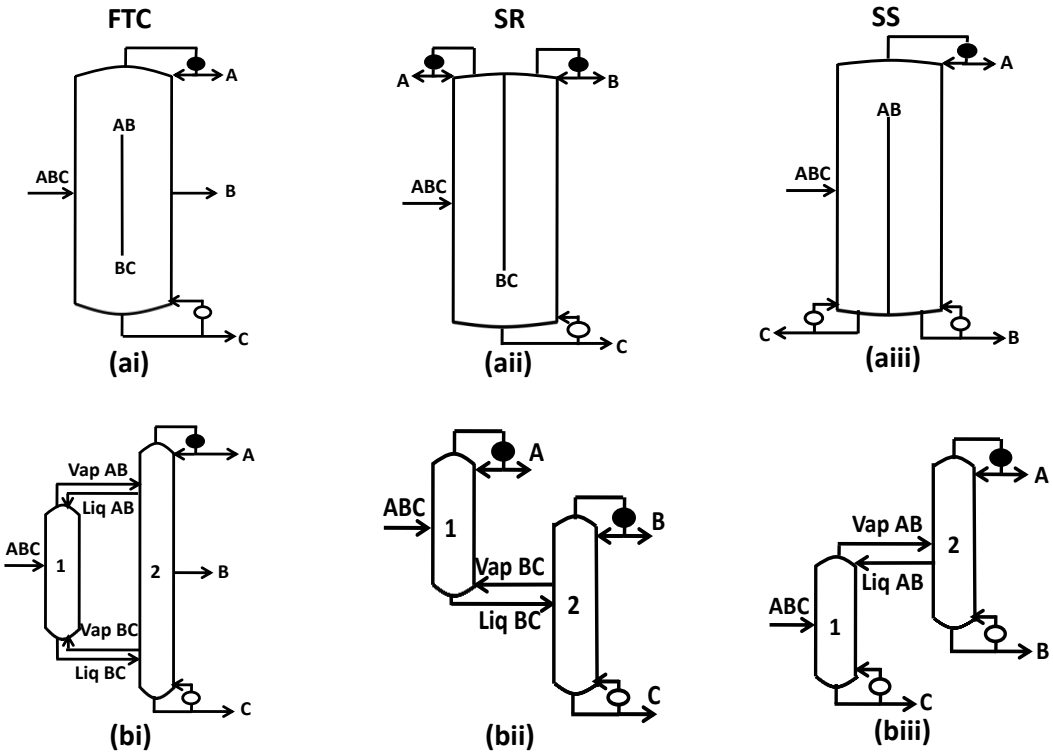

Figure 4.1 (i) FTC (ii) Side-rectifier (iii) Side-stripper

The advantage of the FTC system is that, theoretically, it always consumes the least heat duty for any ternary separation. However, some of the issues associated with the FTC system are as follows. The FTC DWC in Figure 4.1(a(i)) has a vapor split at the bottom of the partition that is unregulated during operation. So, the theoretically promising heat duty benefits may not be retrieved during operation if the DWC operates away from optimality. Another issue with

the FTC system is that it is not always the thermodynamically most efficient system for ternary separations.[8] This is because all the heating and cooling for the FTC system are provided respectively at the highest and lowest temperatures. On the other hand, the SR and SS DWCs, by virtue of fewer submixture stream transfers, additional heat exchanger and fewer sections, are generally easier to build and operate than the FTC DWC. Further, the vapor flow in each section of the SR and SS DWC can be regulated by external means. This can be achieved by using the condensers and reboilers at the top and bottom of the SR and SS DWCs.[9] In addition, not all of the heating/cooling utility needs to be at the highest/lowest possible temperature. However, the SR and SS DWCs will have a heat duty similar to that of the FTC for a fraction of the feed conditions, and for such feed conditions, SR/SS DWC would very likely be the choice for implementation over the FTC DWC. Refer to the work by Agrawal and Fidkowski[10] for such feed conditions.

In the context of the discussion in the previous paragraph, the question to ask is whether there are other DWCs like the SR/SS DWC, that are easier to build and operate, and have the same heat duty as the FTC DWC, at least for a few feed conditions. To answer this question, observe that each of the three thermally coupled ternary configurations in Figure 4.1(b) has a unique DWC corresponding to it. Since each thermally coupled configuration leads to a unique DWC, to identify new, potentially useful ternary DWCs, one must look for known thermally coupled configurations that have been overlooked for DWC implementation. We identify such ternary thermally coupled configurations in the

following lines. In Reference 10, Agrawal and Fidkowski, presented the ternary thermally coupled configurations shown in Figure 4.2. The arrangements in Figure 4.2(a) and 4.2 (b) respectively, will be referred to as the side-rectifier with liquid connection (SRL) and side-stripper with liquid connection (SSL). In their

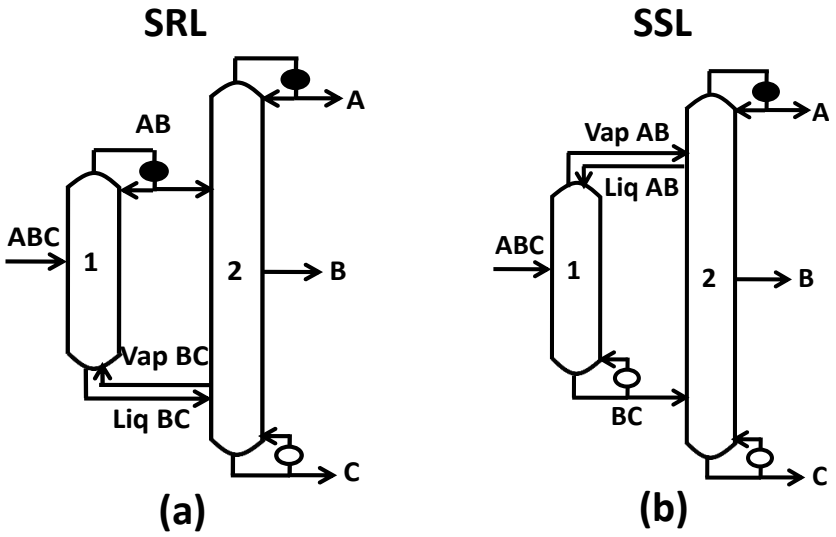

Figure 4.2 (a) Side-rectifier with Liquid Connection (b) Side-stripper with Liquid Connection.

work, Agrawal and Fidkowski extensively compared the minimum heat duty requirement of the FTC, SS, SR, SSL and SRL arrangements for various feed conditions. Based on their results, certain observations are presented in Figures 4.3(a) and 4.3(b) when the relative volatilities between the consecutive components are respectively $\{\alpha_{AB}, \alpha_{BC}\}$ = {2.5, 2.5} and {1.1, 1.1}. The shaded regions in these composition triangles signify the following. For example, in the

shaded region (drawn approximately) of the composition triangle of Figure 4.3(a), the best of SSL/SRL has a heat duty very similar to that of the FTC, but, using the best of SS/SR instead of the best of SSL/SRL incurs a heat duty penalty of 20-40%. So, to separate a feed condition that falls in the shaded regions of these composition triangles, while the SS/SR DWCs would not be useful, the DWC versions of the SSL/SRL would be very useful and preferred over the FTC DWC for the same reasons described in an earlier paragraph (1-equal/close to FTC

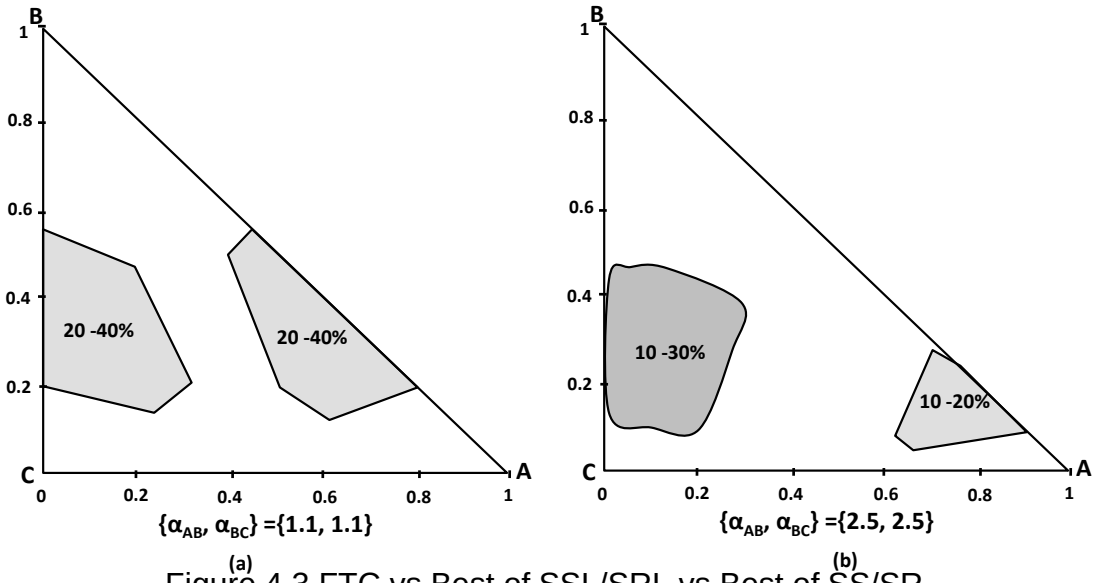

Figure 4.3 FTC vs Best of SSL/SRL vs Best of SS/SR.

heat duty for the highlighted feed conditions; 2-easier to build and operate because of fewer streams and additional heat exchanger; 3-controllability of vapor flow in each section of the DWC by external means during operation; 4-not all of the heating/cooling utility is needed to be at the highest/lowest temperature). The DWC versions of the SSL/SRL are presented here in Figure 4.4.

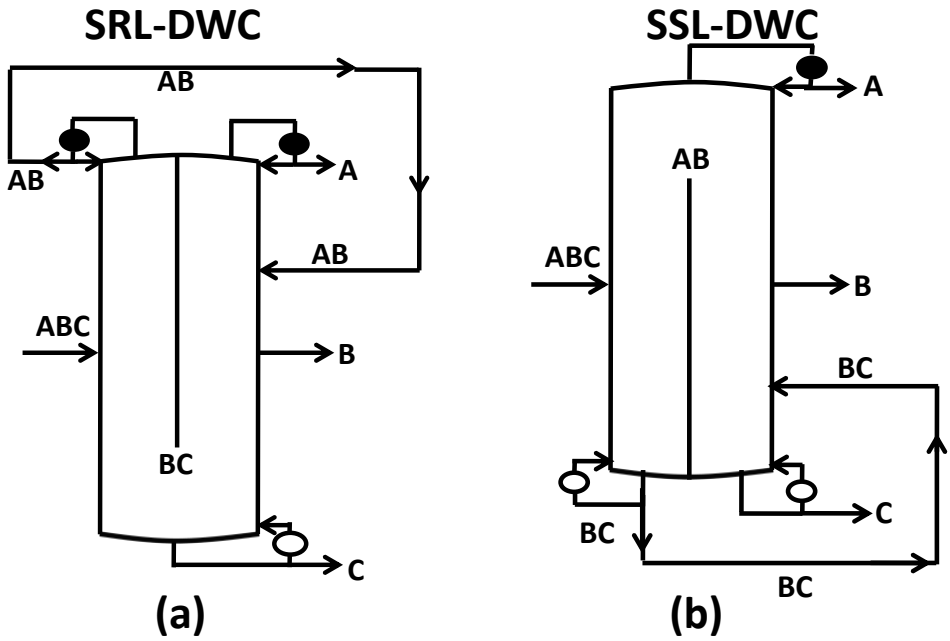

Figure 4.4 DWC version of (a) Figure 4.2(a); (b) Figure 4.2(b).

Even though the DWCs in Figure 4.1 have been known for quite some time, the SSL/SRL DWCs shown in Figure 4.4 have been surprisingly missing from literature. One reason for this is the identification of new DWCs has been through sporadic inventive activity, and not through systematic procedures. The goal of this work is to address the issue of a lack of a systematic procedure to synthesize DWCs so as not to miss potentially implementable solutions. We do this by first systematically synthesizing all possible distillation flowsheets, and then redrawing all DWCs that can be derived from each one of the distillation flowsheets.

4.2 Classes of distillation configurations

The preliminary step to synthesizing all DWCs is to first synthesize all the distillation configurations using a systematic method. We use the Shah & Agrawal[11] method to do this. At the end of the method, one has the complete distillation flowsheet, with/without heat exchangers at submixtures that are transferred between distillation columns. For the purposes of this chapter, during the synthesis, (though not required) we assume that, whenever a submixture is produced simultaneously from a stripping and rectifying section, it is produced as a liquid. Furthermore, every submixture that has a reboiler or condenser associated it is assumed to be in the liquid phase. Subsequent to the synthesis, the distillation configurations are divided into four categories. The four categories of distillation configurations are 'satellite-configurations'[12], 'satellite-like-configurations', 'heat-and-mass-integrated-configurations-at-product-end (HMCP)' and 'normal-configurations'. Such a categorization is needed for the following reason. Using a single method to redraw configurations belonging to each category as DWCs leads to complicated/unrealistic DWC partitioning. So, we designate two independent methods, one for normal-configurations, and another for the rest. In the following paragraph, we briefly explain each category mentioned above, so that configurations can be easily categorized during synthesis.

Satellite-configurations were introduced by Agrawal.[12] Such configurations comprise of columns between which there is a back-and-forth flow of net mass. An example satellite-configuration is shown in Figure 4.5(a). In this figure, the

back-and-forth net flow of mass is between distillation columns 2 and 3. Likewise, an example satellite-like-configuration is shown in Figure 4.5(b). While a satellite-like-configuration does not have a back and forth exchange of net mass between

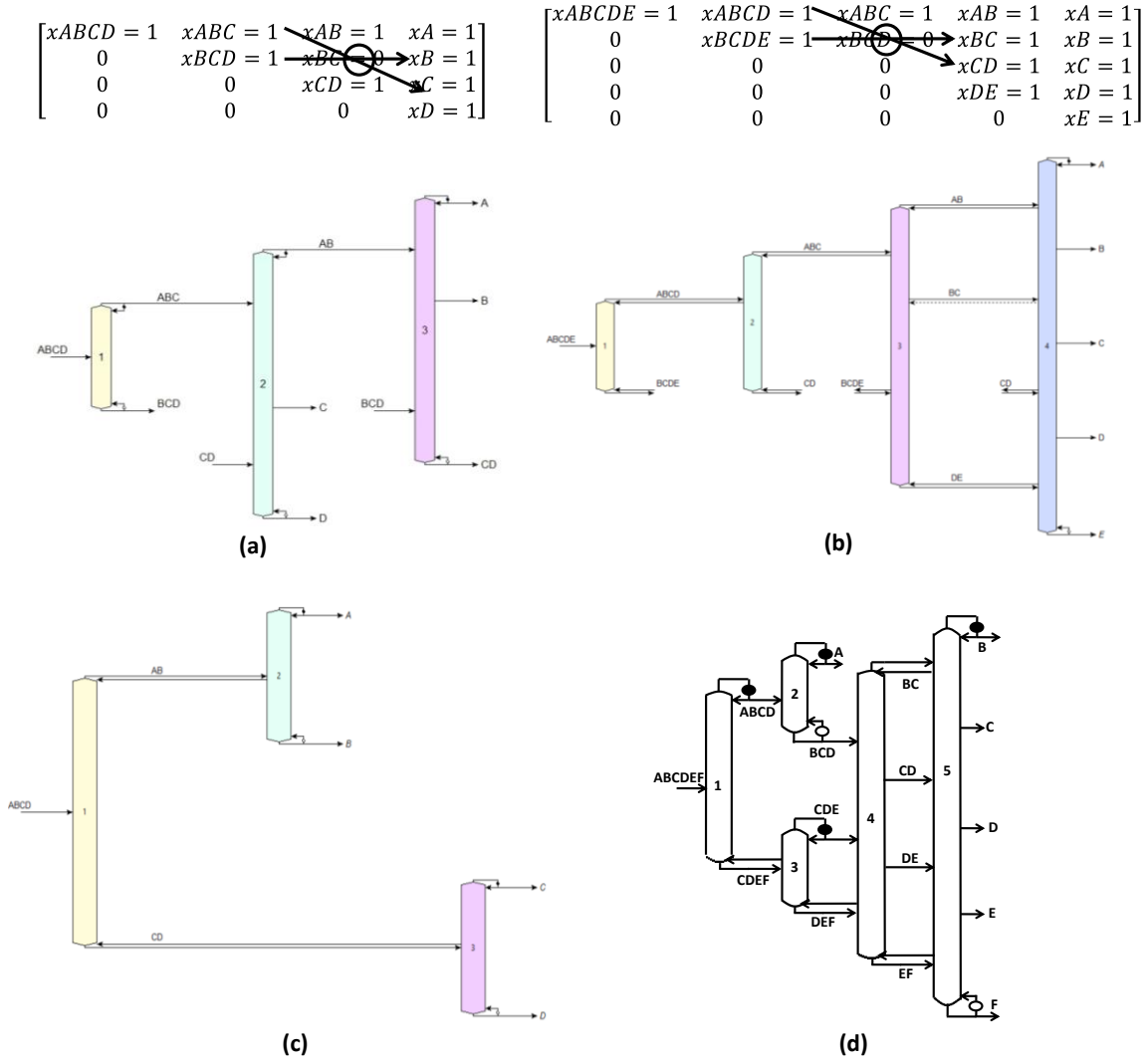

Figure 4.5 Example of (a) Satellite configuration; (b) satellite-like configuration; (c) HMCP configuration; (d) normal-configuration.

the same distillation columns, both satellite- and satellite-like-configurations can be flagged using a common property that both these categories share. In the matrix representation (Shah & Agrawal[11]) of these categories, there is a pair of

distinct submixture nodes from which the top product branch and the bottom product branch intersect each other at a ‘zero’. This can be observed even in the matrices placed above the configurations in Figures 4.5(a) and 4.5(b). On the other hand, HMCP configuration is one which has a condenser associated with a pure component that is heavier than a reboiler producing a pure component. In the example HMCP configuration shown in Figure 4.5(c), there is a condenser at *C* which is heavier than the reboiler at *B*. A configuration not belonging to any of the above mentioned categories is, for convenience, categorized as a normal-configuration. An example is shown in Figure 4.5(d).

A separate, common method for drawing the DWC versions of the configurations belonging to the categories: satellite/satellite-like/HMCP configurations is presented later in the chapter. For the normal-configurations, which comprise of the majority of the search space of configurations, a method for drawing their DWC versions is presented in the next section.

4.3 DWCs for normal-configurations

The methodology presented in this section is applicable for normal-configurations only. Before beginning the methodology, we introduce some preliminaries that will be used for the presentation of the methodology. In the normal-configurations, as shown in the example of Figure 4.5(d), the net mass flow is in a particular direction, from the main-feed column towards the pure-component product columns. For convenience, this direction of net mass flow

from the feed towards the pure-component product end will be treated as net mass flow from left to right. So, there is a sense of ‘left’/’right’ used for convenience in the discussions that follow, and ‘left’ relative to something implies towards the ‘feed-side’ of it. This sense of direction is also used for the next critical step, which is the numbering of the distillation columns of the synthesized configurations. The distillation columns are numbered in increasing order (starting from 1) from left to right, i.e., any numbering procedure is admissible as long as mass is fed from a lower-numbered column to a higher-numbered column. The numbering of columns, in certain cases can present ambiguities. For example, while the columns of the configuration in Figure 4.5(d) are numbered as shown, an alternate system where the column-numbers of columns 2 and 3 are interchanged, is also admissible. For now, this ambiguity is disregarded, and the steps to follow will neutralize the effect of this ambiguity.

A DWC of a distillation configuration with n-1 columns, to separate an n-component mixture, has n-2 vertical partitions. At this point, we make a distinction between a ‘vertical partition’ and the two outer ‘vertical boundaries’ of any DWC, the left vertical boundary (to which the feed is fed) and the right vertical boundary (from which pure component products are typically withdrawn). Likewise, a distinction is made between a ‘horizontal partition’ within a DWC, and the two ‘outer horizontal boundaries’ of any DWC: the top horizontal boundary and the bottom horizontal boundary. The intersection of the bottom horizontal boundary and the left vertical boundary, i.e., the bottom left corner of the DWC-boundary, for the sake of the development of the method, is assumed to be the

origin. Having introduced the preliminaries, we present the rules to be used for synthesizing DWCs from distillation configurations.

4.3.1 Steps for DWCs of completely thermally coupled configurations

A synthesized distillation configuration may or may not have heat exchangers at submixtures. Irrespective of the configuration at hand, in our procedure, we first draw the DWC of its completely thermally coupled version.[13] In the completely thermally coupled version of a distillation configuration, all submixtures at which heat exchangers appear are replaced by thermal couplings. As an example, the completely thermally coupled version of Figure 4.5(d) is shown in Figure 4.6. Here, we present the rules for drawing DWCs of such

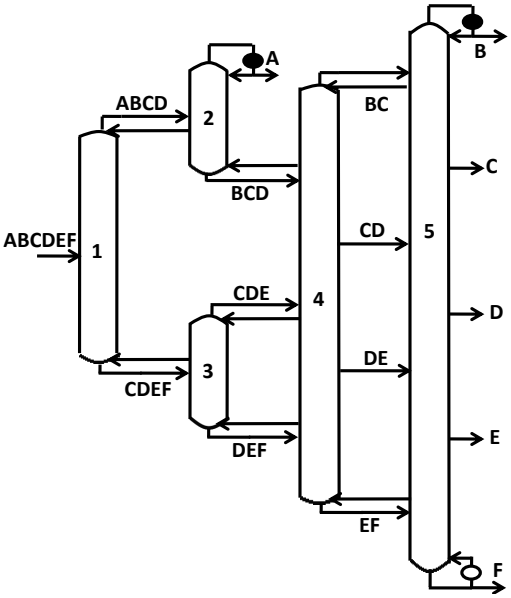

Figure 4.6 Completely thermally coupled version of Figure 4.5(d).

completely thermally configurations, and use the example of Figure 4.6 for demonstration. Once these DWCs are obtained, heat exchangers are then introduced at the desired submixtures at the next stage.

Step 1: The first objective is to identify the vertical coordinate/height of the DWC at which the various submixtures and pure component products are produced. Note that the pure component products which are produced at the condensers (e.g., *A* and *B* in Figure 4.6) and reboilers (e.g., *F* in Figure 4.6), are respectively, produced from the top and bottom of the column. So, fix the vertical coordinate/height of the respective pure component products at the top and bottom horizontal boundaries. The remaining submixtures and pure component products are produced at an intermediate height of the DWC. To fix these vertical coordinates, we assign numbers (denoting artificial volatilities) *n*, *n*-1, *n*-2, …, in alphabetical order to components *A, B*, *C*, …, and calculate an average volatility for each submixture produced in the concerned distillation configuration. For example, *AB* would have an artificial volatility of [(n)+(n-1)]/2, while ABC would have [(n)+(n-1)+(n-2)]/3. Using the fact that a more volatile submixture/product is produced above a less volatile submixture/product, the submixtures and products are accordingly ordered along the height of the DWC boundary. For the example of Figure 4.6, the ordering looks like what is shown in Figure 4.7(a).

Step 2: Each distillation column of the completely thermally coupled configuration has a corresponding vertical partition inside the DWC, except the last distillation column. So, there are (*n*-2) vertical partitions inside the DWC, corresponding to the first (*n*-2) distillation columns. For the purposes of the method, a vertical partition is a simple vertical line. The objective of this step is to fix the end points of the *n*-2 vertical lines. Start this step with j=1 inside the boundary of the DWC. Assume that the current iteration is the j^{th} iteration, i.e.,

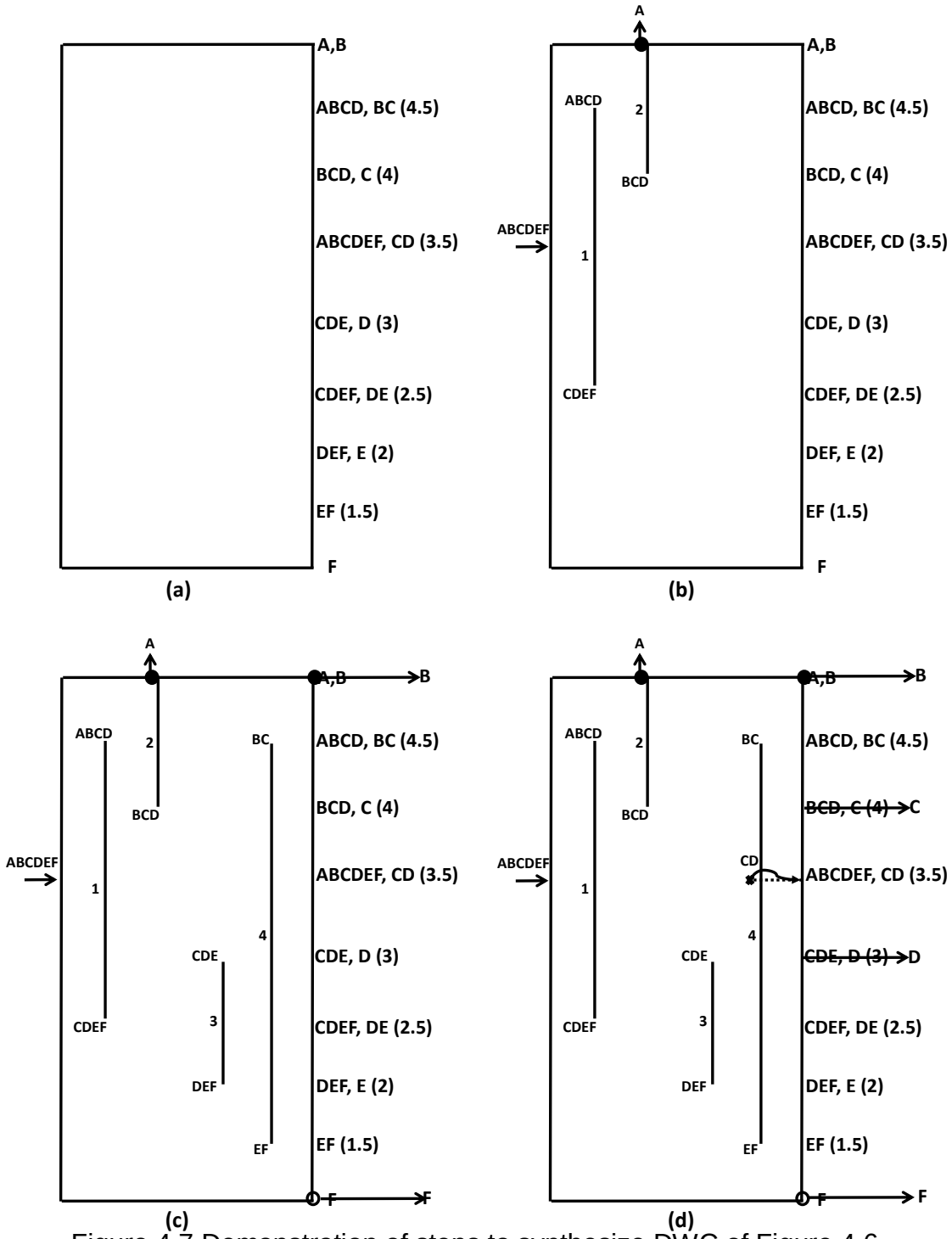

Figure 4.7 Demonstration of steps to synthesize DWC of Figure 4.6.

the vertical partition corresponding to the j^{th} distillation column is to be located, with the first (j-1) vertical partitions already located inside the DWC. The x-

coordinate of this partition is anything greater than that of the $(j-1)^{th}$ vertical partition, within the boundary of the DWC. To locate the vertical coordinates of the end points of the vertical partition, identify the top product and bottom product of the j^{th} distillation column. The vertical coordinates of the top and bottom products of the j^{th} distillation column have already been fixed in Step 1 alongside the DWC, and the j^{th} vertical partition inside the DWC under construction is between these vertical coordinates. This fixes the j^{th} vertical partition inside the DWC. Number the vertical partition as j. Name the submixtures/products at the top and bottom of the j^{th} vertical partition to the immediate left of the partition. If the j^{th} partition terminates at the top/bottom horizontal boundary of the DWC, implying pure component product withdrawal at the location, place a condenser/reboiler at the withdrawal location accordingly. Repeat this step with j=j+1, and stop when the vertical partition for j=*n*-2 has been drawn. As an example, the DWC for the example of Figure 4.6, after j=2 is shown in Figure 4.7(b).

Step 3: While the $(n-1)^{th}$ distillation column of the distillation configuration does not have a corresponding vertical partition in the DWC, the top and bottom products produced from this distillation column are withdrawn from the right vertical boundary of the DWC. The top and bottom products of the $(n-1)^{th}$ distillation column are always pure components with heat exchangers. So they are produced from the top and bottom of the DWC always. Continuing with the example of Figure 4.6, the DWC version of this configuration should appear as shown in Figure 4.7(c) by the end of this step.

Step 4: Note that, while Steps 2 and 3 locate the top and bottom products of every distillation column in the DWC, this step locates the side-draw streams that are produced from an intermediate height/location of a distillation column. Repeat this step for every column, starting at Column 1. Assume the iteration is at column j. Span the length of distillation column j to identify all the streams withdrawn from an intermediate location of this distillation column. These streams are withdrawn in the DWC from the immediate left of partition j at the vertical height fixed in Step 1. This locates the withdrawal location of the side-draw streams. Among the withdrawn streams, the feed locations of streams that are submixtures and not pure component products are to be fixed. To fix the feed location, we use what we call the 'stream-feed-rule'. This rule is explained in the following paragraph, and is used in the latter parts of the chapter for other scenarios as well.

Stream-feed rule: This rule is used to fix the feed-location of a stream, the withdrawal location of which is known. The feed location of such a stream is at the same vertical height as the withdrawal location. Since the direction of mass flow is from left to right, the stream withdrawn from the left of the partition is to be fed to the right of the partition. To fix this location in the zone that is to the immediate right of partition at the same vertical height, the right-most point within the zone is chosen. A construction is shown in Figure 4.8 to understand this rule in the general case.

Step 4 ends when it has been applied to the (n-1)th column. Note again that the $(n\text{-}1)^{th}$ column has no vertical partition corresponding to it, and its side-

draw streams are withdrawn in the DWC from the right vertical boundary. The DWC for Figure 4.6, at the end of Step 4 appears as shown in Figure 4.7(d). This completes the steps to be followed to draw a DWC for a given completely thermally coupled distillation configuration. The DWC obtained for Figure 4.6, without the intermediate constructions, is shown in Figure 4.9(a). At his point, it is worth mentioning that, once a DWC, as in Figure 4.9(a) is obtained, the vertical partitions can be moved horizontally to alter the area designated for each zone as long as the vertical partitions do not physically cross over each other. So, another version of the DWC shown in Figure 4.9(a), obtained by horizontally

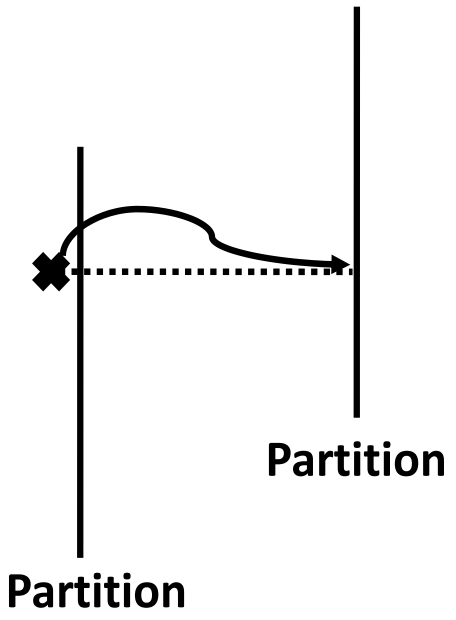

Figure 4.8 Demonstration of the 'stream-feed' rule.

moving the vertical partitions relative to each other is shown in Figure 4.9(b). Note that the vertical partitions in Figure 4.9(b) are re-numbered from left to right. While the DWC in Figure 4.9(a) is preferred when, in the configuration of Figure 4.6, the vapor flow leaving the top of Column 3 is greater than the vapor flow entering the bottom of Column 2, the DWC in Figure 4.9(b) is preferred when the vapor flow leaving the top of Column 3 is less than the vapor flow entering the bottom of Column 2. In fact, the DWC in Figure 4.9(b) would have directly followed from the four steps described in this section if the Columns 2 and 3 in Figure 4.6 were interchangeably numbered. In conclusion, once a DWC is drawn

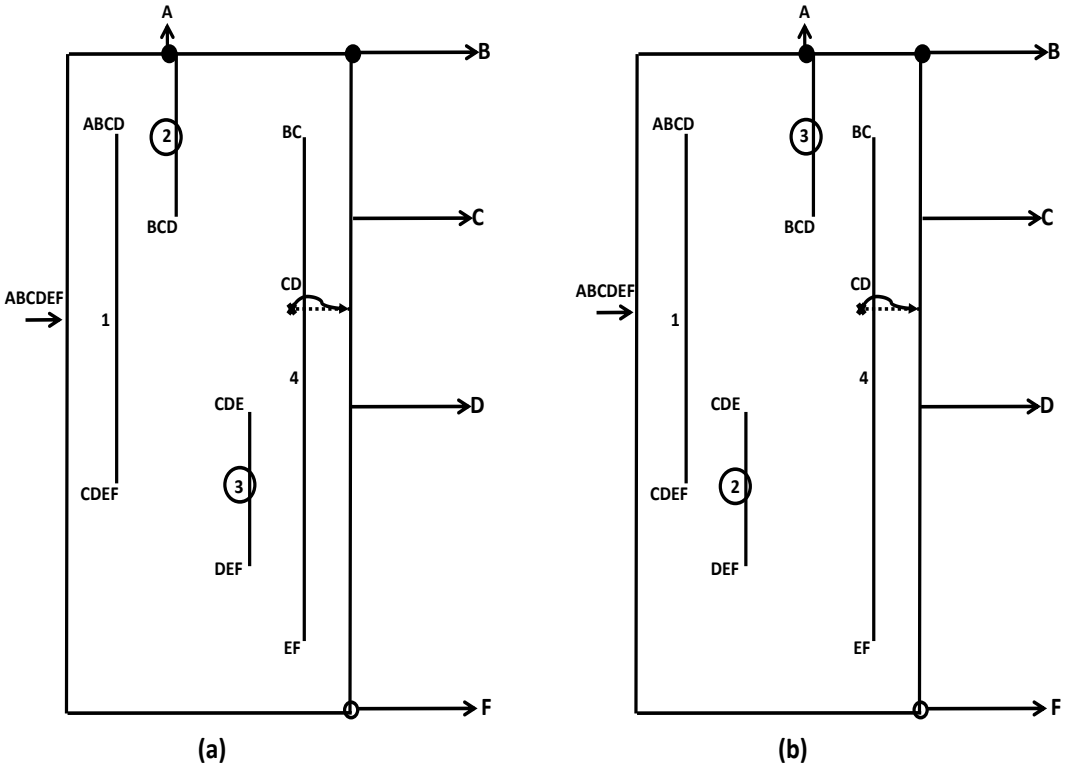

Figure 4.9 Both are DWCs of Figure 4.6. The difference between the two is the horizontal placement of the vertical partitions relative to each other.

following the steps in this section, the vertical partitions may be moved horizontally relative to each other according to the vapor flow and the cross-sectional area needed for the various distillation zones.

4.3.2 Steps for DWCs of partially thermally coupled configurations

Partially thermally coupled configurations are thermally coupled configurations which have heat exchangers at one or more submixtures. To obtain the DWC versions of such configurations, the DWC obtained in the previous section for completely thermally coupled distillation is used as the starting point, and heat exchangers are systematically introduced at the respective submixtures, as elucidated in the following steps.

Step 5: The objective of this step is to enumerate all the partially thermally coupled DWCs that could be derived from the completely thermally coupled DWC obtained at the end of Step 4. If one's goal is not enumeration, but simply redrawing a given partially thermally coupled distillation flowsheet, then the reader can disregard this step and directly go to Step 6. To do the enumeration, first, identify separately the submixtures produced at the top and bottom of each vertical partition (e.g., using Figure 4.9(a)) in order of increasing partition-number. There is a choice at each identified submixture whether to use a heat exchanger or not. If the total number of identified submixtures is w, then, there are 2^w unique combinations of the presence/absence of heat exchanger at the w submixtures, that lead to 2^w unique DWCs. Find all these combinations. One way of doing this systematically is through tabulation, a demonstration of which is shown in Table 4.1 for the example of Figure 4.9(a). The table is divided into two ordered sets of

submixtures, one set which is produced at the top of a vertical partition, and the other produced at the bottom. Assigning unique combinations of 0s and 1s (denoting absence or presence of heat exchanger) to the *w* submixtures enumerates all DWCs.

Table 4.1 Ordered set of submixtures with 0s and 1s assigned.

Top Of Partition			Bottom Of Partition			
ABCD	CDE	BC	CDEF	BCD	DEF	EF
0	0	0	0	0	0	0
0	0	0	0	0	0	1
0	0	0	0	0	1	0
⋮	⋮	⋮	⋮	⋮	⋮	⋮

Step 6: In this step, based on available information (directly from a synthesized distillation flowsheet as in Figure 4.5(d) or from a table like Table 4.1) about the submixtures where condensers are present, the condensers are introduced into the DWC one at a time. The condensers are introduced iteratively (and hence this step is repeated) in the same order as the identified ordered set of submixtures. Suppose a condenser is to be introduced at a submixture on top of the j^{th} vertical partition. To do this, introduce a horizontal partition, starting from the top of the j^{th} vertical partition, leftward, till you hit another vertical partition/boundary. This horizontal partition is always attached to the top of the j^{th} vertical partition. Place a condenser on the horizontal partition. The condenser serves as a source of liquid stream of the respective submixture. To locate the

feed-location of this stream, we use the stream-feed rule discussed in the previous section. Consider the example of synthesizing the DWC version of Figure 4.5(d) using the DWC of Figure 4.9(a) as an intermediary. A demonstration of the procedure discussed in Step 6 so far, applied to the first vertical partition, is shown in Figure 4.10(a).

Step 6 continues as follows. Check whether the introduced horizontal partition attached to the top of the j^{th} partition is connected at the other end to the left vertical boundary or to a vertical partition that is attached to the top of the DWC. If this is not so, repeat Step 6 for the next submixture in the ordered set. However, if this true, then, the horizontal partition and the condenser, along with the j^{th} vertical partition is extended all the way to the top of the DWC. Note that the feed location of the liquid stream from the condenser does not change. Applying this rule to the DWC of Figure 4.10(a) results in the DWC of Figure 4.10(b). Note that this extension of the j^{th} vertical partition along with its horizontal partition to the top of the DWC is not always straightforward. For example, from the DWC of Figure 4.10(b), the next step towards obtaining the DWC of Figure 4.5(d) is to introduce a condenser at submixture *CDE*. In Figure 4.10(b), with the introduction of the horizontal partition and the condenser on top of vertical partition 3, the introduced horizontal partition connects the top of vertical partition 3 with vertical partition 1 at the other end. Since vertical partition 1 is attached to the top of the DWC, the introduced horizontal partition, along with the third vertical partition should be extended to the top of the DWC. However, the existence of vertical partition 2 obstructs the upward extension of the horizontal

partition along with vertical partition 3. This is overcome by displacing the

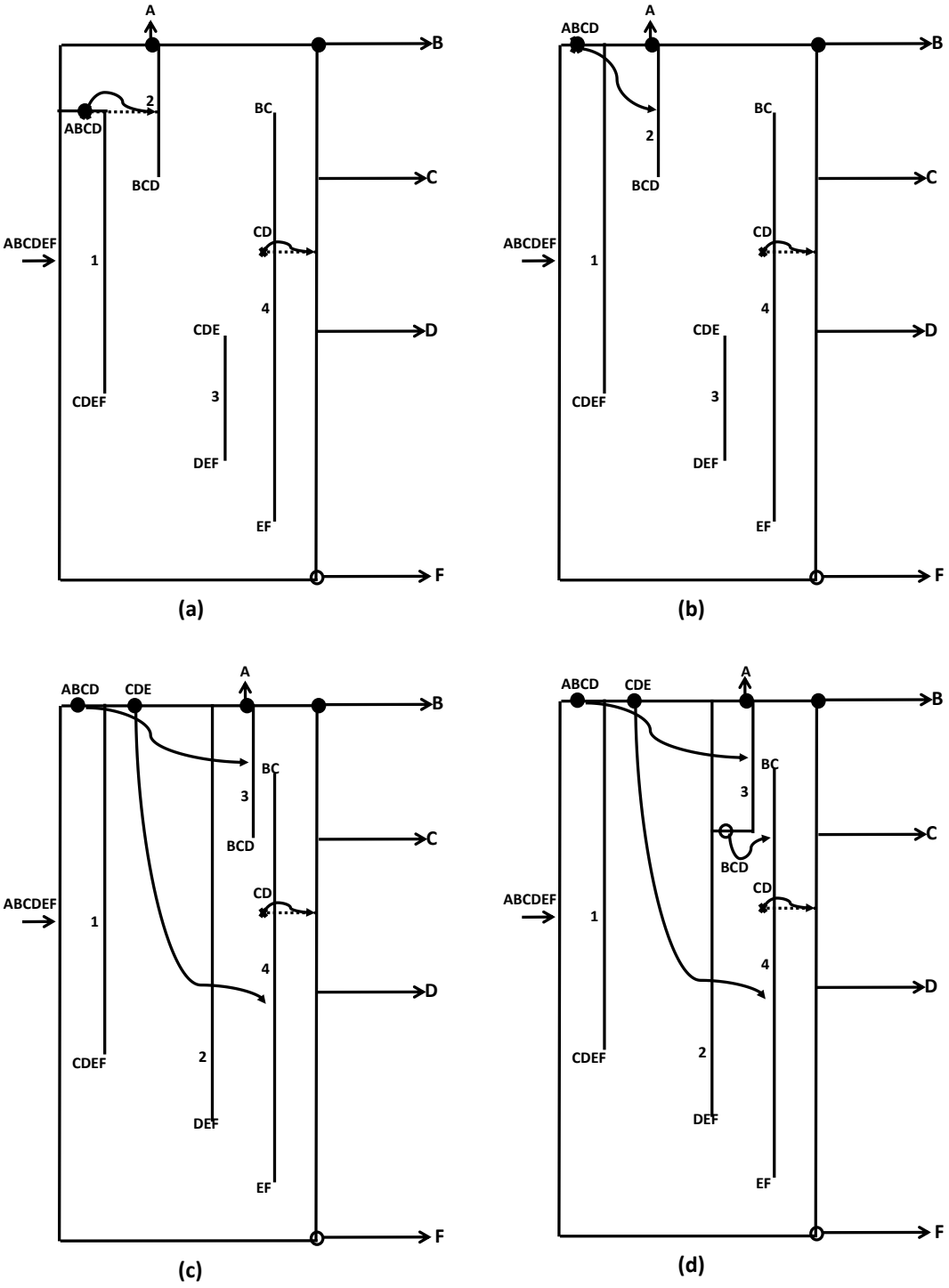

Figure 4.10 Intermediate steps to draw the DWC of Figure 4.5(d) starting from the DWC of Figure 4.9(a).

obstructing vertical partition 2 to the right to make way for the upward extension of the horizontal partition along with its vertical partition 3. Since this step has resulted in a change in the positioning of the vertical partitions along the horizontal coordinate relative to the other, the vertical partitions are renumbered. At the end of this step, the DWC in Figure 4.10(b) is converted to the one in Figure 4.10(c).

Step 7: This step is the exact same as Step 6, but accordingly modified to introduce a reboiler at the respective submixtures. The Step 6 had everything to do with up, upwards and top, while this step has to do with down, downwards and bottom. By the end of this step, the DWC in Figure 4.10(c) is converted to the one in Figure 4.10(d), which is the DWC version of the configuration in Figure 4.5(d). This completes the steps to draw DWCs of partially thermally coupled configurations.

4.4 DWCs for satellite, satellite-like and HMCP Configurations

In this section, we present a general method to draw DWCs of the satellite, satellite-like, and HMCP configurations. To start with, the columns of any given configuration are numbered arbitrarily from 1 to (*n*-1). Because the direction of mass flow between the columns in a configuration of these categories is complicated, the method presents the DWCs for these configurations in three-dimensions. We first demonstrate how to draw the DWC for the completely thermally coupled version of the given configuration.

Step 1: The first step is the same as Step 1 used for normal-configurations. This step assigns the vertical coordinate/height at which each submixture/pure component-product is produced from the DWC.

Step 2: The objective of this step is to list all the thermal-coupling-interactions between distillation columns, which is elaborated below. Note that a thermal coupling at the bottom of a column splits the vapor flow between two distillation columns. Likewise, a thermal coupling at the top of a distillation column feeds the vapor flow into another column. To achieve this in a DWC, wherever a thermal coupling exists, a vertical partition should begin/terminate. So, each submixture associated with a thermal coupling dictates/fixes the vertical end point of some vertical partition. Now, we look at which vertical partition does a given thermal coupling begin/terminate. To answer this, if the thermal coupling is between Columns ‘j’ and ‘k’, then, this thermal coupling begins/terminates the vertical partition separating the zones in the DWC that represent the Column j-k pair (irrespective of whether Column ‘j’ feeds into Column ‘k’ or vice-versa). So, in this step, information for each thermal coupling (or more specifically, each submixture that is a thermal coupling) is collected about the column-pair it connects, and whether it is at the top or bottom of a distillation column. For the example of Figure 4.5(b), this information is collected in Table 4.2. A further interpretation of this table is provided in subsequent steps as the methodology develops.

Step 3: In this step we determine the top view of the DWC, i.e., project the DWC onto a cross-section. Note that the DWC has a zone corresponding to each distillation column. Delineate the zones for each column in the projected cross-section (refer to Figure 4.11 for the example of Figure 4.5(b)). The delineation is constrained by the following. Observe that the column-pairs identified in Table 4.2 have vapor interactions between them through a thermal coupling, and hence, in the DWC, the corresponding zone-pairs must be next to each other to allow for the vapor-interaction. Any delineation of zones that satisfies the above constraint is admissible. Furthermore, all side-draws between the respective zones are also marked on this cross-section (e.g., *BC* in Figure 4.11).

Table 4.2 Column-pair connections.

	Top	Bottom
1-2	ABCD	-
1-3	-	BCDE
2-3	ABC	-
2-4	-	CD
3-4	AB	DE

Step 4: In this step and the next, the boundaries of the vertical partitions are fixed. To do this, the table obtained from Step 2 (e.g., Table 4.2) is to be

interpreted in the following way (the interpretation follows directly from the explanation in Step 2). The left-most column indicates a vertical partition between

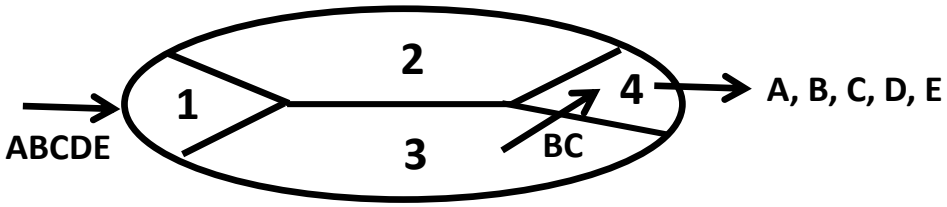

Figure 4.11 Delineated zones for the example of Figure 4.5(b) derived from the information in Table 4.2.

the respective zone-pairs. The entries alongside a vertical partition in the table indicate the submixtures where the vertical partition terminates at the top and bottom. If an entry is missing, then, the respective (top/bottom) vertical end point is not known, and will be fixed in the next step. As an example, from Table 4.2, the vertical end points of the vertical partition separating zones 3 and 4 are at submixtures *AB* and *DE* respectively. Using the vertical coordinates of the submixtures fixed in Step 1, the delineations from Step 3, and the tabular interpretation in this step, fix the boundaries of the vertical partitions in the DWC. The vertical partitions for which both the vertical end points are known, complete the partition. For the example under consideration, the progress by the end of this step is depicted in Figure 4.12.

Step 5: In this step, the vertical end points of the vertical partitions unfixed from the table obtained in Step 2 are fixed. The unfixed ends of the vertical partitions take the lowest/highest plane/cross-section, i.e., the most extreme plane/cross-section at which all the vertical partitions in that cross-section, along

with the circumference of the DWC, form a closed figure in that plane/cross-

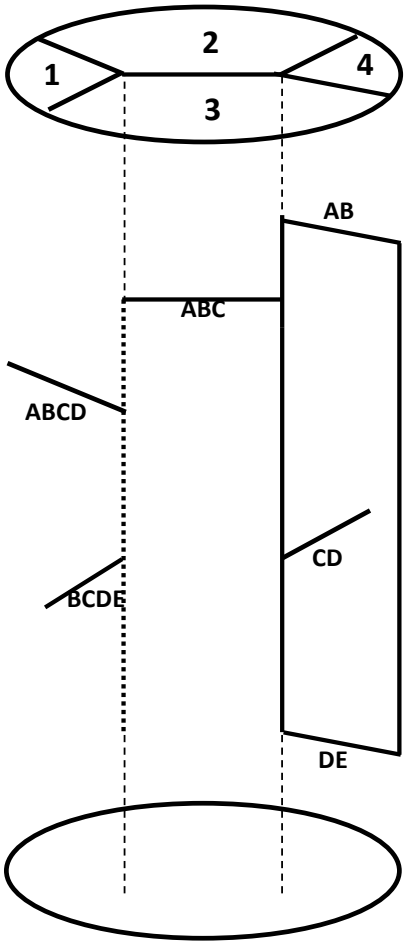

Figure 4.12 Incomplete DWC of the completely thermally coupled version of Figure 4.5(b) after the intermediate Step 4.

section. For example, in the Figure 4.12, the lowest plane/cross-section the vertical partition1-2 and vertical partition 2-3 can take is the bottom of the DWC. However, if these vertical partitions are extended all the way to the bottom of the DWC, in the bottom plane of the DWC, the vertical partitions 1-2 and 2-3, along with the circumference of the DWC do not form a closed planar figure, but, instead form what is shown in Figure 4.13(a). The lowest plane at which the

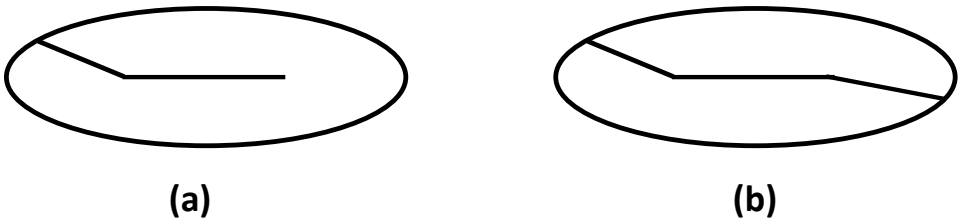

Figure 4.13 Cross section of DWC when vertical partitions 1-2 and 2-3 are extended to (a) bottom of the DWC (b) the vertical height of submixture *DE*.

bottom end points of vertical partitions 1-2 and 2-3, along with the circumference of the DWC, can form a closed planar figure is at the vertical height of submixture *DE* because it is at this height that vertical partition 3-4 also has its bottom end point. In this plane the vertical partitions 1-2, 2-3 and 3-4 along with the circumference of the DWC form a closed figure as shown in Figure 4.13(b). So, this fixes the bottom end points of vertical partitions 1-2 and 2-3. In this manner, the vertical end points of all the vertical partitions are fixed.

Step 6: In this step, the fixed vertical partitions obtained from Step 5 are superimposed with the delineated top view obtained from Step 3. This is the last step and gives the final DWC. The DWC of Figure 4.5(b) is shown in Figure 4.14.

The same method is used for DWCs of satellite and HMCP configurations as well. This method could be used for drawing DWCs of normal-configurations as well. However, using this method for normal-configurations leads to very complicated partitioning in the resulting DWC as opposed to what could be obtained using the procedure elucidated in the prior sections.

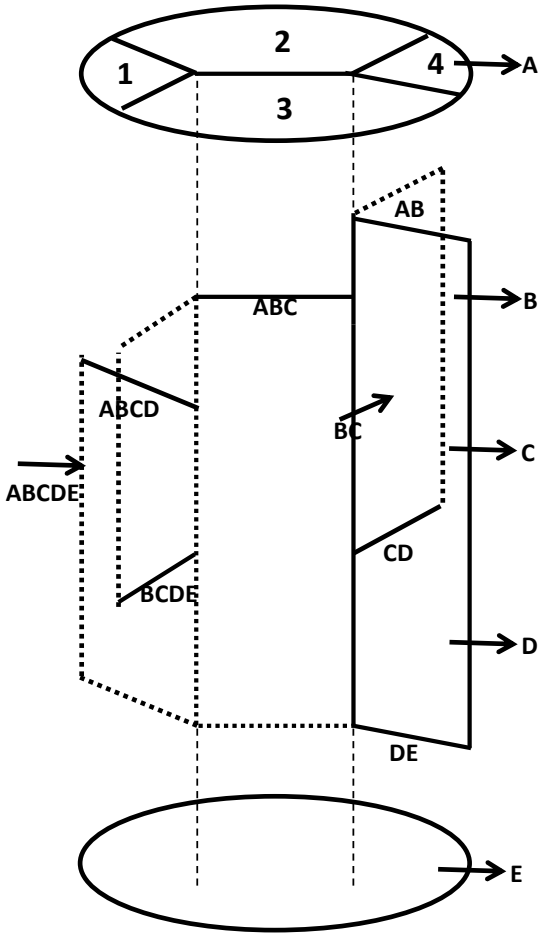

Figure 4.14 DWC of Figure 4.5(b).

4.5 Conclusions

For distilling an *n*-component mixture, various methods have been presented in the literature to synthesize all possible distillation configurations. However, no such systematic method exists for synthesizing all possible DWCs for *n*-component distillation. Because of this reason, the DWCs that have been implemented industrially have been synthesized from experience or sporadic inventive activity. We showed that, as a result of this haphazard procedure,

potentially very useful DWCs have been missing from the literature. In this work we addressed this need of a systematic DWC-synthesizing procedure.

Here, we presented an easy-to-use method to draw all possible DWCs corresponding to all possible distillation flowsheets. Precursory to the presented method, we first obtained all possible distillation flowsheets from the Shah and Agrawal[11] method. Then, simple rules were presented to first draw the DWCs of only the completely thermally coupled configurations. The DWCs obtained from the completely thermally coupled configurations were used as a starting point to systematically introduce heat exchangers (reboiler/condenser) at the various thermally coupled submixtures.

We identified that the presented method to draw DWCs of conventional configurations cannot be used for complicated configurations like the satellite-configurations. For such configurations, we presented an alternative method, which redrew the configuration as a DWC in 3-dimensions. As a result of this work, any energy-efficient distillation flowsheet can be implemented as a DWC. This presents an industrial practitioner with a plethora of options to choose from for any given application. The presented method can be extended further to obtain thermodynamically equivalent versions of the drawn DWCs by converting thermal couplings to liquid-only transfer streams (discussed in the prior chapters), which will further lead to hitherto unknown DWCs.

References

1. Wright RO. Fractionation Apparatus. 1949. US Patent 2,471,134.
2. Kaibel G. Distillation Columns with Vertical Partitions. Chem Eng Tech. 1987;10(1):92-98.
3. Monro DA. Fractionating apparatus and method of fractionation. 1938. US Patent 2,134,882.
4. Ognisty TP, Manley, DB. Partitioned distillation column. 1998. US Patent 5,709,780.
5. Dejanovic I, Matijasevic L, Olujic Z. Dividing wall column—A breakthrough towards sustainable distilling. Chem Eng Process. 2010;49:559-580.
6. Madenoor Ramapriya G, Tawarmalani M, Agrawal R. Thermal Coupling Links to Liquid-only Transfer Streams: A Path for New Dividing Wall Columns. AIChE J. 2014;60(8):2949-2961.
7. Cameretti LF, Demicoli D, Meier R. A new application of dividing-wall columns for the separation of middle-boiling impurities. Chem Eng Res Des. 2015;99:120–124.
8. Agrawal R, Fidkowski ZT. Are Thermally Coupled Distillation Columns Always Thermodynamically More Efficient for Ternary Distillations? Ind Eng Chem Res. 1998;37(8):3444–3454.
9. Agrawal R. Multicomponent Columns with Partitions and Multiple Reboilers and Condensers. Ind Eng Chem Res. 2001;40(20):4258-4266.
10. Agrawal R, Fidkowski ZT. New thermally coupled schemes for ternary distillation. AIChE J. 1999;45(3):485–496.
11. Shah, V.H.; Agrawal, R. A Matrix Method for Multicomponent Distillation Sequences. AIChE J. 2010, 56 (7), 1759.
12. Agrawal R. Synthesis of Distillation Column Configurations for a Multicomponent Separation. Ind Eng Chem Res. 1996;35(4):1059-1071.
13. Agrawal R. Synthesis of Multicomponent Distillation Column Configurations. AIChE J. 2003;49(2):379-401.

CHAPTER 5. HEAT AND MASS INTEGRATION OF DISTILLATION COLUMNS

Heat and mass integration to consolidate distillation columns in a configuration is often characterized by elimination of a reboiler and condenser associated with the same components. In this chapter, we study a new and more general approach to column-consolidation, of which the conventional approach is a special case. In the new approach, reboiler of a column is coupled with condenser of another, through heat and mass integration in an additional section (HMA-section). The introduction of an HMA-section eliminates multiple connecting streams/valves, reduces the number of reboilers, condensers, and distillation columns by one each, and reduces the heat duty of the configuration. We exhaustively enumerate HMA-sections, and lay out a framework to identify all configurations with HMA-sections. Through examples, we show that both heat integration and mass integration resulting from introducing an HMA-section contribute to reduce the heat duty significantly.

5.1 Introduction

There are two aspects to the overall cost of a distillation configuration – the operating cost and the capital cost. The operating cost of a distillation configuration is directly related to the sum total of heat input at all the reboilers while the capital cost of a configuration is dependent on the number of distillation columns, reboilers, condensers, and transfer streams the configuration utilizes. Much of the research in distillation aims to reduce the operating and/or capital

costs of a configuration. One avenue to achieve this reduction is heat and mass integration of distillation columns. We explain this technique in more detail below.

Figure 5.1 illustrates one of the earliest cases of heat and mass integration between distillation columns producing the same pure product streams.[1] In Figure 5.1(a), pure product *B* is produced from two locations of the configuration; the reboiler of distillation column 2 and the condenser of distillation column 3. This reboiler and condenser are eliminated, and the two distillation columns are

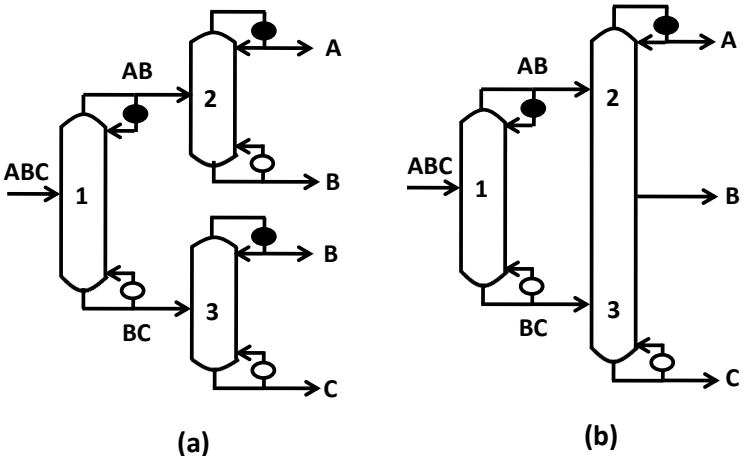

Figure 5.1 (a) A three-column distillation configuration for the separation of a three-component feed mixture; (b) A basic configuration obtained by the heat and mass integration of distillation columns 2 and 3 of the configuration in (a).

heat and mass integrated, to obtain the Column 2-3 of the configuration in Figure 5.1(b). A single product stream *B* is withdrawn from the resulting distillation column. The configuration of Figure 5.1(b) utilizes one less distillation column, reboiler, condenser and produces one less product stream than the configuration in Figure 5.1(a). Also, the vapor generated in the reboiler of Column 2-3 (see Figure 5.1(b)) is utilized for both splits, *BC* -> *B**C* and *AB* -> *A**B*. Thus, the vapor generated at the reboilers of Columns 2 and 3 of Figure 5.1(a) is replaced

by the greater of the two vapors and is now generated at the reboiler of Column 2-3 in Figure 5.1(b). The resulting capital and operating cost reduction achieved from heat and mass integration makes this approach attractive for industrial application.

However, heat and mass integration of distillation columns is not limited to eliminating reboilers and condensers associated with the same final product streams. Figure 5.2 shows an example of heat and mass integration between distillation columns producing submixtures with the same components from the

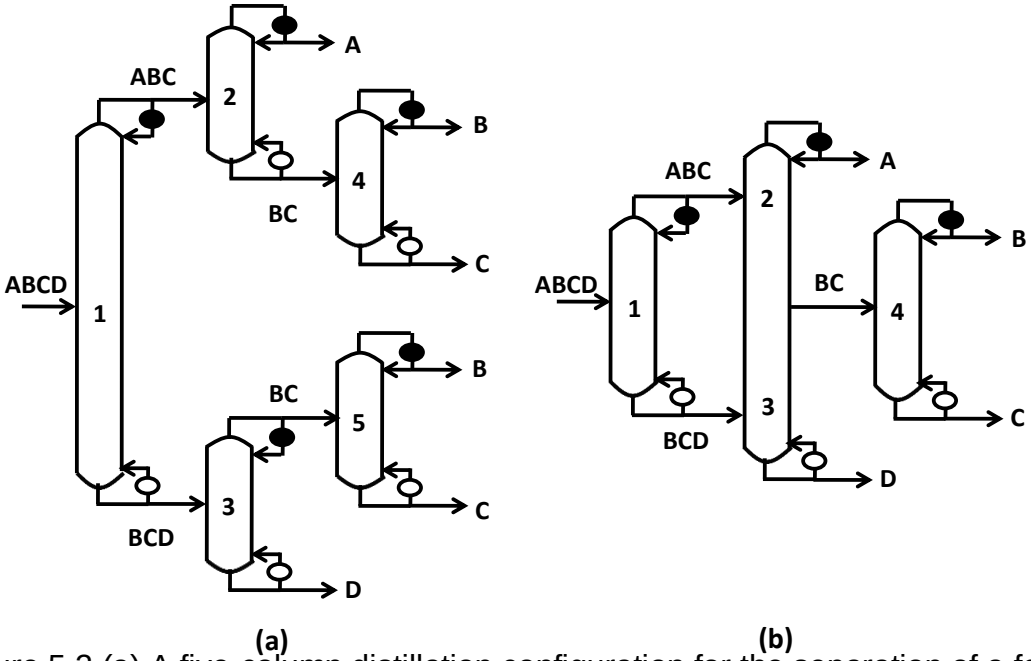

Figure 5.2 (a) A five-column distillation configuration for the separation of a four-component feed mixture; (b) A basic configuration obtained by the heat and mass integration of distillation columns 2 and 3 of the configuration in (a).

stripping and rectifying sections. Observe the configuration of Figure 5.2(a). From this configuration, the reboiler and condenser associated with the two *BC* submixtures are eliminated, and the two distillation columns are heat and mass

integrated, to obtain the Column 2-3 of the configuration in Figure 5.2(b). One stream containing both components *B* and *C* is withdrawn from the resulting distillation column. Also, note that due to heat and mass integration, Column 5 in the configuration of Figure 5.2(a) is eliminated. Heat and mass integration resulting of this kind has been commonly used in the literature to synthesize configurations,[2-11] and we will refer to it as conventional heat and mass integration.

Another example of heat and mass integration, due to Brugma,[12] is shown in Figure 5.3(b). In the configuration of Figure 5.3(a), the bottom product *B*, of the second distillation column, is more volatile than the top product *C*, of the third

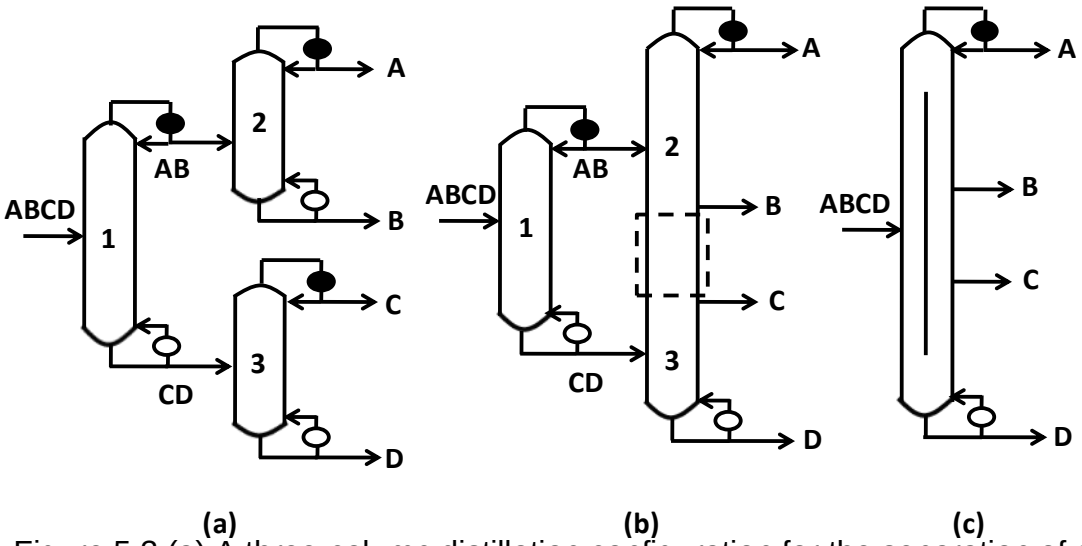

Figure 5.3 (a) A three-column distillation configuration for the separation of a four-component feed mixture; (b) Brugma configuration[12]; (c) DWC of Brugma configuration.[13]

distillation column. With the introduction of an additional section, the vapor from the third distillation column, which is rich in component *C*, is used as boilup for the second distillation column. This eliminates the reboiler associated with

product stream *B*. Likewise, the liquid from the second distillation column, which is rich in component *B*, is used as reflux for the third distillation column. This eliminates the condenser associated with product stream *C*. The product streams associated with the eliminated reboiler and condenser have different components, leading to two separate streams being withdrawn from the consolidated distillation column with an intermediate section between the two streams, shown in Figure 5.3(b) by a dotted box. The intermediate section is provided with sufficient stages, so that mass exchange takes place between the entering *C*-rich vapor at the bottom and *B*-rich liquid at the top to get *B*-rich vapor and *C*-rich liquid leaving the section. The two-column Brugma configuration[12] can be thus obtained from the configuration in Figure 5.3(a). Furthermore, its dividing wall column implementation,[13] shown in Figure 5.3(c), can be derived from the Brugma configuration after introducing thermal couplings at submixtures *AB* and *CD*,[14] and incorporating the two columns into a single shell. Note that the heat duty savings achieved in the Brugma configuration over the configuration shown in Figure 5.3(a) can also be achieved by heat integration.[15,16]

The heat and mass integration in the Brugma configuration differs in nature from conventional heat and mass integration discussed earlier, due to the appearance of an additional section in Column 2-3 of Figure 5.3(b). The additional section appears because the product streams participating in the heat and mass integration are comprised of different components. In this chapter, we refer to this kind of heat and mass integration as *Heat and Mass integration link with an Additional section*, and, in short, as *HMA*. HMA has received little

attention in the literature. Fidkowski[7] briefly mentions about the possibility of HMA between submixtures containing different components, but never considers it relevant for his enumeration/evaluation. Shenvi et al.[17] establish the relevance of HMA, and explore opportunities to introduce HMA between distillation columns of previously known distillation configurations. Madenoor Ramapriya et al.[18] identify more such opportunities. In this chapter, we introduce a systematic method to identify all HMAs for *n*-component distillation, which facilitates exploration of the configurations that use HMA. As an example, we explicitly show all HMAs that can arise in up to six-component distillation. Furthermore, the chapter aims to clarify the operational and mass integration aspects of any HMA, so that maximum benefits from this kind of heat and mass integration may be derived.

5.2 Heat and mass integration link with an additional section (HMA)

Heat and mass integration link in Figure 5.4(a) depicts the HMA of the Brugma configuration. The additional section, denoted in the figure by a dotted box, will be referred to as the *HMA-section*, and the column with such a section, an *HMA-column*. For convenience, the stream associated with the eliminated reboiler (for instance, stream *B* in Figure 5.4(a)) will be referred to as the *top stream of the HMA*, and the stream associated with the eliminated condenser (for instance, stream *C* in Figure 5.4(a)) will be referred to as the *bottom stream of the HMA*. The top and bottom streams of an HMA offer the HMA-column additional operational degrees of freedom.

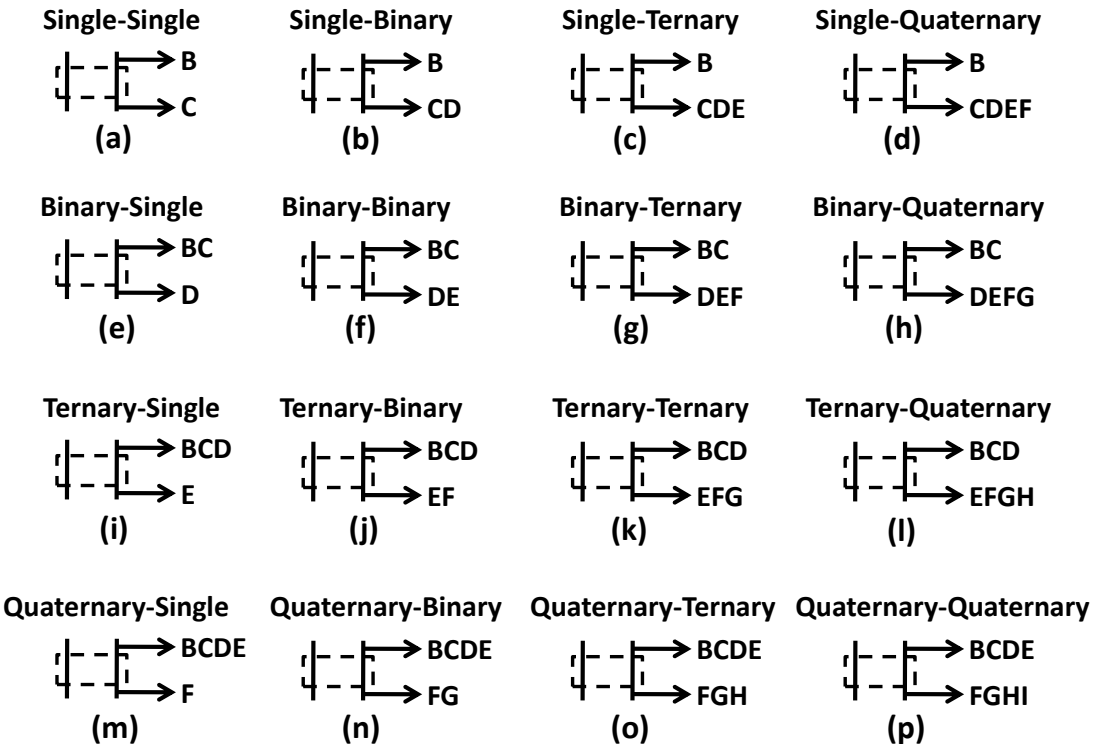

Figure 5.4 HMAs with no-overlap.

We propose that, in general, an HMA can be introduced between any two distillation columns if the bubble point temperature of the liquid stream exiting the eliminated condenser is higher than the dew point temperature of the vapor stream exiting the eliminated reboiler. This generally means that the ratio of mole fractions of each component in the reboiler stream relative to that in the condenser stream decreases with decreasing volatility of the components. Usually, the reboiler stream does not have a component that is heavier than the heaviest component in the condenser stream, and likewise, the condenser stream does not have a component that is more volatile than the most volatile component present in the reboiler stream. With such a condition, the more volatile stream is always withdrawn above the less volatile stream from an HMA.

5.3 Generalized class of HMAs

In order to present the general class of HMAs, we divide the HMAs into categories based on the number of components that are common between the

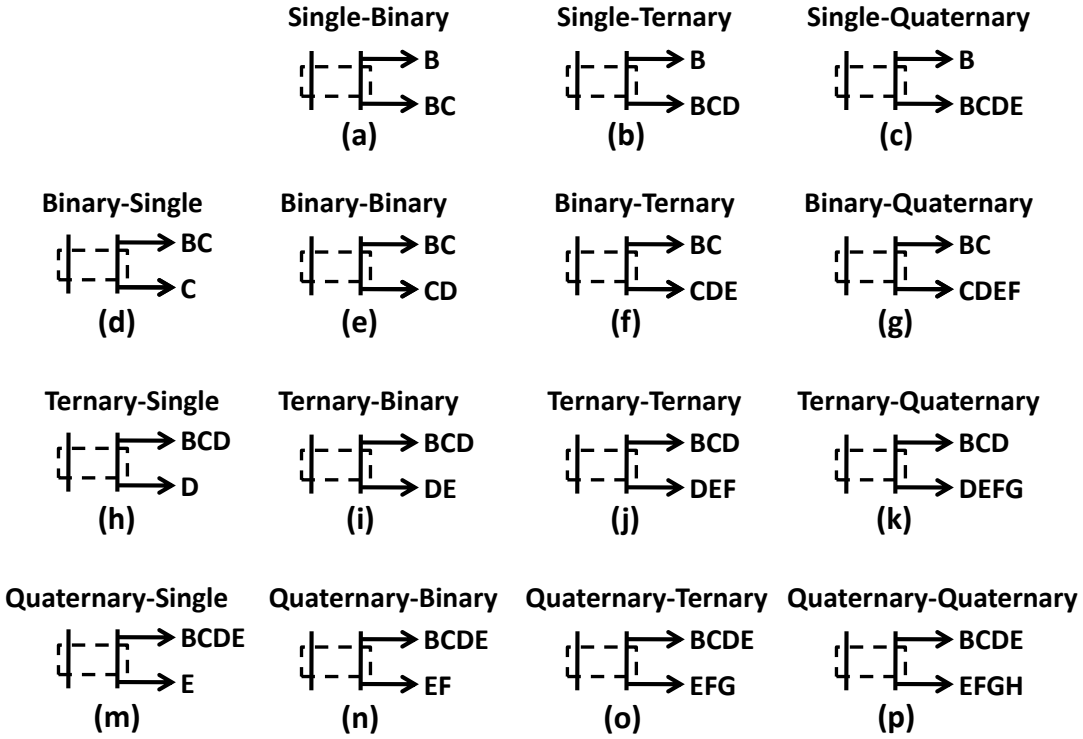

Figure 5.5 HMAs with one-overlap.

top and bottom streams of the HMA. For the HMA of Figure 5.4(a), with *B* and *C* as top and bottom streams, there are no overlapping components. Hence, such an HMA is called an 'HMA *with no-overlap*'. The categories of no-overlap, one-overlap, two-overlaps, etc., are further sub-categorized based on the number of components that make up the top and bottom streams of the HMA. Thus, the HMA of Figure 5.4(a), with a single component in each of its top and bottom streams, is an example of a *'single-single HMA with no-overlap'*, while the HMA of Figure 5.4(b), with one component in the top stream and two in the bottom

stream, is an example of a '*single-binary HMA with no-overlap*'. Figures 5.4, 5.5, 5.6, 5.7 and 5.8, respectively show the various sub-categories of HMAs with no-overlap, one-overlap, two-overlaps, three-overlaps, and four-overlaps (no stream in these figures contains more than four components). For *n*-component distillation (n≥3), in all, there are exactly (n^3-13n+12)/6 unique sub-categories of HMAs. A derivation of this number is provided in Appendix D. Specifically, under the *k*-overlap case, the number of sub-categories of HMAs is given by:

$$\begin{cases} (n-2)(n-3)/2 & k=0 \\ \dfrac{(n-k)(n-k-1)}{2}-1 & k=1 \\ \dfrac{(n-k)(n-k-1)}{2} & 2\le k\le n \end{cases}$$

Observe in Figures 5.6(a), 5.7(a) and 5.8, we show HMAs that have same

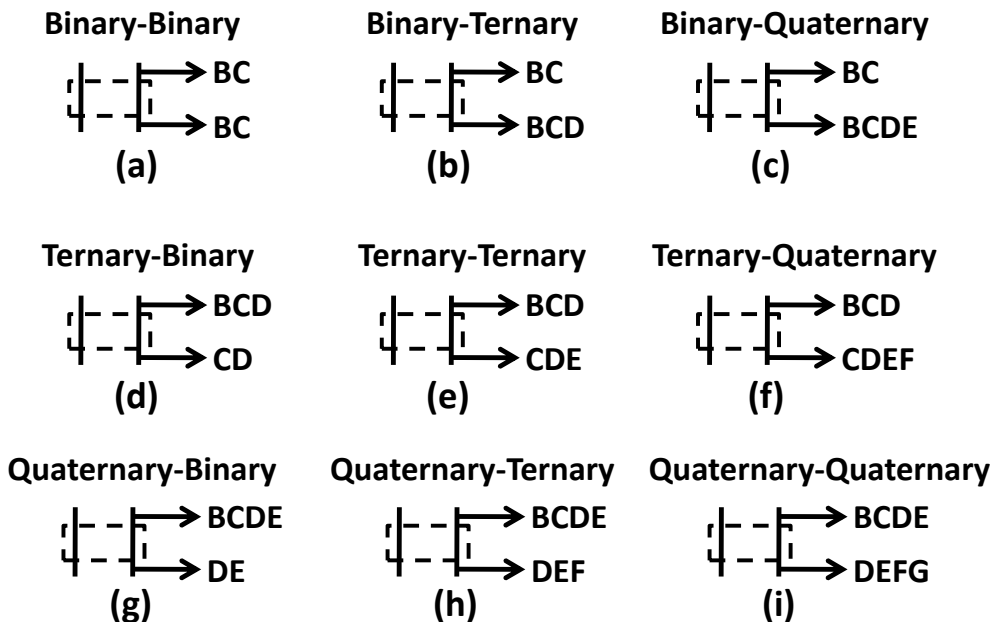

Figure 5.6 HMAs with two-overlaps.

components in the top and bottom streams of the HMA.[18] If the composition of the vapor entering at the bottom of the HMA-section is in equilibrium with the

liquid entering from the top, then, the HMA is not required, and columns are consolidated using conventional heat and mass integration, as was demonstrated in Figure 5.1. For this reason, the conventional heat and mass integration can be considered a special case of the proposed HMA. On the other hand, the proposed HMAs in Figures 5.6(a), 5.7(a) and 5.8 allow for the possibility of withdrawing streams at different compositions. Thus, in Figure 5.6(a), *BC* from the top is considered to have more lighter component (*B*) than the bottom *BC* stream, and vice-versa for the heavier component (*C*). Note that in Figure 5.5, we do not show an HMA with *B* at the top and another *B* at the bottom; the reason being that we assume that a final product stream is produced at a single purity. If two *B* product streams, each at different purity, were to be produced, then, an HMA could be used between them.

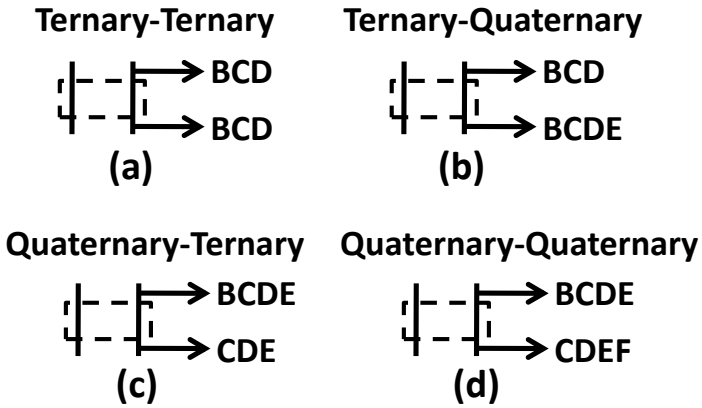

Figure 5.7 HMAs with three-overlaps.

Also note that the components used in any HMA of Figures 5.4, 5.5, 5.6, 5.7 and 5.8 are only representative. For instance, Figure 5.4(a) showing a *B-C* HMA represents all feasible ‘single-single HMAs with no-overlap’, and includes, for example, the *B-D, C-D*, *C-E*, etc. HMAs. Similarly, the ‘single-binary *B-CD*

HMA with no-overlap' of Figure 5.4(b) includes, for example, the *B-DE, B-EF, C-DE, C-EF,* etc. HMAs. When this multiplicity of components is accounted for, the exhaustive space comprises of $\frac{n(n-1)^2(n-2)}{12} - (n-2)$ HMAs for an *n*-component

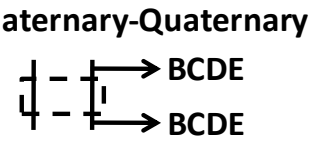

Figure 5.8 HMAs with four-overlaps.

distillation. See Appendix E for a derivation. Thus, the 25 sub-categories for six-component distillation actually include 46 feasible HMAs.

5.4 On the synthesis of distillation configurations with HMAs

Once a complete set of feasible HMAs are known, all possible *n*-component configurations can be drawn by incorporating them in a synthesis method for multicomponent distillation configurations. Shah and Agrawal[10,11] proposed a six-step method to synthesize multicomponent distillation configurations that result from conventional heat and mass integration. We use the method proposed by Shah and Agrawal[10,11] as an example to highlight the characteristics of any synthesis method that would synthesize distillation configurations with HMAs.

Figure 5.9(a) shows an example intermediate flowsheet that is obtained at the end of Step 5 of Shah and Agrawal's six-step method. In the final Step 6, distillation columns 4 and 5, the bottom and top products respectively of which

are pure *C*, are consolidated into a single column to obtain the configuration of Figure 5.9(b). This is the only four-column distillation configuration that the

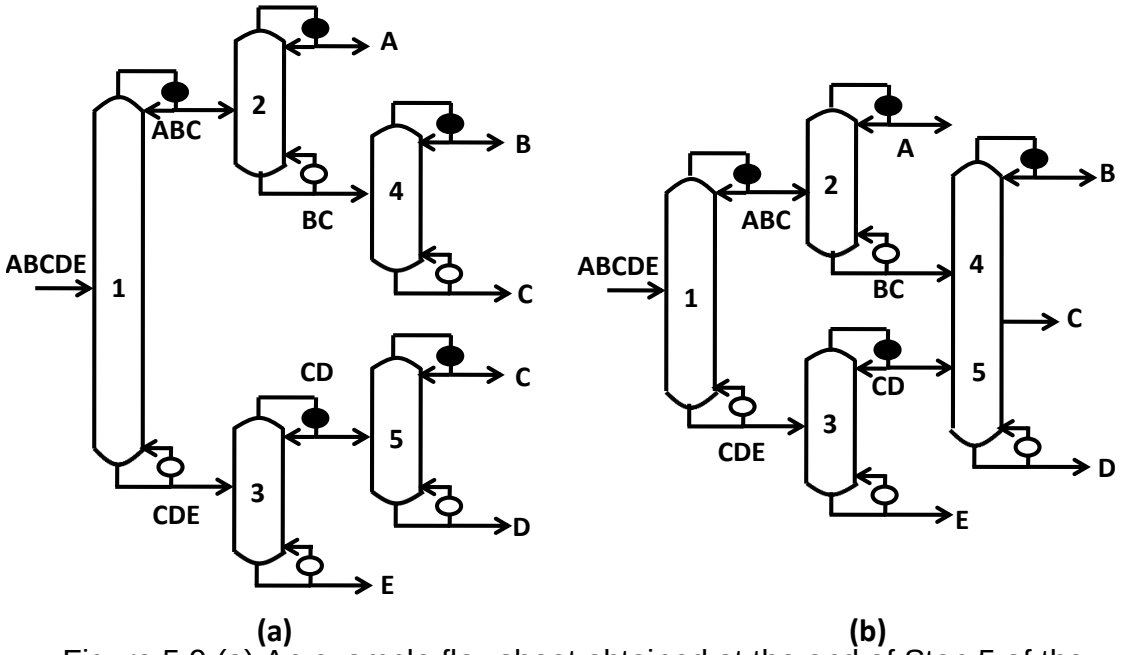

Figure 5.9 (a) An example flowsheet obtained at the end of Step 5 of the method proposed by Shah and Agrawal;[10,11] (b) Configuration synthesized at the end of Step 6.

method synthesizes from the flowsheet of Figure 5.9(a). The method, as published, does not consider consolidation of columns using HMA. We can modify Step 6 of the method to allow for column consolidations using HMA. For the configuration in Figure 5.9(a), we observe that there are three possible HMAs: 'binary-single HMA *BC-C* with one-overlap' (Figure 5.5(d)), 'single-binary HMA *C-CD* with one-overlap' (Figure 5.5(a)) and 'binary-binary HMA *BC-CD* with one-overlap' (Figure 5.5(e)). If we further consider the consolidation of *C*-producing columns 4 and 5 as another option, then there are a total of six possible ways to consolidate all the columns as shown in Figures 5.9(b) and 5.10. Four

configurations in Figures 5.10(a)-(c) and 5.9(b) result from single consolidations, while configurations in Figures 5.10(d) and (e) result from two consolidations at a

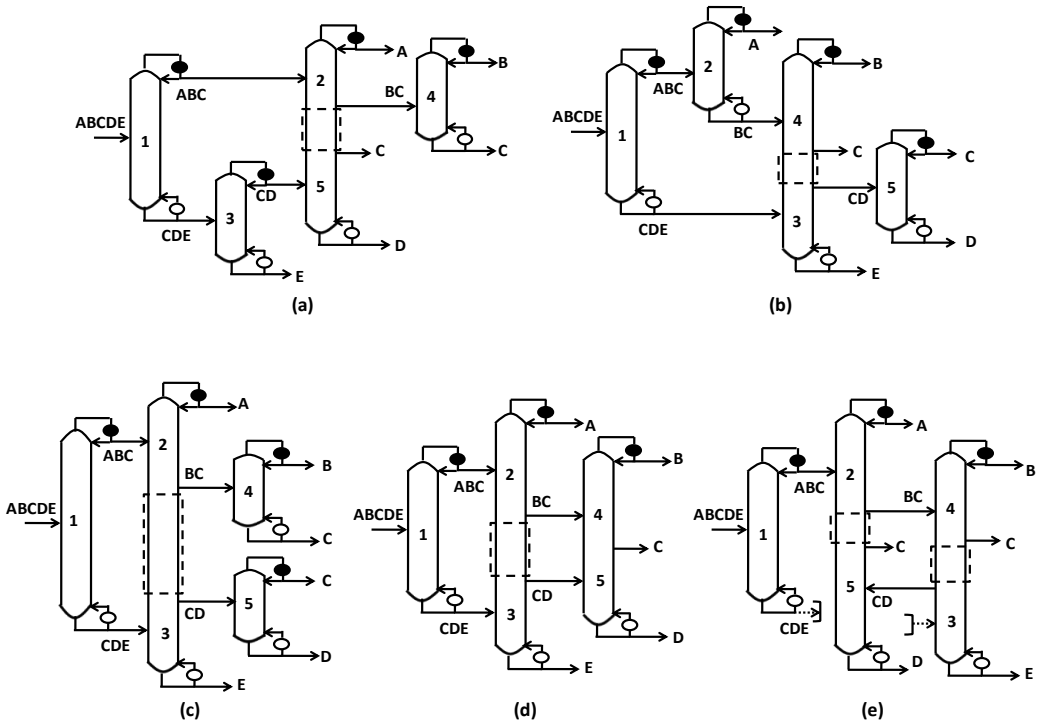

Figure 5.10 Configurations obtained by combining columns of Figure 5.9(a).

time. Note that a configuration such as the one in Figure 5.10(c) is rarely of interest as columns producing same product streams are generally consolidated, resulting in the corresponding configuration of Figure 5.10(d). Therefore, in this case, we actually have five distinct configurations: one that has been known (Figure 5.9(b)), and four new ones with HMAs (Figures 5.10(a), (b), (d) and (e)).

An important observation to be made is that the configurations of Figures

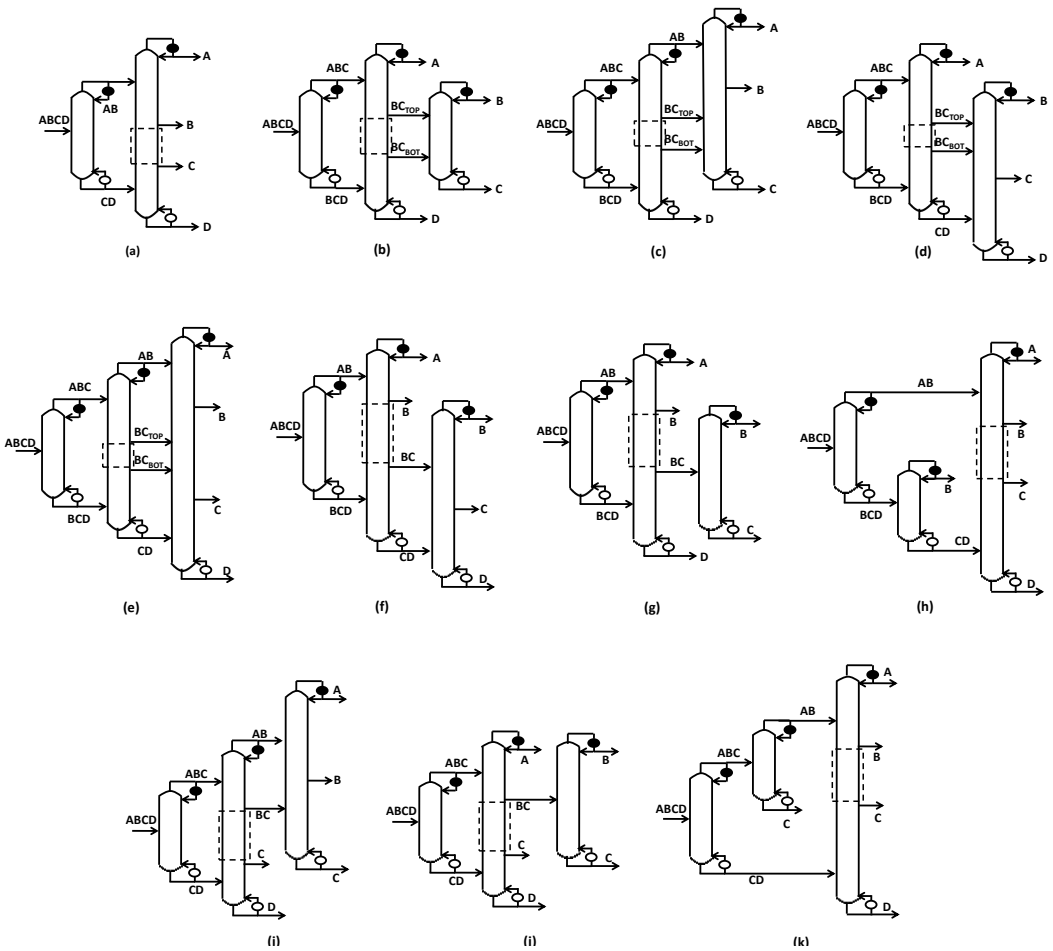

Figure 5.11 All 4-component configurations with 3 or less columns that use HMA.

5.10(a), 5.10(b) and 5.10(e) would have escaped our synthesis if we had looked for opportunities to introduce HMAs between distillation columns of the known/synthesized configuration of Figure 5.9(b). This clearly demonstrates the peril of looking for HMAs in the (*n*-1)-column basic configurations. Thus, as demonstrated here, once all feasible splits have been identified after Step 5 of Shah and Agrawal's method, and before any column consolidation is done, one must identify all feasible HMA-sections, and then create configurations containing

all possible combinations of these sections. Such an exercise becomes an integral part of Step 6 of the method. Using this procedure, we have identified a total of eleven configurations with less than or equal to three columns for four-component distillation (Figure 5.11; the ones which use more than three columns are omitted here for brevity). Of all the configurations in Figure 5.11, the one in 5.11(a) has been known for a while[12]. In the earlier synthesis method, for Figures 5.11(b), (c), (d) and (e), BC_{TOP} was assumed to be equal to BC_{BOT} resulting in the corresponding configurations with no HMA. However, to our knowledge, Figures 5.11(f) through (k) are entirely new in the literature. For an *n*-component feed in general, the introduced framework creates a much expanded search space of distillation configurations containing not only configurations with (*n*-1) columns, but also those with less than (*n*-1) columns which have the ability to produce pure products.

5.5 Operational aspects of the HMA-sections

To understand the functioning of an HMA-section, we will study one representative HMA from each category of Figures 5.4, 5.5, 5.6 and 5.7. The distillation columns used for the study, containing the representative HMAs, are shown in Figure 5.12. The distillation columns of Figures 5.12(a), 5.12(b), 5.12(c) and 5.12(d), respectively contain the HMAs shown in Figures 5.4(f), 5.5(e), 5.6(e) and 5.7(d). The numbers inside the distillation columns denote the number of stages that are used in a particular section for all the simulations of the distillation columns in ASPEN Plus®. Stages are provided in excess in each of these

sections. The number of stages that are used in any HMA-section of Figure 5.12 is denoted by **N**. All simulations use the stage-by-stage distillation model RADFRAC in ASPEN Plus®.

The feeds are ideal mixtures of any of the components *A*, *B*, *C*, *D*, *E*, *F* and *G*. Relative volatilities between all components are **2.5** unless specified. ***In all***

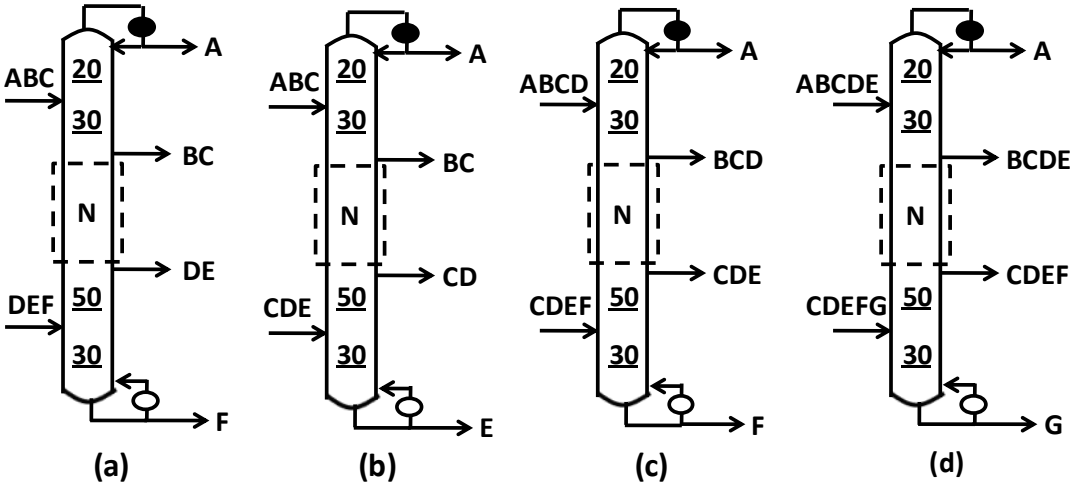

Figure 5.12 Simulated distillation columns having an HMA-section with: (a) no-overlap; (b) one-overlap; (c) two-overlaps; (c) three-overlaps.

our simulations in this section, all component flows in each of the two feed streams are set to 25 kmol/hr. Thus for component overlap cases in particular, each overlapping component has a flow rate of 25 kmol/hr in each feed stream. The top feed stream to all distillation columns is saturated vapor while the bottom feed stream is saturated liquid. All the streams leaving the column are assumed to be in the liquid phase.

Each of these distillation columns is assigned two splits. In the top split of each distillation column, the most volatile component is separated from the top feed mixture. Likewise, in the bottom split of each distillation column, the least

volatile component is separated from the bottom feed mixture. The distillation columns are simulated for different boil-up ratios (BR) in their reboilers (defined as the ratio of the vapor molar flow rate to bottom product molar flow rate). The lower limit of this boil-up ratio is the value at which one of the two splits in the distillation column only just fails (that is, when either the most volatile component from the top feed (component *A*) just appears in the top stream of the HMA-section, or, when the least volatile component from the bottom feed just appears in the bottom stream of the HMA-section). This boil-up ratio will be referred to as the minimum boil-up ratio of the column. *Furthermore, for preliminary studies, the flowrate in the top and bottom streams of HMA-sections of Figure 5.12 is maintained the same as prior to the introduction of an HMA. This makes the HMA-section a no-net mass flow section.* Such an operation will potentially make it possible for the top and bottom streams of the HMA-section to retain the same composition as before the introduction of the HMA-section.

For brevity, not all simulation results are presented here. Instead, only the main observations about the respective HMAs are presented below.

5.5.1 HMA with no-overlap

- The components in the top and bottom streams of an ‘HMA with no-overlap’ are mixed in the HMA-section. An adequate number of stages in the HMA-section is generally sufficient to prevent the components in the top and bottom streams from contaminating each other. An additional expenditure of

energy is not required to separate the components which are mixed in the HMA-section. This is mostly possible in ‘HMAs with no-overlap’ because the most volatile component in the bottom stream of the HMA, which has the highest tendency to move up and contaminate the top stream of the HMA, is less volatile than the least volatile component in the top stream of the HMA.

- Among the components that are mixed in the HMA-section, the separation of the least volatile component in the top stream from the most volatile component in the bottom stream of the HMA is the critical separation. As an example, for Figure 5.12(a), the separation of component *C* from *D* in the HMA-section is most critical. So, the relative volatility between these two components, to a great extent, decides the number of stages needed in the HMA-section to keep each stream free from contaminating-components of the other stream. For the feed composition in our example, with **N**=25, the contamination of the top and bottom streams is insignificant for relative volatilities given by $\{\alpha_{BC}, \alpha_{CD}, \alpha_{DE}\}$ = {2.5, 2.5, 2.5}, {1.1, 2.5, 2.5}, {2.5, 2.5, 1.1} and {1.1, 2.5, 1.1}, while for {2.5, 1.1, 2.5}, as shown in Table 5.1(a), it is significant. This table and the tables to follow show the net component-flows in the HMA-section for the components participating in the HMA. A positive quantity implies net movement of a component up the section and appearance in the top stream of the HMA, while a negative quantity implies the opposite. From the simulations, the minimum boil-up ratio for the column is observed to be 3.4. The bottom split of the column (*DEF->DE\F*) decides the minimum boil-up ratio of the column. This is also the case for every subsequent simulation in this section where the minimum boil-up

ratio is listed. Further, from Table 5.1(b), it is observed that the net component flows in the HMA-section are significantly reduced when **N** is increased to 150 for the same boil-up ratios.

Table 5.1 Net component flows in the HMA-section of the column in Figure 5.12(a) with $\{\alpha_{BC},\alpha_{CD},\alpha_{DE}\} = \{2.5, 1.1, 2.5\}$ and (a) N=25; (b) N=150; for different boil-up ratios, BR (the top and bottom stream flow rates are fixed at 50 kmol/hr).

	MOLE-BR	**Net *B***	**Net *C***	**Net *D***	**Net *E***
		kmol/hr			
CASE (a)	3.4 (min BR)	0	-1.711	1.711	0
	4	0	-1.919	1.919	0
	7	0	-2.703	2.703	0
	10	0	-3.221	3.221	0
	MOLE-BR	**Net *B***	**Net *C***	**Net *D***	**Net *E***
		kmol/hr			
CASE (b)	3.4 (min BR)	0	-0.005	0.005	0
	4	0	-0.006	0.006	0
	7	0	-0.009	0.009	0
	10	0	-0.010	0.010	0

- The mixing tendencies between the two streams of an ‘HMA with no-overlap’ are higher at larger boil-ups in the distillation column. This trend can be observed in Table 5.1. It would thus be appropriate to operate columns containing ‘HMAs with no-overlap’ close to the minimum boil-up (or reflux) ratio.

5.5.2 HMA with one-overlap

- Sufficient stages in the HMA-section of an ‘HMA with one-overlap’ ensure that the same composition is retained in the two streams of the HMA as before the introduction of the HMA-section. This is because, in such HMAs, the most volatile component in the bottom stream of the HMA, which has the highest tendency to move up the HMA-section, is the same as the least volatile component in the top stream of the HMA, which has the highest tendency to move down the HMA-section.
- At any given boil-up (no less than the minimum boil-up) in a distillation column that contains an ‘HMA with one-overlap’, the direction of net movement of the overlapping component in the HMA-section can be controlled by altering the flowrates of the top and bottom streams of the HMA. This phenomenon is observed in Table 5.2, which presents the results of simulating the distillation column of Figure 5.12(b). In the simulation, flowrates of submixture streams, *BC* and *CD*, are varied for $\{\alpha_{BC}, \alpha_{CD}\}$ = {1.1, 1.1} and **N**=150, at BR=4. The chosen boil-up ratio is slightly higher than the minimum boil-up ratio of 3.3. The net movement of only the overlapping component in the HMA-section in either direction signifies the separation of the overlapping component from its neighboring components in the submixture it was originally present in. Note that the relative volatilities chosen correspond to a difficult-separation scenario. If either relative volatility, α_{BC} or α_{CD}, is greater than 1.1, then the movement of the overlapping component in the HMA-section is more pronounced (because it is easier for the overlapping component to separate from the neighboring

component). This would translate to observance of the described phenomenon over a wider range of flow rates in the top and bottom streams of the HMA. Since α_{BC} and α_{CD} are chosen to be 1.1, **N**=150 is used to keep *B* from contaminating *CD*, and *D* from contaminating *BC*. For higher relative volatility combinations, much fewer stages would be needed. This observation suggests that there is a need to optimize the relative flow rates of streams *BC* and *CD* to minimize the total heat duty of the entire configuration (see next section for more details).

Table 5.2 Net mass and component flows in the HMA-section of the distillation column in Figure 5.12(b) with $\{\alpha_{BC},\alpha_{CD}\} = \{1.1, 1.1\}$ and N=150, at BR=4, for different flowrates of submixture streams *BC* and *CD*.

BC **Flowrate**	***CD*** **Flowrate**	**Net Mass**	**Net *B***	**Net *C***	**Net *D***	**Direction of component flows**
kmol/hr						
56	44	6	0	5.545	0.455	
55	45	5	0	4.989	0.011	**+C, +D**
54	46	4	0	3.999	0.001	
53	47	3	0	3	0	
52	48	2	0	2	0	**+C**
51	49	1	0	1	0	
50	50	0	0	0	0	
49	51	-1	0	-1	0	
48	52	-2	0	-2	0	**-C**
47	53	-3	0	-3	0	
46	54	-4	-0.001	-3.999	0	
45	55	-5	-0.002	-4.998	0	**-B, -C**
44	56	-6	-0.011	-5.989	0	

5.5.3 HMA with two or more overlaps

- It seems impossible to preserve the composition of two streams which have two or more components in common, after an HMA is introduced between them. This is because, in such HMAs, the most volatile component in the bottom stream of the HMA is more volatile than the least volatile component in the top stream of the HMA. Attempts to retain the total molar flow rates of the two streams to be same after the introduction of an HMA result in countercurrent flows of the overlapping components in the HMA-section. This phenomenon of countercurrent flows can be observed from Table 5.3 (+ve *C* and -ve *D*). The table presents the results of simulating the HMA-section of the distillation column in Figure 5.12(c) as a no-net mass flow section, with **N**=150, for $\{\alpha_{BC}, \alpha_{CD}, \alpha_{DE}\}$ = {1.1, 1.1, 1.1}. Even though sufficiently large number of stages is present, the countercurrent flows remain.

Table 5.3 Net component flows in the HMA-section of the distillation column in Figure 5.12(c) with $\{\alpha_{BC},\alpha_{CD},\alpha_{DE}\}$ = {1.1, 1.1, 1.1} and N=150, for different boil-up ratios (the top and bottom stream flow rates are fixed at 75 kmol/hr).

MOLE-BR	**Net *B***	**Net *C***	**Net *D***	**Net *E***
	kmol/hr			
4.46 (min BR)	0	3.225	-3.225	0
5	0	3.587	-3.587	0
8	0	5.475	-5.475	0
11	0	7.135	-7.135	0

- It is interesting to note that, for any given boil-up (no less than minimum boil-up) in a distillation column that contains an 'HMA with two or more overlaps', the direction of movement of the overlapping components in the HMA-section can be controlled by using the relative flow rates of the top and bottom streams of the HMA. Table 5.4 presents the results of simulating the distillation column of Figure 5.12(c) at BR=5 (just above the minimum BR of 4.46), with $\{\alpha_{BC}, \alpha_{CD}, \alpha_{DE}\}$ = {1.1, 1.1, 1.1} and **N**=150, for various flow rates of the top and bottom streams

Table 5.4 Net mass and component flows in the HMA-section of the distillation column in Figure 5.12(c) with $\{\alpha_{BC},\alpha_{CD},\alpha_{DE}\}$ = {1.1, 1.1, 1.1} and N=150, at BR=5, for different flowrates of submixture streams *BCD* and *CDE*.

BCD **Flowrate**	***CDE*** **Flowrate**	**Net Mass**	**Net *B***	**Net *C***	**Net *D***	**Net *E***	**Direction of component flows**
kmol/hr							
88	62	13	0	8.142	4.709	0.150	**+C, +D, +E**
87	63	12	0	7.819	4.173	0.008	
86	64	11	0	7.471	3.528	0.001	
85	65	10	0	7.121	2.879	0	**+C, +D**
⋮	⋮	⋮	⋮	⋮	⋮	⋮	
81	69	6	0	5.721	0.279	0	
80	70	5	0	5.371	-0.371	0	**+C, -D**
79	71	4	0	5.021	-1.021	0	
⋮	⋮	⋮	⋮	⋮	⋮	⋮	
70	80	-5	0	0.748	-5.748	0	
69	81	-6	0	0.115	-6.114	0	
68	82	-7	0	-0.520	-6.480	0	**-C, -D**
⋮	⋮	⋮	⋮	⋮	⋮	⋮	
64	86	-11	0	-3.059	-7.941	0	
63	87	-12	-0.001	-3.693	-8.306	0	**-B, -C, -D**
62	88	-13	-0.002	-4.328	-8.671	0	
61	89	-14	-0.005	-4.960	-9.035	0	

of the HMA. It follows from observations listed in the table that every feasible combination of directions of the overlapping components is achieved in different ranges of flow rates of the top and bottom streams of the HMA. Note that the used relative volatilities are small, and hence separations are difficult. If any relative volatility, α_{BC} or α_{CD} or α_{DE} , is greater than 1.1, the described phenomenon is more pronounced. In such a case, ranges of flow rates of the top and bottom streams become wider. Since the flow rates of the overlapping components can influence downstream distillation and the overall heat duty of the entire configuration, these may be optimized to yield energy savings.

5.6 Energy saving potential of HMAs

In this section, we demonstrate the energy saving potential of HMAs in multicomponent distillations. We compare the energy requirements of conventional configurations with those that result from connecting the distillation columns of these configurations with HMAs. We optimize the distillation configurations using ASPEN Plus® for minimum total reboiler duty requirement assuming constant latent heats of vaporization and relative volatilities between pure components. The stage-by-stage distillation model RADFRAC in ASPEN Plus® is used. Sufficient stages are included in each section to make the results insensitive to the feed and sidestream tray locations. The main *n*-component feed to the overall configuration is an ideal saturated liquid feed mixture of any of components *A*, *B*, *C*, *D*, *E,* and *F*. ***Each component flow in the feed is set to***

25 kmol/hr. All submixtures and products are withdrawn in the liquid phase. Pure products of molar purities greater than 99.9% are desired.

The initial guesses to ASPEN Plus® optimization of the conventional configurations are obtained from the Global Minimization Algorithm (GMA)[19] to ensure reliable and quick convergence. The GMA uses the Underwood's equations[20] to determine the minimum total vapor requirement of a configuration.

5.6.1 HMA with no-overlap

The configuration of Figure 5.13(a) is optimized for $\{\alpha_{AB}, \alpha_{BC}, \alpha_{CD}, \alpha_{DE}, \alpha_{EF}\}$ = {2.5, 1.5, 1.5, 1.5, 1.5} and the vapor duty requirement in the reboiler of each

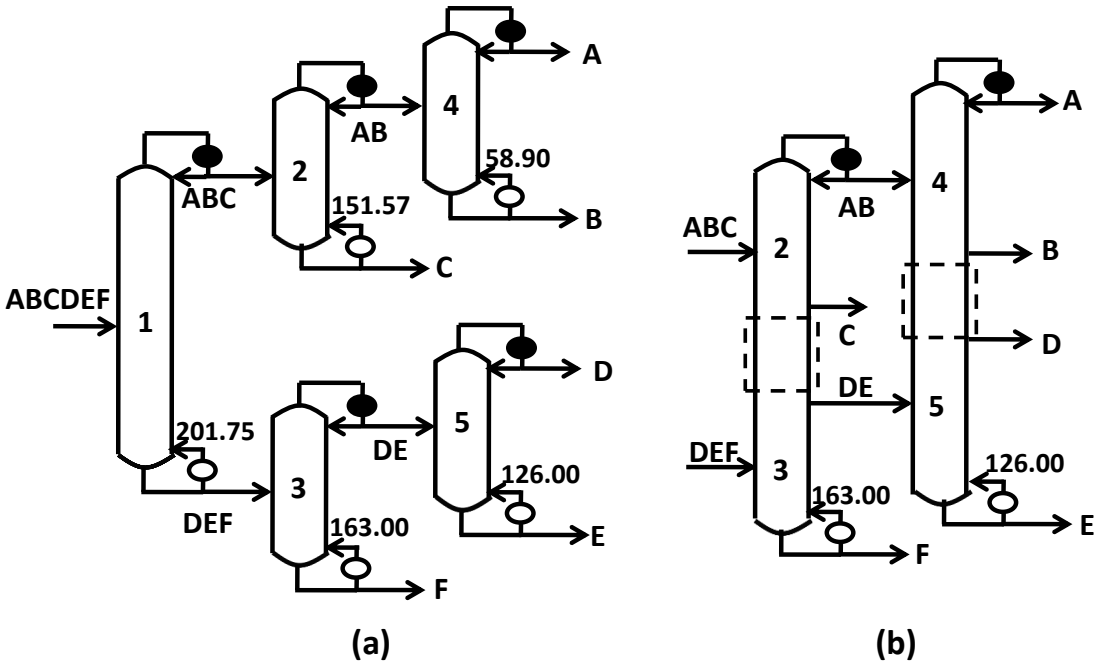

Figure 5.13 (a) Optimized 6-component configuration with vapor requirements in every reboiler; (b) The combination of columns of (a) yielding the highest energy saving.

column is shown in Figure 5.13(a). From this flowsheet, there are four possible HMAs leading to six different combinations. The six combinations are listed in Table 5.5 along with their heat duty savings. The configurations are labeled by the columns that have been combined through the use of corresponding HMA-sections. The vapor requirement in the reboiler of the HMA-column is the larger of the two vapor requirements at the reboilers of the columns which are combined. Thus, when columns 2-3 and 4-5, as shown in Figure 5.13(b), are combined, the highest heat duty saving of 30% is achieved because the combined columns have 'close-valued' heat duties. Furthermore, due to HMAs, the number of distillation columns has reduced to three, accompanied by a reduction in reboilers and condensers. In this case, the heat duty is saved without using an additional higher temperature heat source, albeit the cold utilities at condensers *AB* and *A* have increased. Nevertheless, by using an intermediate condenser at *D*, as shown in Figure 5.13(b), it is possible to condense more than half of the vapor supplied at *E*, thereby reducing the load on the condenser at *A*.

Table 5.5 Total heat duty savings obtained by combining the different pairs of columns in the configuration of Figure 5.13(a).

Column Pairs of Figure 13(a)	(2-3)	(2-5)	(4-3)	(4-5)	(2-3),(4-5)	(2-5),(4-3)
Heat Duty Savings (%)	21.6	18.0	8.4	8.4	30.0	26.4

5.6.2 HMA with one-overlap

The configuration of Figure 5.9(b) is optimized for two feed conditions, F1 and F2, for which $\{\alpha_{AB}, \alpha_{BC}, \alpha_{CD}, \alpha_{DE}\}$ are set to {2.5, 2.5, 1.5, 1.5} and {1.5, 1.5, 2.5, 2.5} respectively. The flowrates of *ABC* and *CDE* are obtained by optimizing for each feed condition separately. These flowrates are then used to feed Column 2-3 of the configuration in Figure 5.10(d). The vapor duty requirement in the reboiler of Column 2-3 of Figure 5.10(d) is assigned the larger of the two vapor requirements at reboilers of Columns 2 and 3 of Figure 5.9(b). The remainder of the configuration in Figure 5.10(d) is optimized for heat duty. It is found that for F1 (resp. F2), the configuration in Figure 5.10(d) requires a total vapor duty that is 22.2% (resp. 21.7%) less than the configuration in Figure 5.9(b). However, the heat duty shared between the two splits, *ABC->A\BC* and *CDE->CD\E* using an HMA, accounts only for 64.1% (resp. 84.4%) of the total vapor duty saving. The rest of the saving results from mass integration capabilities of an HMA, which we detail below.

The Column 4-5 of Figure 5.9(b) performs two splits, *BC->B\C* and *CD->C\D*. For feed F1, among the two splits, split *CD->C\D* is more difficult, and controls the vapor requirement in the reboiler of Column 4-5. From the simulation for the configuration of Figure 5.10(d), we observe that, there is a net movement of 12.68 kmol/hr of *C* up the HMA-section in Column 2-3. This movement of *C* in Column 2-3, reduces the amount of *C* by 12.68 kmol/hr in the submixture *CD* fed to Column 4-5, making the *CD->C\D* split less energy intensive. This reduces the vapor duty requirement in the reboiler of Column 4-5, shown in Figure 5.10(d), by

31.5% compared to that in Column 4-5 shown in Figure 5.9(b). For the case of feed F2, split *BC->B\C* is more difficult than split *CD->C\D* in Column 4-5 of Figure 5.9(b). A net flow of 7.31 kmol/hr of *C* down the HMA-section in Column 2-3 of Figure 5.10(d) makes the separation of submixture *BC* easier in Column 4-5, due to which the vapor duty in the reboiler of the column is reduced by 13.6%. An optimization of the overall configuration in Figure 5.10(d) including Column 1 could further increase heat duty savings for the same feeds F1 and F2.

5.6.3 HMA with two or more overlaps

The operating conditions for the configuration of Figure 5.14(a) are optimized to minimize the total heat duty for two feed conditions, F3 and F4, for

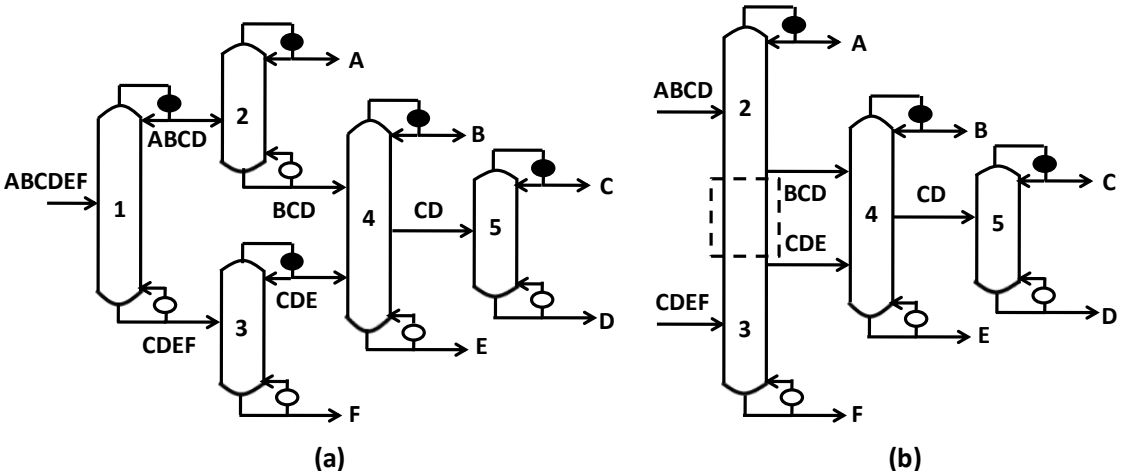

Figure 5.14 (a) A conventional six-component configuration; (b) The HMA-linked configuration obtained after introducing HMAs between columns 2 and 3 of (a).

which $\{\alpha_{AB}, \alpha_{BC}, \alpha_{CD}, \alpha_{DE}, \alpha_{EF}\}$ are set to {2.5, 2.5, 1.5, 1.5, 1.5} and {1.5, 1.5, 2.5, 2.5, 2.5} respectively. The flowrates of *ABCD* and *CDEF* are obtained by optimizing for each feed condition, and used to feed Column 2-3 of Figure 5.14(b). The vapor duty in the reboiler of this column is assigned the larger of the two vapor duty requirements at reboilers of Columns 2 and 3 of Figure 5.14(a). Optimizing the remainder of the configuration in Figure 5.14(b) yields a total vapor duty saving of 16.5% and 23.5% for feed conditions F3 and F4 respectively (the comparison includes Column 1 in configurations of Figures 5.14(a) and 5.14(b)). Here, sharing the heat between the two splits, *ABCD->A\BCD* and *CDEF->CDE\F*, using an HMA, accounts for a total vapor duty saving of only 10.4% and 20.4%, for F3 and F4 respectively. The rest of the saving is observed in the reboiler of the Column 4 due to movement of mass in the HMA-section. By optimizing the composition of streams *BCD* and *CDE*, the reboiler duty of Column 4 in Figure 5.14(b) is reduced by 30.3% and 14.2% for the two feed conditions, compared to that of Column 4 in Figure 5.14(a), yielding the overall saving mentioned above.

For feed F3, in Column 4 of Figure 5.14(a), it is found that the split *CDE->CD\E* controls the vapor duty requirement in the reboiler of the column. In Column 2-3 of Figure 5.14(b), a net flow of 6.21 kmol/hr of *C* and 9.18 kmol/hr of *D* up the HMA-section eases the separation of the *CDE* submixture into *CD* and *E* in Column 4. Likewise, for feed F4, in Column 4 of Figure 5.14(a), split *BCD->B\CD* controls the vapor duty requirement in the reboiler of the column. In Column 2-3 of Figure 5.14(b), a net flow of 8.11 kmol/hr of *C* and 3.06 kmol/hr of

D down the HMA-section makes the separation of submixture *BCD* in the next column less energy intensive.

Similar to the above optimization, optimization of the configuration in Figure 5.15(b) for $\{\alpha_{AB}, \alpha_{BC}, \alpha_{CD}, \alpha_{DE}\}$ = {2.5, 2.5, 2.5, 2.5} gives an overall vapor duty saving of 7.3% over that in Figure 5.15(a). The vapor requirement in the reboilers

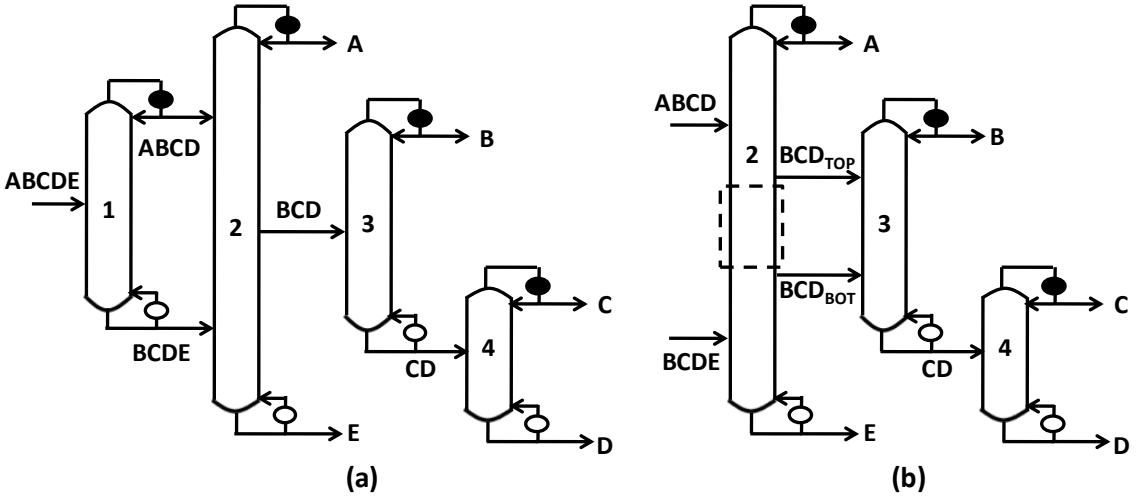

Figure 5.15 (a) A conventional five-component configuration; (b) Configuration of Figure (a) with the *BCD* transfer stream replaced by the HMA of Figure 5.7(a).

of Column 2 in both configurations is the same. All the energy saving in the configuration of Figure 5.15(b) is obtained at the reboiler of the third distillation column in the form of a 31.9% reduction in its reboiler duty. In the HMA-section of Column 2, a net upflow of 5.24 kmol/hr of *B*, and a net downflow of 3.23 kmol/hr and 1.00 kmol/hr of *C* and *D* respectively, make the BCD_{TOP} submixture 92.2% rich in *B*, and the BCD_{BOT} submixture 44.5% and 46.6% rich in *C* and *D* respectively, with little *B*. In comparison, the feed to Column 3 in Figure 5.15(a) is 33.3% rich in each of *B*, *C* and *D*. This makes the overall separation of *B* from

CD in Column 3 of Figure 5.15(b) less energy intensive compared to Column 3 of Figure 5.15(a). This example is an illustration of the need to include HMAs such as those shown in Figures 5.6(a), 5.7(a) and 5.8.

5.7 On the use of intermediate reboilers and condensers with HMA-sections

Although introducing HMAs between distillation columns offers benefits in terms of heat duty savings, it may incur temperature level penalties. For example, in Column 2-3 of Figure 5.13(b), if the split *DEF->DE\F* is more energy intensive than *ABC->AB\C*, then all the condensing duty for the *DEF->DE\F* split is provided at the lower temperature of *AB* condenser. In such a case, the cooling duty at condenser *AB* in Figure 5.13(b) compared to Figure 5.13(a) is higher. Similarly, if the split *ABC->AB\C* is more energy intensive than *DEF->DE\F*, then the heating duty at reboiler *F* of Figure 5.13(b) is higher when compared to Figure 5.13(a). These temperature level penalties in the configuration of Figure 5.13(b) can be reduced by incorporating an intermediate condenser at submixture *DE* when the bottom split is more energy intensive than the top split, and an intermediate reboiler at *C* for the converse case.

Unlike the usage of intermediate reboilers and condensers, as discussed in the previous paragraph for ‘HMAs with no-overlap’, other considerations are needed for HMAs with one or more overlaps. Consider Column 2-3 of Figure 5.10(d) for example. Figure 5.16 shows four versions of the column with an intermediate reboiler or a condenser introduced at different submixtures. Note

that the minimum vapor duty requirement of the configuration in Figure 5.10(d) is not always equal to the minimum vapor duty requirement of the same configuration with the Column 2-3 replaced by the ones in Figures 5.16(a) or 5.16(b). This is because the vapor traffic in the HMA-section of the columns in

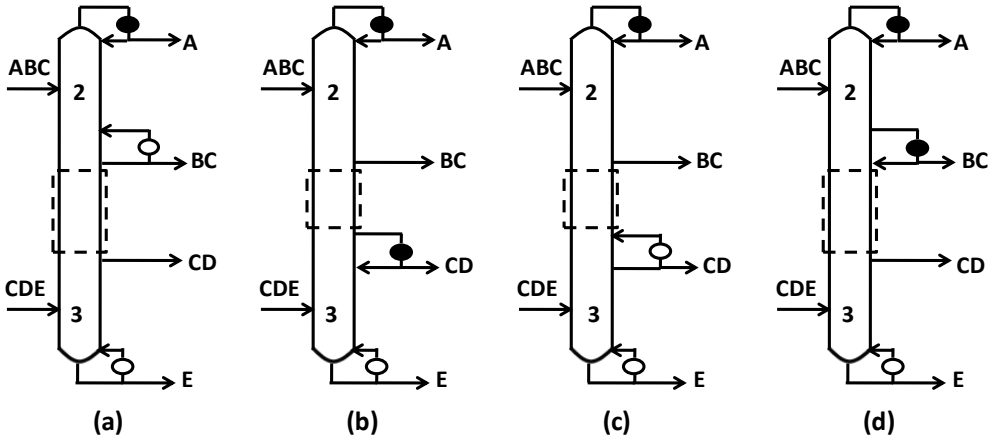

Figure 5.16 Column 2-3 of the configuration in Figure 5.10(d) with an intermediate (a) reboiler at *BC*; (b) condenser at *CD*; (c) reboiler at *CD*; (d) condenser at *BC*.

Figures 5.16(a) and 5.16(b) is lower than the vapor traffic in the HMA-section of Column 2-3 in Figure 5.10(d). With lower vapor traffic in the HMA-section, the maximum quantity of the overlapping *C* component that can be transported up or down the HMA-section is definitely reduced. This may affect the vapor duty requirement in the reboiler of the next distillation column. Alternative intermediate reboiler and condenser arrangements are shown in Figures 5.16(c) and 5.16(d). These columns retain the same vapor traffic in their HMA-section as in Column 2-3 of Figure 5.10(d). However, the reboiler *CD* in Figure 5.16(c) boils at a higher temperature than reboiler *BC* in Figure 5.16(a), and the condenser *BC* in Figure 16(d) condenses at a lower temperature than the condenser *CD* in Figure 5.16(b).

The above factors must be considered while implementing intermediate heat exchangers at the top and bottom streams of HMAs with one or more overlapping components.

5.8 A column connected through multiple HMA-sections

So far, we have discussed cases whereby a column is consolidated with only one another column through one HMA. For example, Figure 5.13(b) is

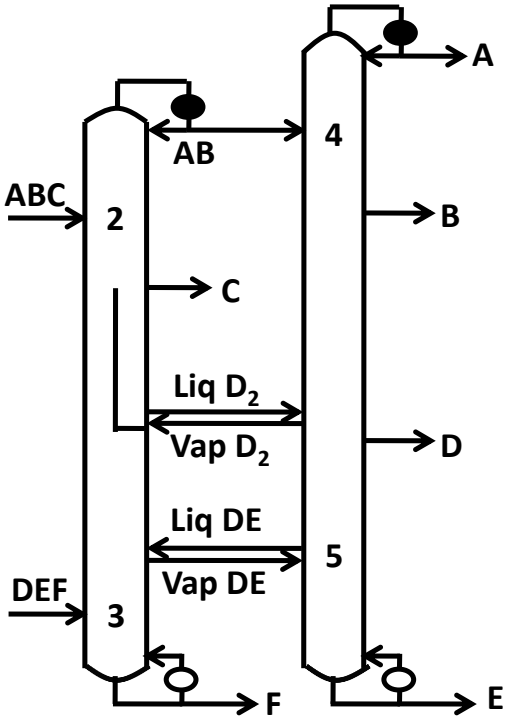

Figure 5.17 An implementation of configuration of Figure 5.13(a), where all potential HMA-linkable condensers are HMA-linked with all potential HMA-linkable reboilers.

obtained by connecting Columns 3 and 2, and, Columns 5 and 4. Similarly, in another option, Column 3 can be connected to 4, and Column 5 to 2, each with

one HMA-section. These connections limit the splits that can share heat duties. For example, in the configuration of Figure 5.13(b), the heat supplied at reboilers *F* and *E* is respectively not conveyed to splits *AB->A\B* and *ABC->AB\C*. Thus, in a flowsheet such as the one in Figure 5.13(a), it is lucrative to connect a condenser simultaneously with more than one reboiler through the HMA-section. One way to achieve this for the configuration of Figure 5.13(b) is shown in Figure 5.17. The excess vapor generated in reboiler *F* is conveyed to split *AB->A\B* through the vapor stream in the back and forth *DE* liquid-vapor communication, with net mass flow equal to the sum of the total component *D* and *E* flows in the feed. This connection is somewhat similar to using an HMA-section between condenser *DE* and reboiler *B*. Since an HMA-section already exists between condenser *D* and reboiler *B*, the *DE* vapor takes advantage of it. The condenser *D* is also connected to reboiler *C* through the use of a dividing wall column. Some of the vapor generated in reboiler *E* is conveyed to split *ABC->AB\C* through the vapor stream in the back and forth D_2 vapor-liquid communication, with no net transfer of mass in D_2 between the two columns. If needed, in Figure 5.17, the condenser *AB* may also be eliminated through the use of conventional thermal coupling to achieve more sharing of vapor traffic through various sections. Conceptually, connecting one column simultaneously with multiple columns through the use of multiple HMAs has a potential to further reduce overall heat duty, however, due to added complexity, the usefulness of this strategy will depend on the practicality of an onsite implementation.

5.9 HMAs with additional intermediate streams

Observe the HMA of Figure 5.5(e). Shenvi et al.[17] found that for a configuration which uses this HMA, a pure product stream *C* could be withdrawn

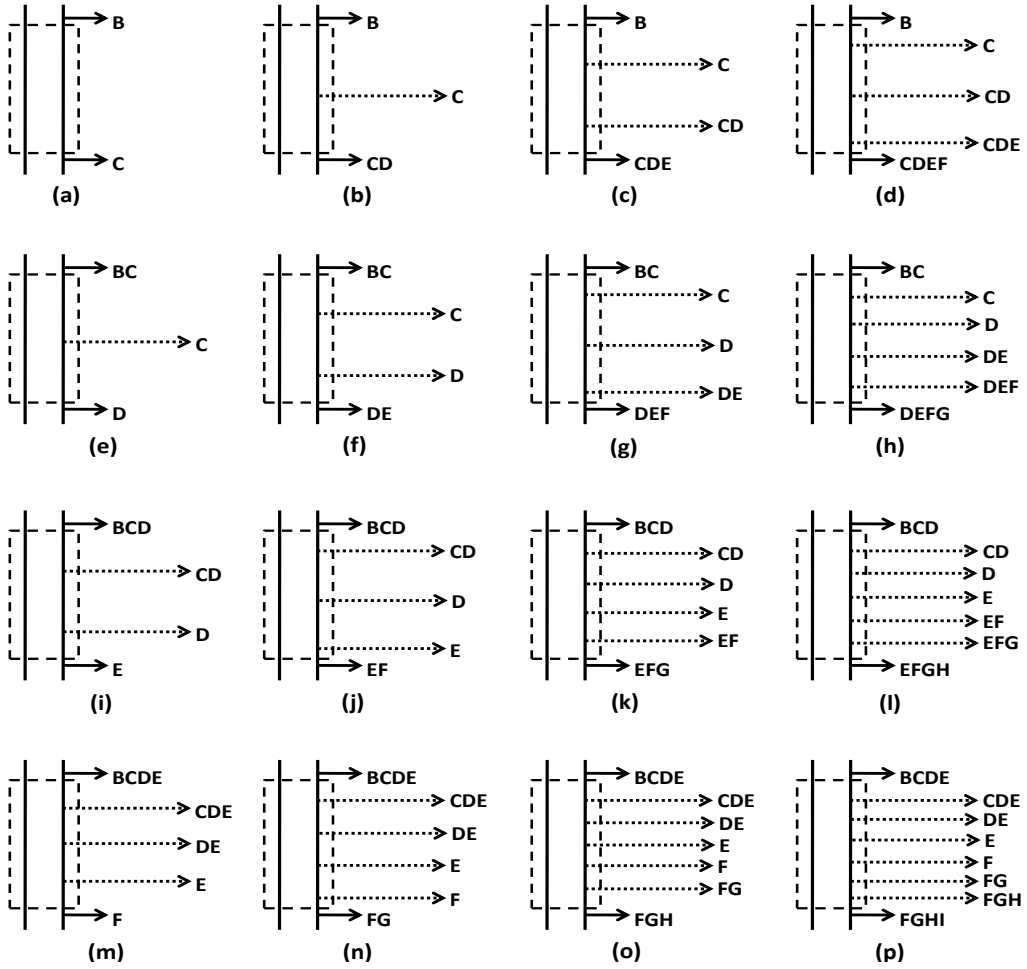

Figure 5.18 Additional streams shown for the no-overlap HMAs of Figure 5.4.

from an intermediate location of the HMA. This is possible because, as the liquid rich in *BC* descends down the HMA-section, it becomes leaner in *B*. Thus, there is a tray at an intermediate location where the liquid is rich only in *C*, but lean in *B*

and *D*. Further descent of the liquid down the section makes it richer in *D*, in addition to the existing *C*. Withdrawing pure *C* from such an intermediate location is potentially beneficial from a heat duty perspective because the *C* that is withdrawn does not need to be separated subsequently. The logic described here to withdraw additional intermediate streams from the HMA-section is extendable to any HMA. All possible useful intermediate streams that may be drawn from HMAs of Figures 5.4, 5.5, 5.6 and 5.7 are shown in Figures 5.18, 5.19, 5.20 and 5.21 by dotted rightward arrows. If such an arrow is absent from any HMA (for e.g, Figure 5.18(a)), it means that a useful (in terms of heat duty) intermediate stream is not available for withdrawal. This way of drawing intermediate streams leads to a further set of new configurations characterized by HMAs with additional intermediate streams. For example, in the configurations of Figures 5.10(d), 5.13(b) and 5.14(b), any/all intermediate streams from the respective HMAs may be withdrawn as shown in Figures 5.19(e), 5.18(b) and 5.20(e) respectively. These configurations, when optimized, can result in larger heat duty savings than reported in the previous sections, improving the savings from the use of HMAs.

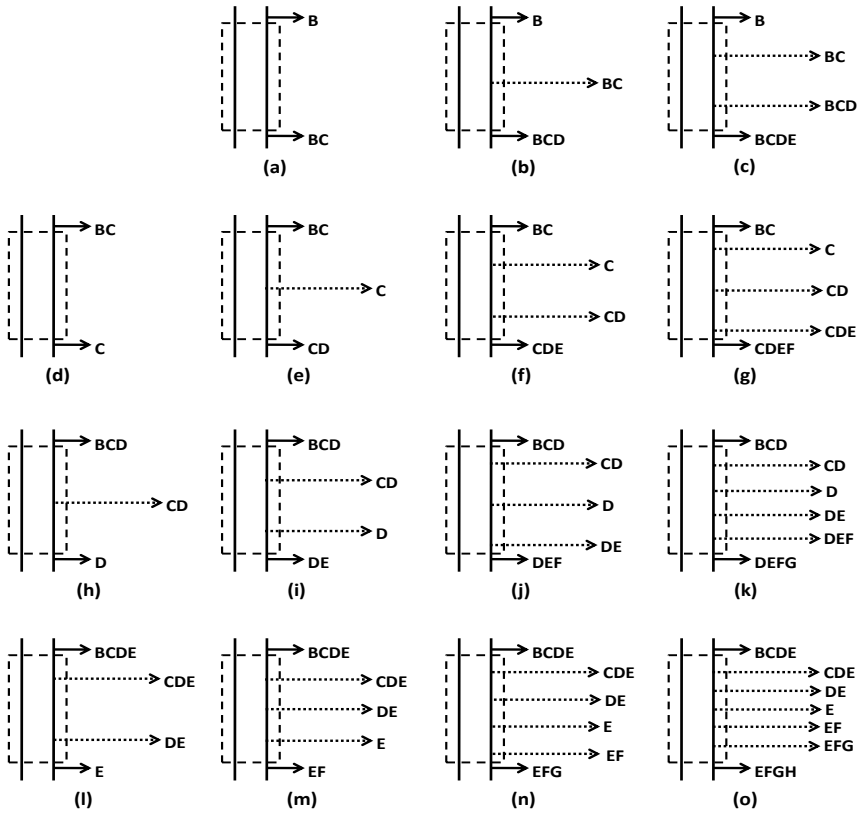

Figure 5.20 Additional streams shown for the one-overlap HMAs of Figure 5.5.

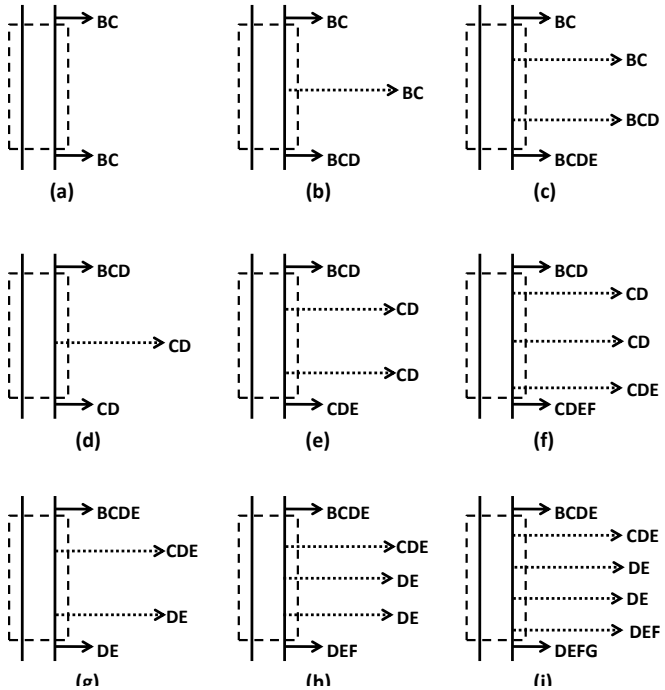

Figure 5.19 Additional streams shown for the two-overlap HMAs of Figure 5.6.

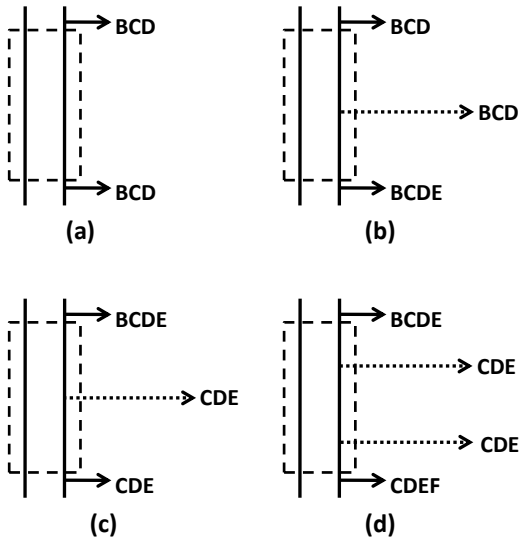

Figure 5.21 Additional intermediate streams shown for the three-overlap HMAs of Figure 5.7.

5.10 Conclusions

We have extended our earlier study by Shenvi et al.[17] on heat and mass integration links that use additional sections, called the HMAs. Here, we propose a new framework for consolidating columns in a configuration, and it is unlike the conventional approach which only consolidates columns that produce streams with the same components. The conventional approach turns out to be a special case of the multitude of possible HMAs that result from our new framework. The usage of an HMA in a configuration eliminates one reboiler, one condenser, one distillation column, multiple connecting streams and valves from the parent configuration, and reduces its overall heat duty requirement.

First, we introduced a systematic method to identify and enumerate all HMAs for an *n*-component feed. We then demonstrated a method to exhaustively draw all configurations containing HMAs. For this purpose, we modified Step 6 of

the Shah and Agrawal's method used to draw basic configurations with (n-1) columns. Sometimes, the use of HMAs leads to configurations with less than (n-1) columns, which still produce pure products. Finally, we studied the functional characteristics of HMAs to determine their operational behavior, and verified their suitability for onsite implementation.

Through several examples, we demonstrated that HMAs have significant potential in saving heat duty. We also distinguished the heat duty savings due to heat integration from those due to mass integration in an HMA. In particular, the mass integration alters compositions in a way that makes the separations in the subsequent distillation columns less energy-intensive. Further, we also discussed mechanisms to minimize temperature level penalties that result from introducing HMAs. In addition, we identified opportunities to withdraw intermediate streams from the HMA-section which can further reduce heat duty.

Considering their capital cost and operating cost saving potential, configurations with HMAs need to be included in the search space of multicomponent distillation configurations. This warrants the development of a method that systematically evaluates their total cost for separating a given feed.

References

1. Petlyuk FB, Platonov VM, Slavinskii DM. Thermodynamically Optimal Method for Separating Multicomponent Mixtures. Int Chem Eng. 1965;5(3):555-561.
2. Sargent, R.W.H.; Gaminibandara, K. Optimum Design of Plate Distillation Columns. In Optimization in Action; Dixon. L.W.C. Ed.; Academic Press: London, 1976; 267-314.
3. Agrawal, R. Synthesis of Distillation Column Configurations for a Multicomponent Separation. Ind. Eng. Chem. Res. 1996, 35 (4), 1059.
4. Caballero, J.A.; Grossmann, I.E. Generalized Disjunctive Programming Model for the Optimal Synthesis of Thermally Linked Distillation Columns. Ind. Eng. Chem. Res. 2001, 40 (10), 2260.
5. Agrawal R. Synthesis of Multicomponent Distillation Column Configurations. AIChE J. 2003, 49 (2), 379.
6. Rong, B.; Kraslawski, A.; Turunen, I. Synthesis of Functionally Distinct Thermally Coupled Configurations for Quaternary Distillation. Ind. Eng. Chem. Res. 2003, 42 (6), 1204.
7. Fidkowski, Z.T. Distillation Configurations and their Energy Requirements. AIChE J. 2006, 52 (6), 2098.
8. Ivakpour, J.; Kasiri, N. Synthesis of Distillation Column Sequences for Nonsharp Separations. Ind. Eng. Chem. Res. 2009, 48 (18), 8635.
9. Giridhar, A.V.; Agrawal, R. Synthesis of Distillation Configurations: II. A Search Formulation for Basic Configurations. Comp. Chem. Eng. 2010, 34 (1), 84.
10. Shah, V.H.; Agrawal, R. A Matrix Method for Multicomponent Distillation Sequences. AIChE J. 2010, 56 (7), 1759.
11. Shah, V.H.; Agrawal, R. Conceptual Design of Zeotropic Distillation Processes in: Gorak, A.; Sorensen, E. (Editors). Distillation: Fundamentals and Principles; Academic Press, 2014.
12. Brugma, A.J. Process and Device for Fractional Distillation of Liquid Mixtures, More Particularly Petroleum. 1942. US Patent 2,295,256.
13. Kaibel, G. Distillation Columns with Vertical Partitions. Chem. Eng. Tech. 1987, 10 (1), 92.
14. Cahn, R.P.; Di Miceli, A.G. Separation of multicomponent mixture in single tower. 1962. US Patent 3,058,893.
15. Christiansen, A.C.; Skogestad, S.; Lien, K. Partitioned Petlyuk Arrangements for Quaternary Separations. Inst. Chem. Eng. Symp. Ser. 1997, 142, 745.

16. Rong, B.; Kraslawski, A.; Turunen, I. Synthesis of Heat-Integrated Thermally Coupled Distillation Systems for Multicomponent Separations. Ind. Eng. Chem. Res. 2003, 42 (19), 4329.

17. Shenvi, A.A.; Shah, V.H.; Agrawal, R. New Multicomponent Distillation Configurations with Simultaneous Heat and Mass Integration. AIChE J. 2013, 59 (1), 272.

18. Madenoor Ramapriya, G.; Tawarmalani, M.; Agrawal, R. Modified basic distillation configurations with intermediate sections for energy savings. AIChE J. 2014, 60 (3), 1091.

19. Nallasivam, U.; Shah, V.H.; Shenvi, A.A.; Tawarmalani, M.; Agrawal, R. Global Optimization of Multicomponent Distillation Configurations: 1. Need for a Global Minimization Algorithm. AIChE J. 2013, 59 (3), 971.

20. Underwood, A.J.V. Fractional Distillation of Multicomponent Mixtures. Chem. Eng. Prog. 1948, 44 (8), 603.

21. Bjorner, A.; Stanley, R.P. Bijective proofs in: A combinatorial miscellany, L'enseignement mathématique, Monograph no. 42, Genève, (2010), 11.

CHAPTER 6. REMIXING LOSSES DUE TO CONSOLIDATION OF DISTILLATION COLUMNS

Energy penalty due to remixing of separated components is observed often in distillation configurations. To avoid these remixing losses, alternative column-consolidation strategies using the *parallel-feed arrangement, cross-feed arrangement and parallel-feed+section arrangement* have been suggested in the literature. In this work, we make a thorough comparison of these alternatives to understand when they are useful, and when they are not. To make this extensive comparison quickly using short-cut methods, we develop new procedures. A direct consequence of this work is the ability to determine the global minimum vapor duty of certain configurations with more than one feed. We have observed that energy penalties can be as high as 25% due to remixing effects in the conventional configurations over the studied alternatives. Finally, we show that the parallel-feed arrangement and parallel-feed+section arrangement, though independently proposed in the literature, are equivalent to each other.

6.1 Introduction

Consider a feed mixture containing the four components: *A*, *B*, *C* and *D*. Figure 6.1(a) shows a possible distillation configuration to separate this mixture. To reduce the heat duty and capital costs of this configuration, multiple distillation columns of the configuration can be consolidated into fewer columns. The conventional column-consolidation used in the literature is demonstrated in Figure 6.1(b).[1-11] In Figure 6.1(a), the bottom product of Column 2 and top product of Column 3 are streams containing components *B* and *C*. These two

columns are combined, and a single *BC* stream is withdrawn from the resulting Column 2 of Figure 6.1(b). Interestingly, while the described column-

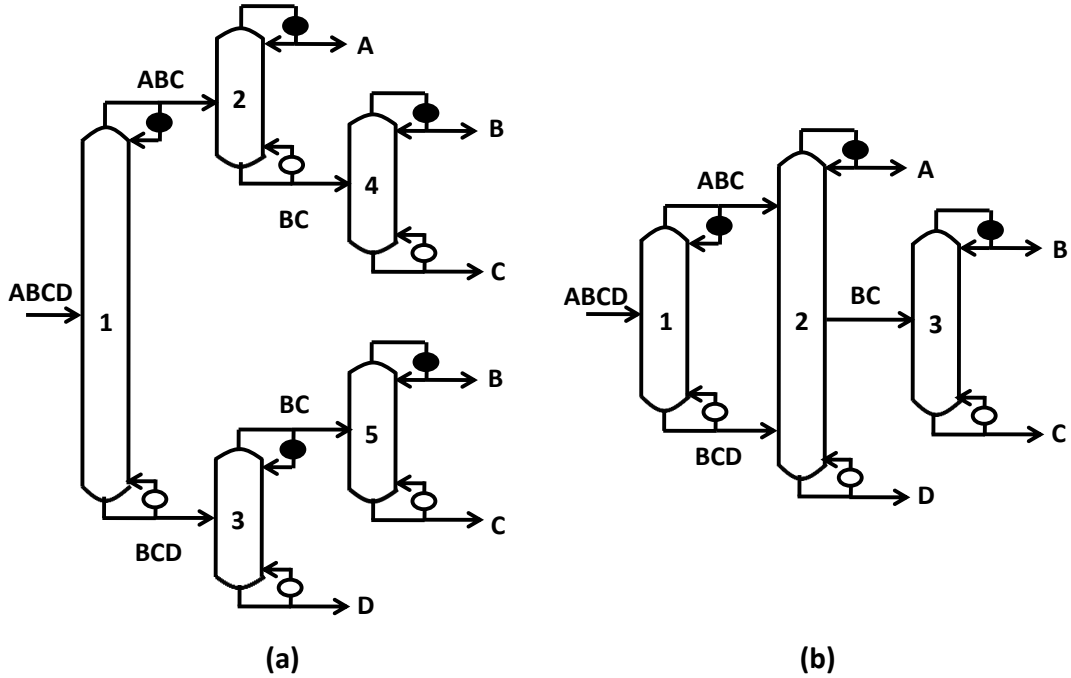

Figure 6.1 (a) A feed mixture *ABCD* separated into pure products using five distillation columns; (b) A three-column configuration to separate the feed mixture *ABCD*, obtained after consolidating columns of (a) by the conventional method.

consolidation is intended to reduce heat duty by sharing heat between multiple splits, it has some unintended accompanying heat duty penalty due to remixing of separated components. For example, in Figure 6.1(b), the components *B* and *C* in *ABC*, and the components *B* and *C* in *BCD* are isolated from each other after the separation in the first distillation column. When a single *BC* stream is withdrawn from the second column, the already separated components are remixed which leads to some inefficiency. Such a scenario arises whenever a

submixture is simultaneously produced from a rectifying and stripping section of a consolidated column.

To avoid the above described remixing losses, alternate column-consolidations have been suggested in the literature. Caballero and Grossmann[12,13] suggested the two-feed thermally coupled arrangements shown in Figures 6.2(a) and 6.2(b). Another column-consolidation, as suggested by Madenoor Ramapriya et al.[14] is shown in Figure 6.2(c). This figure uses 2 *two-*

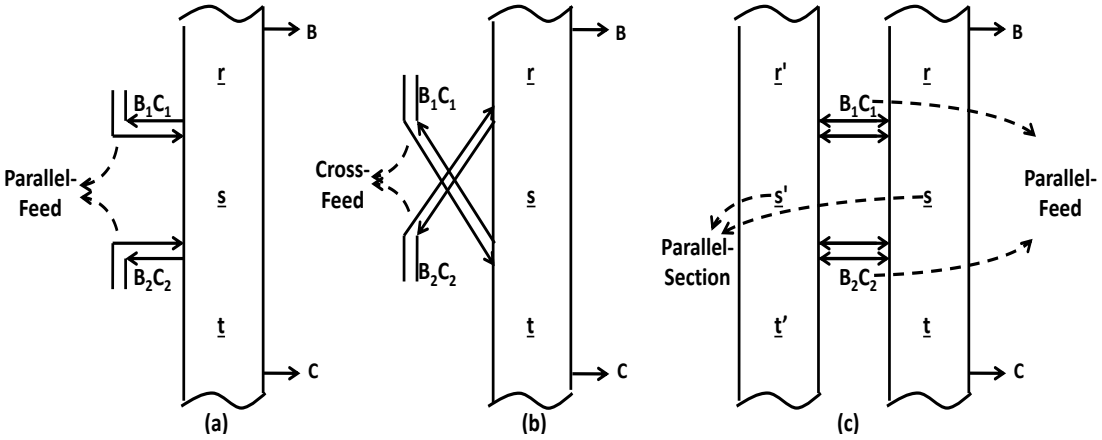

Figure 6.2 (a) Parallel-feed arrangement; (b) Cross-feed arrangement; (c) Parallel-feed+section arrangement.

way communication sets, one for B_1C_1 and another for B_2C_2. The definitions of a two-way communication set and other terms frequently used in this chapter are provided in Appendix F. In the arrangements of Figure 6.2, the proportion of *B* and *C* in the two submixtures B_1C_1 and B_2C_2 can differ, somewhat minimizing the losses due to remixing of the separated components. Following the suggestions in Figure 6.2, the configuration in Figure 6.1(a) can be redrawn as shown in Figures 6.3(b(i)), 6.4 and 6.5(a). In this chapter, for easy repeated reference, the

arrangements of Figures 6.2(a), 6.2(b) and 6.2(c) shall be referred to as the *parallel-feed arrangement*, *cross-feed arrangement* and *parallel-feed+section arrangement* respectively. Any configuration with these arrangements shall be referred to as a *parallel-feed configuration, cross-feed configuration* and *parallel-feed+section configuration* accordingly.

While Caballero and Grossmann[12,13], and Madenoor Ramapriya et al.[14] suggested the respective column-consolidation schemes, neither made a comprehensive study to indicate when such consolidations are useful compared to conventional column-consolidation. A comprehensive comparative study of this kind has its challenges. For such a detailed study, using a commercial process simulator like ASPEN Plus® for evaluation and comparison is a time-consuming exercise, and hence impractical. Instead, to use a short-cut method like that of Underwood's equations[15] for evaluation and comparison, configurations such as the one shown in Figure 6.3(b(i)) are not amenable to its application. This is because the Underwood's equations are only applicable to columns/splits with one feed, one top product and one bottom product. Though a short-cut procedure for comparative evaluation is practical, such a method is currently unavailable for configurations with the arrangements of Figure 6.2.

The objective of this chapter is to analyze the efficacy of all the column-consolidation strategies discussed so far in the chapter using short-cut methods. We do so by examining in detail the relevant configurations for four-component mixtures. To conduct this study, we modify the Underwood's method

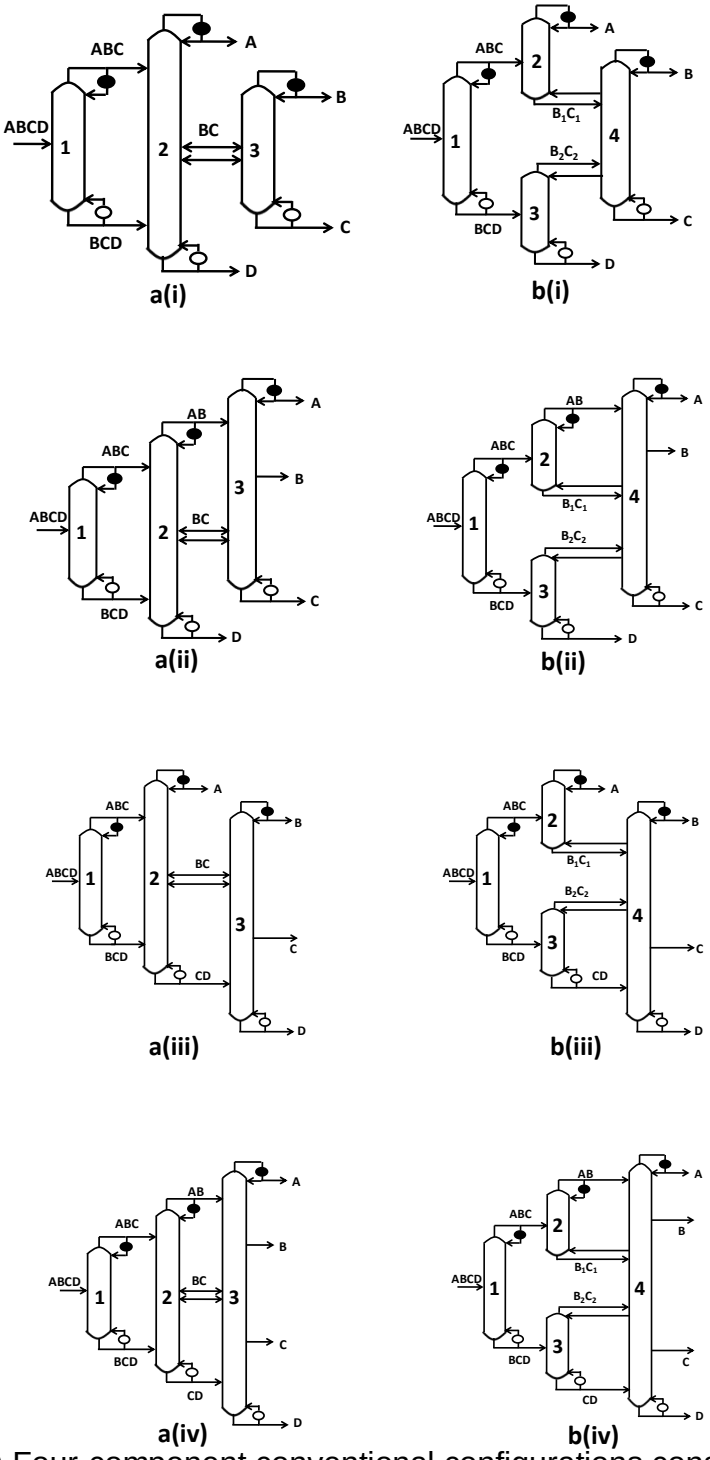

Figure 6.3 (a) Four-component conventional configurations considered for the study; (b) Parallel-feed counterparts of (a).

appropriately to make it extendible to the configurations of interest. Then, the

configurations are analyzed for a variety of feed conditions. Such a study provides an understanding of when the remixing effects due to conventional

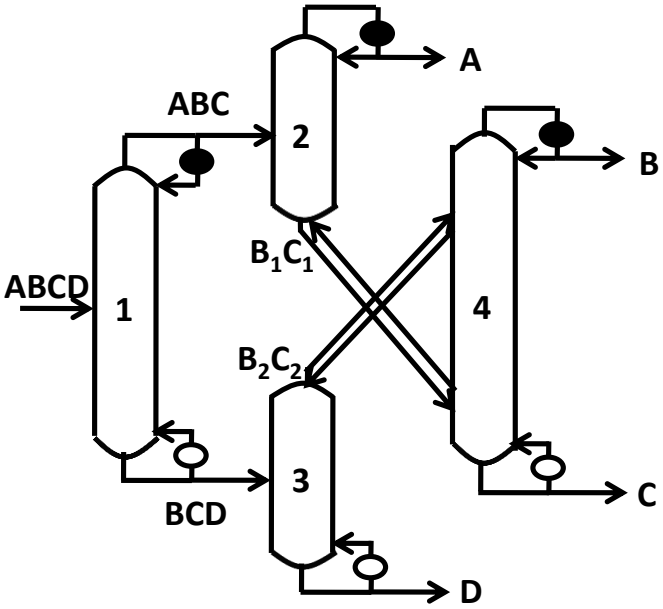

Figure 6.4 Configuration obtained when the columns of Figure 1(a) are consolidated using the cross-feed arrangement.

column-consolidation have negligible impact on the total heat duty. Enroute this exercise, we also answer the curious question of how the fully thermally coupled (FTC) configuration performs in comparison to its counterparts with the parallel-feed, cross-feed and parallel-feed+section arrangements.

6.2 Mathematical model

For a given feed *ABCD*, *BC* is the only submixture in four-component configurations that can be produced simultaneously from a stripping section and a rectifying section. Exactly, there are four such unique scenarios/sequence-of-splits for the four-component case. In each of these scenarios, one of the earlier

described column-consolidations could be used. Refer to Figure 6.3 for more details. In the figure, Set (a) shows configurations which use the conventional column-consolidation, while Set (b) shows their parallel-feed counterparts. Similarly, the cross-feed and parallel-feed+section variants of each of these configurations can be easily drawn.

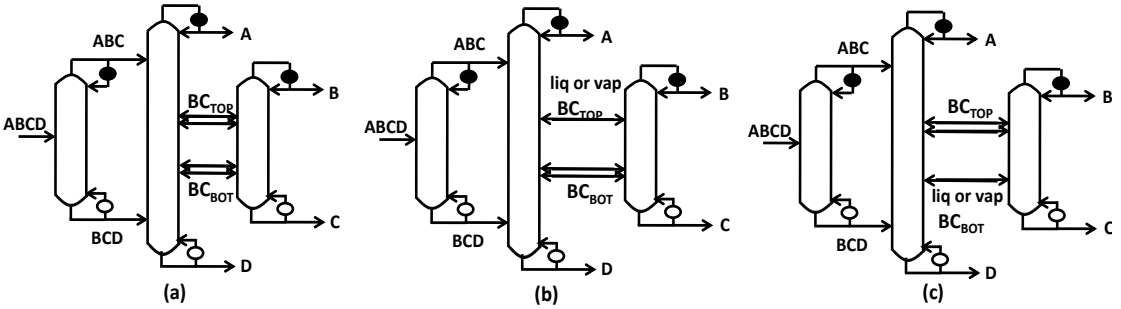

Figure 6.5 (a) Obtained when the columns of Figure 6.1(a) are consolidated using the parallel-feed+section arrangement; Configuration of (a) with one transfer-stream (either liquid or vapor) eliminated from (b) BC_{TOP}; (c) BC_{BOT}.

Having enumerated all the pertinent scenarios, the next step is their evaluation. For evaluation, we first consider the conventional, parallel-feed and cross-feed configurations in this section. The parallel-feed+section configurations will be studied in a latter section.

The total minimum vapor requirement of a configuration is a good indicator of the operating costs and capital costs of a configuration on a plant. So, we use the total minimum vapor requirement of a configuration as a metric for our comparative evaluation. Since each configuration of Set (a) in Figure 6.3 is composed of individual splits with one feed, one top and bottom product, Underwood's equations are applicable to each column. So, we use the Global

Minimization Algorithm (GMA)[16,17] to calculate the overall minimum vapor duty requirement of this set. GMA is a global optimization procedure for determining the minimum vapor duty of a configuration based on the Underwood's equations. The detailed mathematical description of the GMA model is available in References 16 and 17, and is not elaborated here. Observe that, in the configurations of Set (b) in Figure 6.3, the Underwood's equations are still applicable to all columns of the configuration, except the final one due to the parallel-feed (or otherwise cross-feed) arrangement. So, we modify the GMA only to model the two-feed arrangements of Figures 6.2(a) and 6.2(b).

Note that the three sections of the two-feed arrangements shown in Figures 6.2(a) and 6.2(b) are binary sections. In other words, there are no more than two components in the liquid/vapor flowing in these three sections. Therefore, the sections r, s and t of Figures 6.2(a) and 6.2(b) can be represented on the McCabe-Thiele diagram.[18] The underlying assumptions of the McCabe-Thiele representation (of ideal mixtures and constant molar flows) are the same as that for Underwood's equations. So, we construct operating lines, q-lines, etc. on the McCabe-Thiele diagram for the three sections of Figures 6.2(a) and 6.2(b), and incorporate the corresponding equations into the optimization model of GMA.

Take any configuration containing the parallel-feed arrangement of Figure 6.2(a) as an example. The optimized vapor flows in sections r, s and t should be greater than or equal to the cases when the final column pinches at any of its feeds. This condition is enforced in the model for all feeds to the column except

B_1C_1 and B_2C_2 using the Underwood's equations, and is part of GMA. For feeds B_1C_1 and B_2C_2, we use the McCabe-Thiele constructions. When the column pinches at feed B_1C_1, as shown in Figure 6.6(a), the q-line (F_{B1C1}) and operating line for section r (PQ) intersect on the equilibrium curve. Likewise, when the final

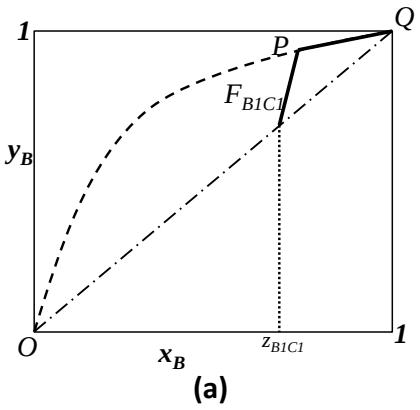

$Q_{B1C1} = \frac{L_{B1C1}}{L_{B1C1} - V_{B1C1}}$	Quality of feed B_1C_1
$Z_{B1C1} = \frac{b1}{b1+c1}$	Overall composition of B in B_1C_1
$y_P = \frac{Q_{B1C1}}{Q_{B1C1}-1} x_P - \frac{Z_{B1C1}}{Q_{B1C1}-1}$	P lies on feed line of B_1C_1
$y_P = \frac{\alpha_{BC}}{1+(\alpha_{BC}-1)x_P} x_P$	P lies on the equilibrium curve
$M_r = b1 + b2$	Net mass flow in section r of Figure 2
$m_{PQ} = \frac{V_{rB\,1C1pin} - M_r}{V_{rB\,1C1pin}} = \frac{1-y_P}{1-x_P}$	Slope of operating line PQ, of section r
$V_r \geq V_{rB1C1pin}$	Minimum vapor flow requirement in Section r

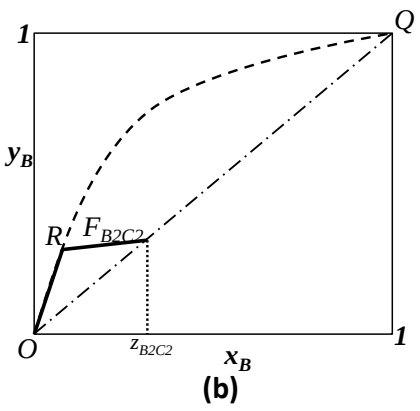

$Q_{B2C2} = \frac{-L_{B2C2}}{V_{B2C2} - L_{B2C2}}$	Quality of feed B_2C_2
$Z_{B2C2} = \frac{b2}{b2+c2}$	Overall composition of B in B_2C_2
$y_R = \frac{Q_{B2C2}}{Q_{B2C2}-1} x_R - \frac{Z_{B2C2}}{Q_{B2C2}-1}$	R lies on feed line of B_2C_2
$y_R = \frac{\alpha_{BC}}{1+(\alpha_{BC}-1)x_R} x_R$	R lies on the equilibrium curve
$M_t = c1 + c2$	Net mass flow in section t of Figure 2
$m_{OR} = \frac{V_{tB\,2C2pin} + M_t}{V_{tB\,2C2pin}} = \frac{y_R}{x_R}$	Slope of operating line OR, of section t
$V_t \geq V_{tB2C2pin}$	Minimum vapor flow requirement in Section t

Figure 6.6 McCabe-Thiele constructions for the parallel-feed arrangement of Figure 6.2(a) when the final column pinches at feed (a) B_1C_1; (b) B_2C_2.

column pinches at feed B_2C_2, as shown in Figure 6.6(b), the q-line (F_{B2C2}) and operating line for section t (OR) intersect on the equilibrium curve. A description of the variables used in the figure are provided in Appendix G. The equations representing the constructions in Figures 6.6(a) and 6.6(b) are shown alongside

the figures. Thus, to the original GMA model, these equations are added to ensure that vapor flows in the sections r, s and t are greater than or equal to the cases when the final column pinches at either of its two feeds, B_1C_1 or B_2C_2. To avoid singularities in the algorithm, some of these equations are cross-multiplied and then implemented, involving products of certain variables.

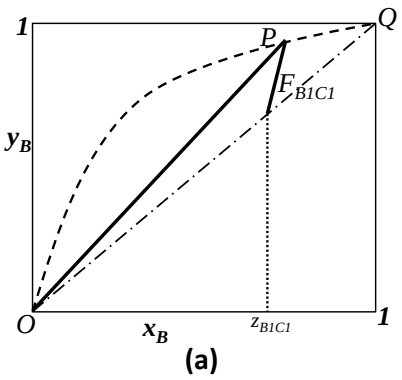

$Q_{B1C1} = \frac{L_{B1C1}}{L_{B1C1} - V_{B1C1}}$	Quality of feed B_1C_1
$Z_{B1C1} = \frac{b1}{b1+c1}$	Overall composition of B in B_1C_1
$y_P = \frac{Q_{B1C1}}{Q_{B1C1}-1} x_P - \frac{Z_{B1C1}}{Q_{B1C1}-1}$	P lies on feed line of B_1C_1
$y_P = \frac{\alpha_{BC}}{1+(\alpha_{BC}-1)x_P} x_P$	P lies on the equilibrium curve
$M_t = c1 + c2$	Net mass flow in section t of Figure 2
$m_{OP} = \frac{V_{tB1C1pin} + M_t}{V_{tB1C1pin}} = \frac{y_P}{x_P}$	Slope of operating line OP, of section t
$V_t \geq V_{tB1C1pin}$	Minimum vapor flow requirement in Section t

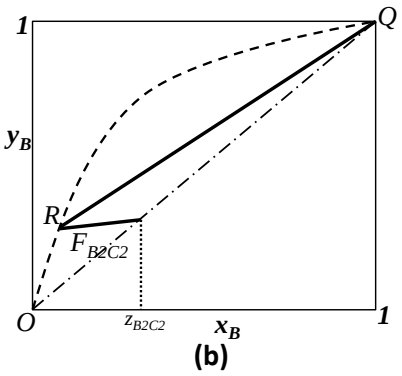

$Q_{B2C2} = \frac{-L_{B2C2}}{V_{B2C2} - L_{B2C2}}$	Quality of feed B_2C_2
$Z_{B2C2} = \frac{b2}{b2+c2}$	Overall composition of B in B_2C_2
$y_R = \frac{Q_{B2C2}}{Q_{B2C2}-1} x_R - \frac{Z_{B2C2}}{Q_{B2C2}-1}$	R lies on feed line of B_2C_2
$y_R = \frac{\alpha_{BC}}{1+(\alpha_{BC}-1)x_R} x_R$	R lies on the equilibrium curve
$M_r = b1 + b2$	Net mass flow in section r of Figure 2
$m_{RQ} = \frac{V_{rB2C2pin} - M_r}{V_{rB2C2pin}} = \frac{1-y_R}{1-x_R}$	Slope of operating line RQ, of section r
$V_r \geq V_{rB2C2pin}$	Minimum vapor flow requirement in Section r

Figure 6.7 McCabe-Thiele constructions for the cross-feed arrangement of Figure 6.2(b) when the final column pinches at feed (a) B_1C_1; (b) B_2C_2.

The cross-feed arrangement of Figure 6.2(b) is modeled very similar to the parallel-feed arrangement of Figure 6.2(a). For the cross-feed arrangement, the McCabe-Thiele constructions when the final column pinches at feeds B_1C_1 and B_2C_2 are presented respectively in Figures 6.7(a) and 6.7(b). The equations

corresponding to the constructions are presented alongside the respective figures. These equations are incorporated into GMA to model the cross-feed configurations.

6.3 Results and discussion

In this section, we use GMA (and its modified version) with a tolerance of 0.001 to compare the overall minimum vapor requirement of the two sets of configurations in Figure 6.3. For an exhaustive comparison, 120 saturated liquid feed conditions[9] are used. Eight different sets of relative volatilities corresponding to all combinations of easy-difficult separations between individual components in the feed, are shown in Table 3.2. Fifteen different compositions corresponding to all combinations of plentiful-lean flowrates in each component in the feed are shown in Table 3.3.

On evaluation, we observe for all 120 feed conditions that, the parallel-feed configurations have a minimum vapor duty requirement lower than or equal to their corresponding conventional configurations. To better understand the efficacy of conventional column-consolidation, we present the following results. Table 6.1 shows the number of instances out of 120 when the vapor duty penalty due to remixing in the conventional configuration is less than 2% and 5% over the corresponding parallel-feed configuration. From the table, for scenarios (b), (c) and (d) of Figure 6.3, the penalty due to remixing in the conventional column-consolidation is less than 5% in comparison to the parallel-feed arrangement for

most feed conditions. On the flip-side, the two worst case vapor duty penalties are shown in Figure 6.8. The table and the figure clearly suggest that the penalty

Table 6.1 Number of instances of vapor duty penalty less than 2% and 5% in the configurations of Figure 6.3(a) compared to those in Figure 6.3(b).

Scenario	**# < 2%**	**# < 5%**
(i)	57	77
(ii)	96	114
(iii)	98	112
(iv)	111	118

due to remixing in the conventional consolidation is more pronounced when both the consolidated splits are sharp splits. For such cases, column-consolidation by the parallel-feed arrangement may be a superior option. This is reasonable to expect because, in a configuration like the one in Figure 6.3(a(i)), with two sharp splits *ABC->A/BC* & *BCD->BC\D* combined in the second distillation column, the extent of remixing of the separated components is high. However, in a configuration like the one in Figure 6.3(a(iv)), with two non-sharp splits *ABC->AB\BC* & *BCD->BC\CD* combined in the second distillation column, the remixing losses are offset by the partial distribution of components *B* and *C* to the top and bottom products respectively. Furthermore, in Figure 6.8, the feed condition [f=aBCd, α=ddd] is a common candidate to three out of the four comparisons. The frequent appearance of this feed condition is attributable to the energy-intensive separation of *B* from *C*.

Now, we present the results for the cross-feed counterparts of the configuration set (a) in Figure 6.3 for all 120 feed conditions. We observe that

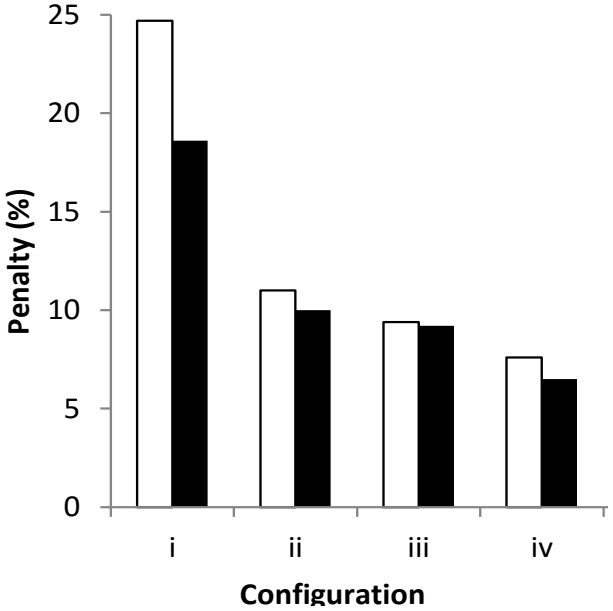

Figure 6.8 Two worst case vapor duty penalties in the configurations of Figure 6.3(a) compared to their parallel-feed counterpart.

using the cross-feed arrangement in place of the conventional column-consolidation never reduces the vapor duty requirement, instead, in many cases, the vapor duty of the configuration increases. In fact, in the worst case, an increase in vapor duty requirement by more than 250% is observed. Hence, the cross-feed column-consolidation should be disregarded for multi-component distillation.

6.4 Does the n-component Petlyuk column have the least heat duty?

An interesting question that arises as a follow-up to the prior study is: what happens when the parallel-feed arrangement is used in the conventional fully

thermally coupled (FTC) configuration? This is an interesting question to answer because the conventional FTC configuration with $n(n\text{-}1)$ sections is historically known to consume the least vapor duty for any given n-component separation (without heat integration).[1,19-21] Here, we investigate how its parallel-feed counterpart, which has $(3n^2\text{-}7n\text{+}6)/2$ sections (this number is derived in Appendix H) performs in terms of overall vapor duty. To do this, we again use the four-component example (Figure 6.9). Figures 6.9(a) and 6.9(b) respectively show the FTC configurations with 12 and 13 sections, while Figure 6.9(c) shows the dividing wall column implementation of the configuration in Figure 6.9(b).

On evaluation using the model, we observe that the vapor duty requirements of the two configurations in Figures 6.9(a) and 6.9(b) are exactly

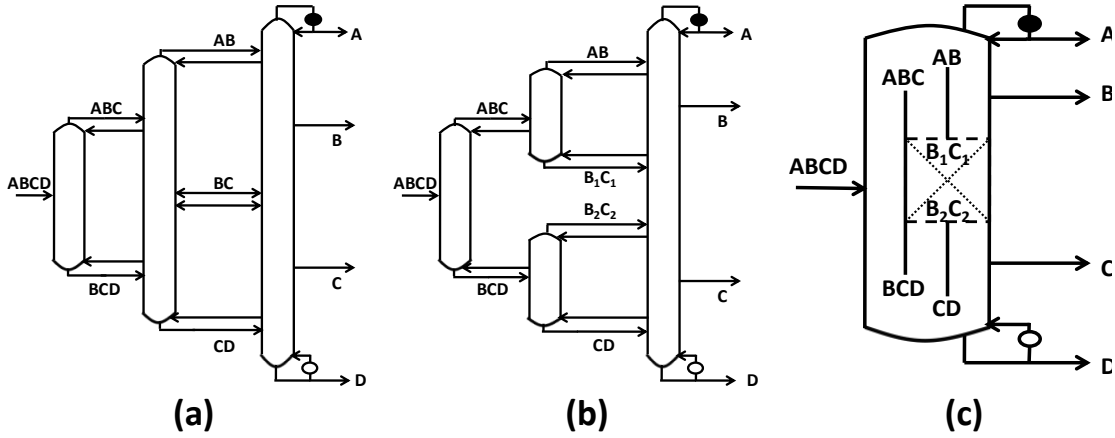

Figure 6.9 (a) 4-component FTC configuration; (b) Parallel-feed counterpart of (a); (c) Dividing wall column implementation of (b).

the same for all 120 feed conditions. This observation can be explained by the following reasoning. For the transition split of the four-component FTC configuration in Figure 6.9(a), Halvorsen and Skogestad[21] showed that the

natural *BC* liquid composition in the stripping section of the *ABC->AB/BC* split, and the natural *BC* liquid composition in the rectifying section of the *BCD->BC/CD* split are equal. Hence, the remixing losses are absent when these two splits are combined into a single column as in Figure 6.9(a). The parity in *BC* liquid compositions from the stripping and rectifying sections is achieved due to the Underwood's root transfer from the first column to the second.[21] So, when this root transfer does not happen, that is, when the assumptions of the Underwood's method (infinite equilibrium stages, ideal mixtures and equality in latent heats) are relaxed, it would interesting to explore whether the additional distillation section in Figure 6.9(b)/(c) could be utilized for some useful separation, leading to a reduced heat duty compared to the configuration in Figure 6.9(a).

6.5 Parallel-feed+section arrangement

In this section, we study the column-consolidation by parallel-feed+section arrangement of Figure 6.2(c). While the use of parallel-feed arrangement (Figure 6.2(a)) for column-consolidation results in configurations with more than *n*-1 columns for distilling an *n*-component feed mixture, the use of parallel-feed+section arrangement (Figure 6.2(c)) for column-consolidation always results in *n*-1 columns. Furthermore, in Appendix I, we show that column-consolidation by parallel-feed arrangement and parallel-feed+section arrangement are *equivalent* to each other, and hence the configurations synthesized from the two consolidation schemes have the same heat duty. So, the heat duty comparisons

made in prior sections for parallel-feed configurations also hold for their parallel-feed+section counterparts. Another interesting result follows from the analysis in Appendix I. To maintain equivalence with the parallel-feed arrangement, in the parallel-feed+section arrangement, unlike what is shown in Figure 6.2(c), it is sufficient to use only one two-way communication set, at either B_1C_1 or B_2C_2. If a two-way communication set is used at B_1C_1, then, B_2C_2 simplifies to a *two-way communication* (defined in Appendix F) in either the liquid or vapor phase, and vice versa. This insight could be useful from an operational perspective. As examples, Figures 6.5(a), 6.5(b) and 6.5(c) show all versions of the parallel-feed+section arrangement used to consolidate the columns of Figure 6.1(a), and are always equivalent to the parallel-feed configuration of Figure 6.3(b(i)).

6.6 Conclusions

In many configurations, there are instances where submixtures containing the same components are produced simultaneously from a rectifying and stripping section. Such sections are usually combined, which may incur a energy penalty due to remixing of the separated components. To overcome such penalties, the use of parallel-feed, cross-feed and parallel-feed+section arrangements suggested in the literature, were investigated extensively in the chapter. Due to unavailability of short-cut methods to thoroughly evaluate these arrangements, we devised a new methodology. We integrated the McCabe-Thiele method with the Underwood's equations into an optimization model. The

model precisely determines the global minimum total vapor requirement of the parallel-feed and cross-feed configurations.

We found the parallel-feed configurations to have a total vapor duty requirement lower than or equal to the corresponding conventional configuration, while the cross-feed configurations had a vapor duty greater than or equal to the corresponding conventional configuration. So, the cross-feed configurations can be discarded from the search space of distillation configurations. On the other hand, the parallel-feed arrangements are likely most useful when a submixture is produced simultaneously from two sharp splits, followed by when the submixture is produced from one sharp and one non-sharp split, and the least when the submixture is produced simultaneously from two non-sharp splits.

Finally, we showed that the parallel-feed arrangement is equivalent to the parallel-feed+section arrangement, and hence configurations with the two arrangements have the same heat duty. So, the heat duty benefits of the parallel-feed arrangement, which uses more than n-1 columns, can always be retrieved in n-1 columns using the parallel-feed+section arrangement.

References

1. Petlyuk FB, Platonov VM, Slavinskii DM. Thermodynamically Optimal Method for Separating Multicomponent Mixtures. International Chemical Engineering. 1965;5(3):555-561.
2. Sargent RWH, Gaminibandara K. Optimum Design of Plate Distillation Columns. In: Optimization in Action. Dixon LCW, Ed., New York: Academic Press, 1976:267-314.
3. Agrawal R. Synthesis of Distillation Column Configurations for a Multicomponent Separation. Ind Eng Chem Res. 1996;35(4):1059-1071.
4. Caballero JA, Grossmann IE. Generalized Disjunctive Programming Model for the Optimal Synthesis of Thermally Linked Distillation Columns. Ind Eng Chem Res. 2001;40(10):2260-2274.
5. Agrawal R. Synthesis of Multicomponent Distillation Column Configurations. AIChE J. 2003;49(2):379-401.
6. Rong B, Kraslawski A, Turunen I. Synthesis of Functionally Distinct Thermally Coupled Configurations for Quaternary Distillation. Ind Eng Chem Res. 2003;42(6):1204-1214.
7. Fidkowski ZT. Distillation Configurations and their Energy Requirements. AIChE J. 2006;52(6):2098-2106.
8. Ivakpour J, Kasiri N. Synthesis of Distillation Column Sequences for Nonsharp Separations. Ind Eng Chem Res. 2009;48(18):8635-8649.
9. Giridhar AV, Agrawal R. Synthesis of Distillation Configurations: I. Characteristics of a Good Search Space. Comput Chem Eng. 2010;34(1):73-83.
10. Giridhar AV, Agrawal R. Synthesis of Distillation Configurations: II. A Search Formulation for Basic Configurations. Comput Chem Eng. 2010;34(1):84-95.
11. Shah VH, Agrawal R. A Matrix Method for Multicomponent Distillation Sequences. AIChE J. 2010;56(7):1759-1775.
12. Caballero JA, Grossmann IE. Design of Distillation Sequences: From Conventional to Fully Thermally Coupled Distillation Systems. Comput Chem Eng. 28(11):2307-2329, 2004.
13. Caballero JA, Grossmann IE. Structural considerations and modeling in the synthesis of heat-integrated-thermally coupled distillation sequences. Ind Eng Chem Res. 2006;45:8454–8474.
14. Madenoor Ramapriya G, Tawarmalani M, Agrawal R. Modified basic distillation configurations with intermediate sections for energy savings. AIChE J. 2014;60(3):1091.

15. Underwood AJV. Fractional Distillation of Multicomponent Mixtures. Chem Eng Prog. 1948;44(8):603-614.

16. Nallasivam U, Shah VH, Shenvi AA, Tawarmalani M, Agrawal R. Global Optimization of Multicomponent Distillation Configurations: 1. Need for a Global Minimization Algorithm. AIChE J. 2013;59(3):971-981.

17. Nallasivam U, Shah VH, Shenvi AA, Tawarmalani M, Agrawal R. Global Optimization of Multicomponent Distillation Configurations: 2. Enumeration based global minimization algorithm. AIChE J. 2016;62(6):2071–2086.

18. McCabe WL, Thiele EW. Graphical Design of Fractionating Columns, Ind Eng Chem Res. 1925;17(6):605–611.

19. Fidkowski ZT, Krolikowski L. Thermally coupled system of distillation columns: optimization procedure. AIChE J. 1986;32:537–546.

20. Fidkowski ZT, Agrawal R. Multicomponent thermally coupled systems of distillation columns at minimum reflux. AIChE J. 2001;47:2713–2724.

21. Halvorsen IJ, Skogested S. Minimum Energy Consumption in Multicomponent Distillation. 3. More Than Three Products and Generalized Petlyuk Arrangements. Ind Eng Chem Res. 2003;42:605-615.

CHAPTER 7. SHORT-CUT METHODS VERSUS RIGOROUS METHODS FOR PERFORMANCE EVALUATION OF DISTILLATION CONFIGURATIONS

A detailed ASPEN Plus study was performed to demonstrate that the relative total minimum heat duty requirement of distillation configurations based on assumptions of ideal mixtures and constant molar overflow (CMO), compares favorably to results obtained using ASPEN Plus. This exercise validates the use of ideal-mixture and CMO assumptions to model the minimum energy requirements of real world zeotropic distillation applications as a first step to identify the top few energy-efficient configurations.

7.1 Introduction

To separate a feed-mixture into a given set of product streams, several distillation configurations are possible. Many methods have been presented in the literature to systematically generate all these possible distillation configurations.[1-5]. Upon obtaining the list of feasible configurations, referred to as the distillation search space, it then becomes useful to reliably identify which arrangements from the search space correspond to desirable candidates to perform the given separation. Many criteria can be considered for this analysis, including energy consumption, thermodynamic efficiency, or total cost; different sources use different methods of calculating and optimizing based on these criteria.[3-8] In this work, we use the overall minimum heat duty requirement of a configuration as the metric for any comparison. The overall minimum heat duty

requirement of a configuration is a good indicator of the configuration's onsite operating and capital costs, and is a suitable performance estimator.

To quickly evaluate the large search space of available distillation configurations and identify the top performing candidates according to a chosen criterion, many researchers have used short-cut methods (e.g., Underwood's equations[9]) for performance evaluation based on ideal-mixture and CMO assumptions. Because of these assumptions, the short-cut methods significantly reduce evaluation-time compared to performing generalized, rigorous stage-by-stage calculations over the entire search space. However, in the distillation community, there is a long-standing doubt and skepticism about the validity of the simplifying assumptions of these short-cut methods to real world applications, and hence, the results obtained from such methods. This work attempts to clear this doubt by comparing the minimum heat duty requirement results obtained from the two approaches: the short-cut approach and the rigorous simulation based approach. In this work, we present a case study that compares the ranklists of simulated distillation configurations generated by the two approaches.

7.2 Procedure

For short-cut calculation of total minimum heat duty requirement of configurations, we use the Global Minimization Algorithm (GMA) proposed by Nallasivam et al.,[10,11]. GMA is an optimization model that determines the globally overall minimum heat duty requirement of all distillation configurations in the

search space. It uses the well-known Underwood's equations as basis, as a result of which the critical underlying assumptions of GMA are as follows:

1) Infinite number of stages in every section
2) Ideal feed mixture (implies constant relative volatility throughout the configuration)
3) Constant molar overflow

To determine minimum heat duty requirement of configurations through the rigorous stage-by-stage simulation procedure, we use the ASPEN Plus software. As the goal of this work is to test the applicability of the assumptions 2 and 3 listed above to model real systems, in order to make assumption 1 a non-factor in the comparative study, and maintain uniformity across ASPEN Plus simulations, excess stages are used in each section of all configurations. The minimum heat duty of each studied configuration from ASPEN Plus is obtained through a combination of extensive, tedious sensitivity analyses and optimization. Since this exercise is immensely time-consuming, using ASPEN Plus to obtain minimum heat duty results for the entire search space of distillation configurations (e.g., a total of 152 and 6128 configurations, respectively, for four- and five-component mixtures) is impractical. So, we limit our search space for this comparative study to the eighteen four-component basic configurations, which are shown in Figure 7.1. In all these configurations, submixtures associated with reboilers and condensers are respectively in the saturated liquid and vapor phase. All products and the *BC* submixture streams withdrawn from

the intermediate location of a distillation column (configurations ‘e’, ‘o’, ‘q’ and ‘r’ in Figure 7.1) are saturated liquids.

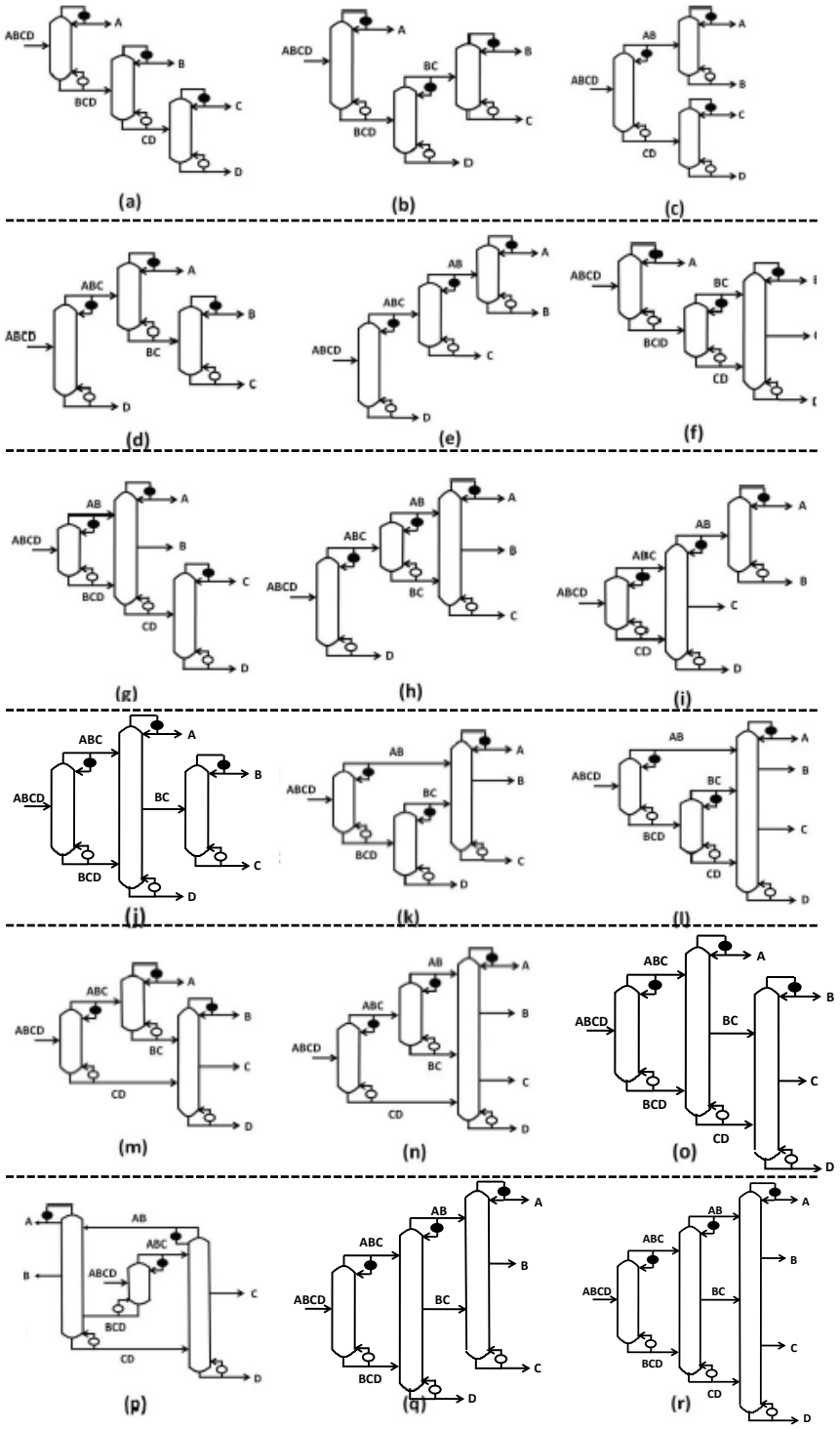

Figure 7.1 All basic configurations for separating a four-component feed mixture.

The feed to be separated, drawn from Kim and Wankat,[12] is a saturated liquid mixture of alkanes at 3 atm. The details of the composition of the components in the feed are shown in Table 7.1. We use the Peng-Robinson equation of state to model the thermodynamics of this system. With this information of the feed, the relative volatility of each component in the feed (shown in Table 7.1) is obtained from the K-values using ASPEN Plus. The feed compositions and obtained relative volatilities are the only inputs to GMA. For the ASPEN Plus simulations, the following additional specifications are made. All columns are operated at a constant pressure of 3 atm. Each product stream is required to be enriched in the respective component by at least 99.9%.

Table 7.1 Feed data.

	Component	Feed Mole Fraction	Relative Volatility w.r.t. *D* (ASPEN Plus)
A	N-butane	0.3	46.21
B	N-pentane	0.4	17.40
C	N-heptane	0.25	2.65
D	N-octane	0.05	1

7.3 Results

Table 7.2 shows the normalized (with respect to configuration ‘r’) minimum heat duties from the GMA method and ASPEN Plus simulations. The heat duty results from each approach are sorted in increasing order down the table. For easy interpretation, we divide the set of configurations into three bands: ‘attractive (A)’ (within 10% of the minimum), ‘border-line (B)’ and ‘unattractive (U)’ (more than 15% of the minimum). The most important observation to be made

from the table is that both the approaches put the same set of configurations in each band. So, the GMA approach neither misplaces a configuration that is attractive into the other bands nor does it wrongly identify an unattractive configuration as attractive. Secondly, there is a close overlap between the rank-lists generated between the two approaches. In the ‘attractive’ band, with only the exception of the position of configuration ‘o’ being different, the rest of the configurations in the band follow the same order in the two approaches, while in the ‘border-line’ band, there is very little to differentiate between configurations ‘g’ and ‘k’ in terms of heat duty. In the ‘unattractive’ band, except the configurations ‘m’ and ‘j’, the rest follow the same ranking order in both the approaches. The above results make a strong case for the applicability of the GMA method as a screening tool for identifying configurations which have low heat duty and pruning out those that don’t, even though GMA makes assumptions that ASPEN Plus does not. To understand the extent of simplification due to the underlying assumptions of GMA, we provide additional information in Table 7.3. In the table, as an example, the relative volatility values at the top and bottom stage of the first column of configuration ‘r’ from the ASPEN Plus simulation are shown. This gives a sample of the actual variation of the relative volatilities across stages of any configuration, and in this context, the matching results obtained from GMA using a single relative volatility set is significant. The simplifying assumptions would also be the reason for any disparity in the heat duty values from the two methods for any configuration in Table 7.2.

Table 7.2 Minimum heat duty results (normalized w.r.t. configuration ‘r’) from ASPEN Plus and GMA for the configurations in Figure 7.1.

		ASPEN Plus Results		GMA Results	
Rank	Band	Configuration	Normalised Heat Duty	Configuration	Normalised Heat Duty
1	**A**	r	1.000	r	1.000
2		o	1.013	n	1.036
3		n	1.021	l	1.036
4		l	1.024	p	1.058
5		p	1.068	o	1.085
6	**B**	k	1.107	g	1.101
7		g	1.109	k	1.103
8	**U**	q	1.188	q	1.242
9		i	1.199	i	1.361
10		m	1.203	f	1.364
11		f	1.226	h	1.372
12		h	1.302	m	1.422
13		c	1.352	j	1.431
14		a	1.374	c	1.439
15		j	1.385	a	1.442
16		b	1.424	b	1.450
17		e	1.438	e	1.455
18		d	1.708	d	1.763

The greatest benefit of using a short-cut method for evaluating distillation configurations over a rigorous approach is the time taken for evaluation. For our case study, we obtained the minimum heat duty requirements for the eighteen configurations using GMA in less than 1 minute. Using ASPEN Plus, to obtain the same results, we adopted a combination of optimization and an extensive, tedious sensitivity analysis for each distillation flowsheet, which took us months for completion!! In reality, even if only estimates of minimum heat duty requirements are sufficient, using rigorous, stage-by-stage methods to span the

search space of available four-component (152 in number) or five-component (6128 in number) configurations would be an immensely time-consuming exercise, and hence impractical. In contrast, a shortcut approach makes the evaluation of each configuration quick, and, as shown here, accurate for practical purposes. These key features of the short-cut approach enable a systematic, complete and reliable evaluation of the search-space of distillation configurations.

Table 7.3 Relative volatilities at the top and bottom stage of the main feed-column in configuration ‘r’.

	Component	Relative Volatility w.r.t. *D* (top stage)	Relative Volatility w.r.t. *D* (bottom stage)
A	N-butane	43.12	26.79
B	N-pentane	16.13	11.21
C	N-heptane	2.62	2.29
D	N-octane	1	1

7.4 Conclusions

The goal of this work was to test the applicability of short-cut performance-evaluation methods and their underlying assumptions to model distillation configurations. To verify this, minimum heat duty results from two approaches: the short-cut approach (GMA) and the rigorous stage-by-stage approach (ASPEN Plus) were obtained and compared for eighteen four-component basic

configurations. The configurations identified as attractive (unattractive) by the short-cut GMA method were also be found to be attractive (unattractive) from ASPEN Plus simulations. The ranklisting of the studied configurations from the two approaches was very similar. However, while the short-cut evaluation of all eighteen configurations took us less than a minute, obtaining reliable minimum heat duty results from ASPEN Plus optimization and detailed sensitivity analysis took us months. These observations establish that the short-cut method (GMA), along with its underlying assumptions, is a computationally efficient and reliable way to identify a set of distillation arrangements that operate with low heat duty requirements. This conclusion also provides a basis to use the same underlying assumptions to develop short-cut procedures for modeling exergy loss or overall cost of distillation configurations in the search-space.

References

1. Agrawal R. Synthesis of Distillation Column Configurations for a Multicomponent Separation. Ind Eng Chem Res. 1996;35(4):1059-1071.
2. Agrawal R. Synthesis of multicomponent distillation configurations. AIChE J. 2003;49:379-401.
3. Giridhar AV, Agrawal R. Synthesis of Distillation Configurations: II. A Search Formulation for Basic Configurations. Comp Chem Eng. 2010;34:84-95.
4. Caballero JA, Grossmann IE. Design of distillation sequences: from conventional to fully thermally coupled distillation systems. Comp Chem Eng. 2004;28:2307-2329.
5. Shah VH, Agrawal R. A Matrix Method for Multicomponent Distillation Sequences. AIChE J. 2010;56(7):1759-1775.
6. Hildebrandt D, Beneke DA, Abbas R, Holland ST, Very M, Glasser D. Column profile maps as a tool for synthesizing complex column configurations. Comp Chem Eng. 2010;34(9):1487–1496.
7. Sargent RWH, Gaminibandara K. (1976). Optimum design of plate distillation columns. In L.W. C. Dixon (Ed.), Optimization in action (pp. 267–314). New York: Academic Press.
8. Zou X, Cui YH, Dong HG, Wang J, Grossmann IE. Optimal design of complex distillation system for multicomponent zeotropic separations. Chem Eng Science. 2012;75:133–143.
9. Underwood AJV. Fractional Distillation of Multicomponent Mixtures. Chem Eng Prog. 1948;44(8):603-614.
10. Nallasivam U, Shah VH, Shenvi AA, Tawarmalani M, Agrawal R. Global Optimization of Multicomponent Distillation Configurations: 1. Need for a Global Minimization Algorithm. AIChE J. 2013;59(3):971-981.
11. Nallasivam U, Shah VH, Shenvi AA, Tawarmalani M, Agrawal R. Global Optimization of Multicomponent Distillation Configurations: 2. Enumeration based global minimization algorithm. AIChE J. 2016;62(6):2071–2086.
12. Kim J, Wankat PC. Quaternary Distillation Systems with Less than N − 1 Columns. Ind Eng Chem Res. 2004;43(14):3838–3846.

CHAPTER 8. A FORMULATION FOR THERMODYNAMICALLY EQUIVALENT THERMALLY COUPLED CONFIGURATIONS

In this chapter, a new formulation is presented to identify the thermodynamically equivalent thermally coupled distillation configurations. The benefits of the formulation, which is a linear integer program, are discussed. An example problem is studied to demonstrate the application of the model. Since this is a work in progress, some guidelines are presented for further progress.

8.1 Introduction

Basic configurations utilize *n*-1 distillation columns, *n*-1 reboilers and *n*-1 condensers for separating an *n*-component mixture.[1] Each submixture/product that is produced is not produced from more than one location of a basic configuration. Basic configurations form an important subset of the exhaustive set of feasible configurations, as exemplified by the numerous studies devoted to them.[1-15] Thermal couplings can be introduced at some or all of the heat exchangers associated with submixtures in a basic configuration. Depending on whether all the replaceable heat exchangers are replaced by thermal couplings or not, a configuration is accordingly referred to as a *completely thermally coupled* or a *partially thermally coupled configuration*.[1] Choosing the best configuration in terms of energy/costs from the set of basic configurations and its thermally coupled derivatives is a problem that has been looked into.[6-8,14-15]

Agrawal and Fidkowski[16] discovered the thermodynamically equivalent configurations of each thermally coupled derivative of basic configurations. The thermodynamically equivalent configurations are obtained by moving sections between distillation columns that are connected by thermal couplings. All such thermodynamically equivalent configurations have the same total number of sections. Figure 2.2 shows the thermodynamically equivalent configurations for the three-component fully thermally coupled Petlyuk configuration (Figure 2.1). These configurations are important for the following reasons. Firstly, these configurations can vary significantly in capital costs, depending on the diameter and height of the individual distillation columns. Secondly, some of the equivalent configurations are more operable than the others. For example, the configurations in Figure 2.2 are more operable than that in Figure 2.1, as a uniformly higher pressure can be maintained in one distillation column relative to the other in the configurations of Figure 2.2. A more detailed explanation on this aspect has been provided in Chapter 2.

Owing to their relevance, multiple attempts have been made in the literature to synthesize these thermodynamically equivalent configurations.[16-19] Agrawal[17] proposed a rule-based procedure to synthesize a few of the thermodynamically equivalent *n*-component fully thermally coupled configurations. Rong et al.[19] presented formulae to determine the total number of thermodynamically equivalent configurations for any thermally coupled derivative of a basic configuration. However, their analysis lacked representation/identifiability for these configurations. Caballero and Grossmann[18] presented a formulation that

could identify/represent all the thermodynamically equivalent configurations uniquely for any given thermally coupled configuration, and have since, incorporated them in their search space. For a given separation flowsheet of a configuration, they solve an extended assignment problem, where they assign the individual sections from the given flowsheet to *n*-1 distillation columns, in conjunction with the mass/component balance constraints that should be satisfied to resemble the originally given separation flowsheet. In their model, they use this formulation to identify the best thermodynamically equivalent configuration of the flowsheet/sequence that has been identified to be the optimal flowsheet/sequence from their optimization model. Thus, identifying the suitable thermodynamically equivalent configuration follows the optimization to identify the best separation flowsheet. A similar procedure will be adopted in this work.

The ultimate goal of the current work is to, for a given distillation flowsheet, be able to identify/draw/represent all the thermodynamically equivalent configurations with the same number of sections of a given sequence/flowsheet, and then, based on some criteria/objective function choose the best among these. To do so, we present an alternate formulation to the one presented by Caballero and Grossmann.[18] Some possible merits of the current formulation over theirs is presented later.

8.2 Definitions

Section: Part of a distillation column between two consecutive streams separated by a few stages that enter or leave a distillation column.

Pseudo Section: A pseudo section comprises of one or more sections. Part of the distillation column from the feed to its top-most rectifying product or from the feed to its bottom-most stripping product is termed a pseudo section. A pseudo section can either be rectifying or stripping.

Rectifying Pseudo Section: A pseudo section comprising of only rectifying sections.

Stripping Pseudo Section: A pseudo section comprising of only stripping sections.

8.3 Formulation

The discussion in this paragraph concerns the rectifying sections and rectifying pseudo sections only. The arguments will be extended to the stripping sections and stripping pseudo sections later. Consider the following reference matrix which has been identified by the matrix method to represent a feasible distillation configuration.

$$\begin{matrix} H & I & J & K & \dots \\ 0 & I' & J' & K' & \dots \\ 0 & 0 & J'' & K'' & \dots \\ 0 & 0 & 0 & K''' & \dots \end{matrix}$$

where *H*, *I*, *I*',… represent unique submixtures. Define a reference vector as follows:

Reference vector = **rv** = $[H \quad I \quad I' \quad J \quad J' \quad J'' \quad K \quad K' \quad K'' \quad K''' \quad ...]$

The way the matrix and reference vector are defined, the product of a submixture lies only to its right in the reference vector. Now, we generate vectors with 0s and 1s of the same length as the reference vector from the feasible matrix. Each generated vector denotes a unique pseudo-section. There is a position-wise correspondence between the generated vectors with 0s and 1s, and the reference vector. The way a generated vector should be interpreted is as follows. The presence of a 1 at a submixture's position implies that only its immediate rectifying product is present in the pseudo section. For example, consider the following vectors **r1, r2** and **r3** with **rv** as reference:

$$\boldsymbol{r1} = [1 \quad 0 \quad 0 \quad 0 \quad 0 \quad 0 \quad 0 \quad 0 \quad 0 \quad 0 \quad ...]$$

$$\boldsymbol{r2} = [1 \quad 1 \quad 0 \quad 0 \quad 0 \quad 0 \quad 0 \quad 0 \quad 0 \quad 0 \quad ...]$$

$$\boldsymbol{r3} = [1 \quad 1 \quad 0 \quad 1 \quad 0 \quad 0 \quad 0 \quad 0 \quad 0 \quad 0 \quad ...]$$

The pseudo section corresponding to vector **r1** has *H*'s immediate rectifying product only (which in this case is *I*). Similarly, the pseudo section corresponding to vector **r2** has *H*'s immediate rectifying product (which is *I*) and *I*'s immediate rectifying product (which is *J*) only. Likewise, the pseudo section corresponding to vector **r3** has *H*'s immediate rectifying product (which is *I*), *I*'s immediate rectifying product (which is *J*) and *J*'s immediate rectifying product (which is *K*) only. Since the presence of a 1 corresponding to a submixture denotes the presence of its immediate rectifying product, the submixture corresponding to the

first 1 in the vector (i.e., the leftmost) is to be interpreted as the feed to the pseudo section. Likewise, the submixture corresponding to the last 1 in the vector (i.e., the rightmost) has its immediate rectifying product as the top product leaving/exiting the rectifying pseudo section. Also, since pure components do not produce rectifying products further, columns corresponding to pure components can be omitted from the vectors. Thus, in this way, a unique vector defines a unique pseudo section. The rectifying pseudo sections defined by **r1, r2** and **r3** are respectively shown in Figures 8.1(a), 8.1(b) and 8.1(c).

It should be noted that only the feasible vectors representing feasible rectifying pseudo sections are generated from the feasible matrix. All feasible rectifying pseudo sections of the sequence/flowsheet the matrix represents can be generated by spanning every submixture in the matrix, and treating it as a feed to the rectifying pseudo section. Pointers to generate the feasible rectifying pseudo sections are presented later. Just following a similar convention as above for stripping, all feasible stripping pseudo sections are generated. We now have all possible rectifying and stripping pseudo sections. We need to combine/group them so that the combination represents a feasible distillation configuration. To do so, we use the simple fact that in a distillation configuration, every submixture (including the feed to be separated) has a single rectifying and stripping product. This is a necessary and sufficient condition for a given set of pseudo rectifying and stripping sections to represent a feasible configuration corresponding to the originally given flowsheet. Notice that the formulation is such, that the mass/component balance constraints are not needed.

A generalized formulation for a four-component feed is presented below, where no assumption is made about the structure of the given matrix. The general matrix is represented as

$$X = \begin{bmatrix} xABCD = 1 & xABC & xAB & xA = 1 \\ 0 & xBCD & xBC & xB = 1 \\ 0 & 0 & xCD & xC = 1 \\ 0 & 0 & 0 & xD = 1 \end{bmatrix}$$

where the *x*s are binary integers, 1 or 0, which respectively denote the presence or absence of a submixture/product, and get fixed when a feasible matrix is given. All feasible rectifying pseudo sections for the above matrix are presented below.

rv	=	$[ABCD$	ABC	BCD	AB	BC	$CD]$
$\boldsymbol{ABCD\ as\ feed}$							
$r1$	=	$[1$	0	0	0	0	$0]$
$r2$	=	$[1$	$xABC$	0	0	0	$0]$
$r3$	=	$[1$	$xABC$	0	xAB	0	$0]$
$\boldsymbol{ABC\ as\ feed}$							
$r4$	=	$[0$	$xABC$	0	0	0	$0]$
$r5$	=	$[0$	$xABC$	0	$xABC * xAB$	0	$0]$
$\boldsymbol{BCD\ as\ feed}$							
$r6$	=	$[0$	0	$xBCD$	0	0	$0]$
$r7$	=	$[0$	0	$xBCD$	0	$xBCD * xBC * (1 - xABC)$	$0]$
$\boldsymbol{AB\ as\ feed}$							
$r8$	=	$[0$	0	0	xAB	0	$0]$
$\boldsymbol{BC\ as\ feed}$							
$r9$	=	$[0$	0	0	0	xBC	$0]$
$\boldsymbol{CD\ as\ feed}$							
$r10$	=	$[0$	0	0	0	0	$xCD]$

In doing so, it is assumed here that the matrix represents a completely thermally coupled configuration, i.e., all heat exchangers associated with submixtures are

replaced by thermal couplings. A small description of the generated vectors is presented in the following paragraph.

In the vectors generated above, if for example, submixture *ABC* is absent in the flowsheet, xABC=0, which makes **r1=r2**. Further, all vectors generated with *ABC* as feed, i.e., **r4** and **r5**, become zero vectors. Thus, for further progress, all the zero vectors should be eliminated and only the unique vectors should be considered. Also notice when xABC=0 that all entries along the *ABC* column will be zero. Further, in the vector **r7**, the term $(1 - xABC)$ appears because the rectifying product of *BC* (i.e., *B*) can be present in the rectifying pseudo section with *BCD* as feed only if *BC* is not simultaneously produced as a stripping product from *ABC*. This can happen when *ABC* is absent.

Furthermore, for the case when heat exchangers associated with submixtures could be present, additional binary integers need to be introduced. Let *q*s be the binary 0 or 1 quantities, indicating the absence or presence of a heat exchanger associated with submixtures. Then, for example, **r1**, **r2** and **r3** become

rv	$=$	$[ABCD$	ABC	BCD	AB	BC	$CD]$
$\boldsymbol{ABCD\ as\ feed}$							
$r1$	$=$	$[1$	0	0	0	0	$0]$
$r2$	$=$	$[1$	$xABC * (1 - qABC)$	0	0	0	$0]$
$r3$	$=$	$[1$	$xABC * (1 - qABC)$	0	$xAB * (1 - qABC) * (1 - qAB)$	0	$0]$

r2, for example, in this case implies that the rectifying pseudo section with *ABCD* as feed can have the rectifying product of *ABC* only if the heat exchanger associated with *ABC* is absent (assuming *ABC* is present). If indeed a heat

exchanger associated with *ABC* is present, observe that **r1**=**r2**=**r3**, which means there is only one unique rectifying pseudo section that is possible with *ABCD* as feed. In this work, only the completely thermally coupled configurations are used as examples and hence all *q*s are set to zero.

Let **r1'**, **r2'**, …**rl'** be the unique non zero vectors out of **r1**, …,**r10**. Define new binary integer 0 or 1 variables, *zr1', zr2', …, zrl'* which respectively denote the absence or presence of rectifying pseudo sections given by **r1'**, **r2'**, …**rl'**.

Now, just like what was done previously for rectifying sections, all feasible stripping pseudo sections for the given feasible matrix are presented below.

rv	$=$	$[ABCD$	ABC	BCD	AB	BC	$CD]$
$\boldsymbol{ABCD\ as\ feed}$							
$s1$	$=$	$[1$	0	0	0	0	$0]$
$s2$	$=$	$[1$	0	$xBCD$	0	0	$0]$
$s3$	$=$	$[1$	0	$xBCD$	0	0	$xCD]$
$\boldsymbol{ABC\ as\ feed}$							
$s4$	$=$	$[0$	$xABC$	0	0	0	$0]$
$s5$	$=$	$[0$	$xABC$	0	0	$xABC * xBC * (1 - xBCD)$	$0]$
$\boldsymbol{BCD\ as\ feed}$							
$s6$	$=$	$[0$	0	$xBCD$	0	0	$0]$
$s7$	$=$	$[0$	0	$xBCD$	0	0	$xBCD * xCD]$
$\boldsymbol{AB\ as\ feed}$							
$s8$	$=$	$[0$	0	0	xAB	0	$0]$
$\boldsymbol{BC\ as\ feed}$							
$s9$	$=$	$[0$	0	0	0	xBC	$0]$
$\boldsymbol{CD\ as\ feed}$							
$s10$	$=$	$[0$	0	0	0	0	$xCD]$

Let **s1'**, **s2'**, …**sm'** be the unique non zero vectors out of **s1**, …,**s10**. Define new binary integer 0 or 1 variables, *zs1', zs2', …, zsm'* which respectively

denote the absence or presence of stripping pseudo sections given by **s1'**, **s2'**, …**sm'**.

Since every submixture must have a single rectifying and stripping product and no more in a distillation configuration, the binary integer variables *zr1', zr2', …, zrl'* and *zs1', zs2', …, zsm'* satisfy the following constraints

$$zr1' * \boldsymbol{r1'} + \cdots + zrl' * \boldsymbol{rl'} = [xABCD \;\; xABC \;\; xBCD \;\; xAB \;\; xBC \;\; xCD]$$

$$zs1' * \boldsymbol{s1'} + \cdots + zsm' * \boldsymbol{sm'} = [xABCD \;\; xABC \;\; xBCD \;\; xAB \;\; xBC \;\; xCD]$$

$$zr1', \ldots, zrl', zs1', \ldots, zsm' \in \{0,1\}$$

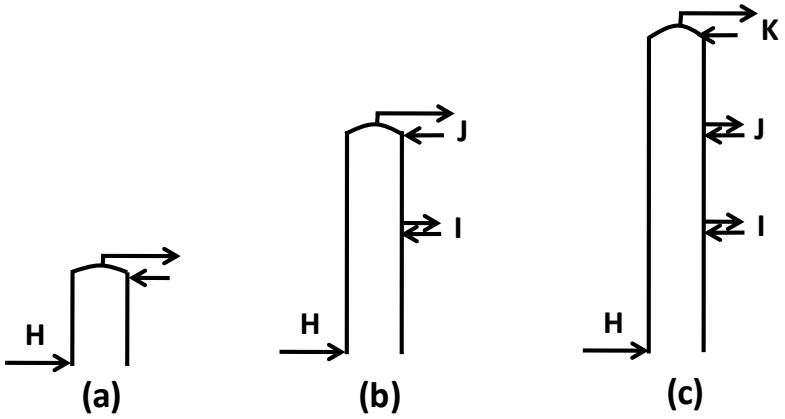

Figure 8.1 Rectifying pseudo sections corresponding to **r1**, **r2** and **r3**.

If any of *xABCD, …, xCD* are zero, then the LHS is also zero automatically corresponding to that element. Any feasible solution to the above constraints represents a unique distillation configuration and all feasible solutions give the total number of thermodynamically equivalent configurations possible for a given flowsheet. Finding this number for any given flowsheet will be a part of the future work of this project. In the current work, I choose the flowsheet that corresponds to the 4-component fully thermally coupled Petlyuk configuration. The vapor flows

in each section under minimum energy conditions are known apriori (transition split). Under the conditions of operation of the flowsheet at 1.2*R_{min} (R_{min} = minimum reflux ratio), the thermodynamically equivalent configuration with the minimum capital cost is desired. The following equations for cost calculations are borrowed from Ignacio Grossmann's website and appropriately modified for pseudo-sections.[20]

$$A_{pseudo} = \frac{PPM * Vap_{\max pseudo}}{\sqrt{\rho_l \rho_v} * 0.6 * 329 * 0.8}$$

where, A_{pseudo}= cross-sectional area of a pseudo section, $Vap_{max\ pseudo}$= maximum of all sectional vapor flows in a pseudo section, ρ_l = liquid density, ρ_v = vapor density, *PPM* = average molecular weight of the feed mixture. Further,

$$H_{pseudo} = 0.5 * N_{pseudo} + 6$$

where, H_{pseudo}= height of the pseudo section, N_{pseudo}= number of trays in the pseudo section. It is assumed that the number of trays per section is a constant and equal to 20. If *t* be the number of sections in a pseudo section, then $N_{pseudo} = 20 * t$ and $H_{pseudo} = 10 * t + 6$.

$$V_{pseudo} = A_{pseudo} * H_{pseudo}$$

where, V_{pseudo}= volume of the pseudo section. If C_{pseudo} is the overall cost of the pseudo section, then it is determined using

$$C_{pseudo} = (603.8 * V_{pseudo} + 5307) * (2.5 + 1.72)$$

and hence, the cost of a given pseudo section, C_{pseudo}, is a known quantity. Let COS_{pseudo}= *[cr1' cr2'…. crl' cs1' cs2'… csm']* be the cost vector of the feasible

pseudo sections that were generated earlier. Let z_{pseudo} = *[zr1' zr2'…. zrl' zs1' zs2'… zsm']*^{T}. Then the optimization problem reduces to:

$$\min COS_{pseudo} z_{pseudo}$$

$$s.t.$$

$$zr1' * \boldsymbol{r1'} + \cdots + zrl' * \boldsymbol{rl'} = [xABCD \;\; xABC \;\; xBCD \;\; xAB \;\; xBC \;\; xCD]$$

$$zs1' * \boldsymbol{s1'} + \cdots + zsm' * \boldsymbol{sm'} = [xABCD \;\; xABC \;\; xBCD \;\; xAB \;\; xBC \;\; xCD]$$

$$zr1', \ldots, zrl', zs1', \ldots, zsm' \in \{0,1\}$$

The feasible region of the above problem is non-convex because of the integer constraints. We solve a relaxation of the above optimization problem by relaxing the integer constraints. The relaxed problem is as follows:

$$\min COS_{pseudo} z_{pseudo}$$

$$s.t.$$

$$zr1' * \boldsymbol{r1'} + \cdots + zrl' * \boldsymbol{rl'} = [xABCD \;\; xABC \;\; xBCD \;\; xAB \;\; xBC \;\; xCD]$$

$$zs1' * \boldsymbol{s1'} + \cdots + zsm' * \boldsymbol{sm'} = [xABCD \;\; xABC \;\; xBCD \;\; xAB \;\; xBC \;\; xCD]$$

$$0 \leq zr1', \ldots, zrl', zs1', \ldots, zsm' \leq 1$$

The feasible region is now an intersection of halfspaces and hyperplanes, and hence is convex. In fact, the original optimization problem is reduced to an LP in which COS_{pseudo} is never parallel to any of the constraint coefficient vectors which are made up of only 0s and 1s. It is observed that the solution returned to the relaxed problem is feasible for the unrelaxed problem as well.

8.4 Example problem

As mentioned earlier, the following matrix which corresponds to the four-component fully thermally coupled Petlyuk configuration is taken as an example.

$$X = \begin{bmatrix} 1 & 1 & 1 & 1 \\ 0 & 1 & 1 & 1 \\ 0 & 0 & 1 & 1 \\ 0 & 0 & 0 & 1 \end{bmatrix}$$

The separation of a feed given in Reference 21 is considered. The feed parameters are given by f=[0.3 0.4 0.25 0.05]; alpha=[13.432 5.891 2.19 1]; feedquality=1. R_{min} is determined using the transition split solution. The vapor flows in all the rectifying and stripping sections at 1.2*R_{min} are given by *vrectABCD = 0.709; vrectABC = 0.915; vrectBCD = 0.265; vrectAB = 1.286; vrectBC = 0.372; vrectCD = 0.312; vstriABCD = 0.709; vstriABC = 0.206; vstriBCD = 0.974; vstriAB = 0.372; vstriBC = 0.312; vstriCD = 1.286;* where, for example, *vrectABCD* = vapor flow in the rectifying section with *ABCD* as feed, and *vstriABCD* = vapor flow in the stripping section with *ABCD* as feed.

Following the determination of the vapor flows, the cost vector COS_{pseudo} is determined, following which, the LP formulated in the previous section is solved. The best thermodynamically equivalent configuration in terms of capital costs for the given feed and operation is shown below in Figure 8.2. It may be reasonable to be expect such a solution because in this configuration, the rectifying section of *AB* and the stripping section of *CD* which have the same, highest vapor flows of all sections, are put into the same distillation column. The stripping section of *ABC* and rectifying section of *BCD* which have similar vapor flows are put into

distillation column 2. Likewise, the stripping section of *AB*, the stripping and rectifying sections of *BC* and the rectifying section of *CD*, all of which have similar vapor requirements are assigned to distillation column 3.

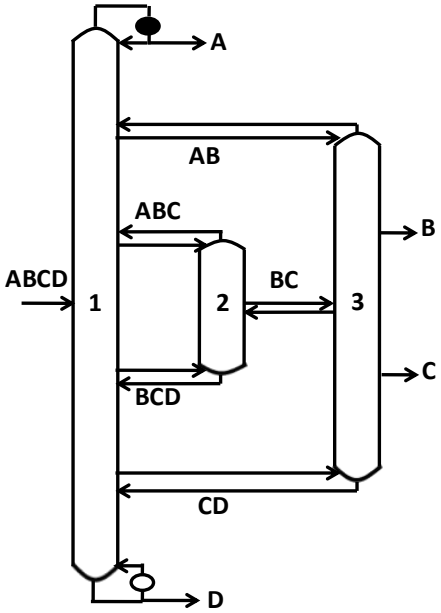

Figure 8.2 Solution obtained from the formulation for the example problem.

8.5 Possible merits over other formulations

In Caballero and Grossmann's formulation,[18] the component/mass balance constraints are explicitly used, while in the current formulation, such constraints are rendered redundant because of the nature of the formulation. The current formulation also does not have to deal with issues of degenerate solutions, as the authors did in Reference 18. Further, the upper bound on the number of variables utilized in their formulation[18] is equal to the maximum number of sections possible times the number of distillation columns, which is $n(n\text{-}1)^2$. In the current formulation, the upper bound on the number of variables

utilized is equal to the maximum number of horizontal and diagonally downward branches possible, which is equal to $\sum_{r=1}^{n} 2 * r * \binom{n-r}{1} = \frac{n(n+1)}{3}$. The maximum number of variables required for different *n* is shown in Table 8.1.

Table 8.1 Variation of the maximum number of variables required for the formulation with number of components in the feed.

n	Caballero	Current
3	12	8
4	36	20
5	80	40
6	150	70
10	810	330

8.6 Future work

This chapter lays the foundation for a formulation to identify thermodynamically equivalent distillation configurations. The formulation presented here can be extended to find the total number of thermodynamically equivalent configurations for any given distillation flowsheet. Further, additional constraints can be incorporated into the current model to identify the thermodynamically equivalent configurations that are more operable than the ones which have pressure-related operational issues. Finally, the formulation could potentially be incorporated into a more robust optimization framework so as to eliminate some of the assumptions that were made in the current work. For example, the presented formulation can be incorporated into an MINLP, thus allowing for the thermodynamically equivalent configurations described here to

be also included as a part of an exercise to determine the distillation flowsheet with the lowest cost.

References

1. Agrawal R. Synthesis of multicomponent distillation configurations. AIChE J. 2003;49:379-401.
2. Petlyuk FB, Platonov VM, Slavinskii DM. Thermodynamically Optimal Method for Separating Multicomponent Mixtures. International Chemical Engineering. 1965;5(3):555-561.
3. Sargent RWH, Gaminibandara K. Optimum Design of Plate Distillation Columns. In: Optimization in Action. Dixon LCW, Ed., New York: Academic Press, 1976:267-314.
4. Agrawal R. Synthesis of Distillation Column Configurations for a Multicomponent Separation. Industrial and Engineering Chemistry Research. 1996;35(4):1059-1071.
5. Rong B, Kraslawski A, Turunen I. Synthesis of Functionally Distinct Thermally Coupled Configurations for Quaternary Distillation. Industrial and Engineering Chemistry Research. 2003;42(6):1204-1214.
6. Caballero JA, Grossmann IE. Design of Distillation Sequences: From Conventional to Fully Thermally Coupled Distillation Systems. Computers and Chemical Engineering. 2004;28(11):2307-2329.
7. Caballero JA, Grossmann IE. Structural Considerations and Modeling in the Synthesis of Heat-Integrated-Thermally Coupled Distillation Sequences. Industrial and Engineering Chemistry Research. 2006;45(25):8454-8474.
8. Fidkowski ZT. Distillation Configurations and their Energy Requirements. American Institute of Chemical Engineers Journal. 2006;52(6):2098-2106.
9. Ivakpour J, Kasiri N. Synthesis of Distillation Column Sequences for Nonsharp Separations. Industrial and Engineering Chemistry Research. 2009;48(18):8635-8649.
10. Giridhar AV, Agrawal R. Synthesis of Distillation Configurations: I. Characteristics of a Good Search Space. Computers and Chemical Engineering. 2010;34(1):73-83.
11. Giridhar AV, Agrawal R. Synthesis of Distillation Configurations: II. A Search Formulation for Basic Configurations. Computers and Chemical Engineering. 2010;34(1):84-95.
12. Shah VH, Agrawal R. A Matrix Method for Multicomponent Distillation Sequences. American Institute of Chemical Engineers Journal. 2010;56(7):1759-1775.

13. Kim SB, Ruiz GJ, Linninger AA. Rigorous Separation Design. 1. Multicomponent Mixtures, Nonideal Mixtures, and Prefractionating Column Networks. Industrial and Engineering Chemistry Research. 2010;49(14):6499-6513.

14. Nallasivam U, Shah VH, Shenvi AA, Tawarmalani M, Agrawal R. Global Optimization of Multicomponent Distillation Configurations: 1. Need for a Global Minimization Algorithm. American Institute of Chemical Engineers Journal. 2012;doi:10.1002/aic.13875.

15. Caballero JA, Grossmann IE. Synthesis of Complex Thermally Coupled Distillation Systems Including Divided Wall Columns. American Institute of Chemical Engineers Journal. 2012;doi:10.1002/aic.13912.

16. Agrawal R., Fidkowski ZT. More Operable Arrangements of Fully Thermally Coupled Distillation Columns. American Institute of Chemical Engineers Journal. 1998;44(11):2565-2568.

17. Agrawal, R. A method to draw fully thermally coupled distillation column configurations for multicomponent distillation. Transactions of IChemE. 2000;78(Part A):454.

18. Caballero JA, Grossmann IE. Thermodynamically Equivalent Configurations for Thermally Coupled Distillation. American Institute of Chemical Engineers Journal. 2003;49(11):2864-2884.

19. Rong B, Kraslawski A, Turunen I. Synthesis and Optimal Design of Thermodynamically Equivalent Thermally Coupled Distillation Systems. Industrial and Engineering Chemistry Research. 2004;43(18):5904-5915.

20. http://egon.cheme.cmu.edu/

21. Kim JK, Wankat PC. Quaternary distillation systems with less than N – 1 columns. Industrial and Engineering Chemistry Research. 2004;43:3838–3846.

CHAPTER 9. SUMMARY

Distillation accounts for 3% of the world energy consumption. Furthermore, it is the predominantly used separation technique in the chemical and petrochemical industries, with 90-95% of the separations being conducted by distillation. Thus, even small improvements to the current practices of conducting distillation can effect significant cost reduction, and influence the plant economy. Process intensification is a method to bring about improvements to chemical processes, whereby both operating cost and capital cost of a process are simultaneously reduced by simultaneously improving energy-efficiency and miniaturizing equipment. In this thesis, we present some novel extensions to pre-existing process intensification methods of multicomponent distillation, which can potentially be used for widespread industrial implementation in the future.

Chapter 2 focused on ternary FTC distillation using DWCs. Ternary FTC DWCs are currently being used in the industry. In such DWCs, to derive maximum energy/cost savings, the vapor split at the bottom of a vertical partition is often critical. But, in practice, the vapor split at the bottom of a partition is left unregulated. To overcome this operational challenge, we identified that, by applying a concept called the conversion of a thermal coupling to a liquid transfer on DWCs, new attractive ternary DWCs can be synthesized. These new DWCs allow independent control of the vapor flowrate in each partitioned zone.

Interestingly, we showed that all the new ternary DWCs have the same minimum heat duty requirements as the FTC configuration.

Chapter 3 extended the concepts presented in Chapter 2 to *n*-component FTC distillation. A full set of DWCs with *n*-2 dividing walls were obtained for FTC distillation of mixtures with *n*-components. While historically only one DWC has been known for FTC distillation of any mixture, for example, for 4-component mixtures, we identified thirty five new DWCs. Among the new DWCs, we identified rules to detect the subset of DWCs in which the vapor flow could be regulated in each section of the DWC during operation by external means. This feature makes it possible to build and operate the DWCs near optimality and ensure purity of product streams.

In Chapter 4, we presented a very easy-to-follow procedure to draw all possible DWCs for any given distillation flowsheet. Two methods were needed for different categories of distillation configurations. The methods comprised of a comprehensive set of rules to draw a DWC for any given thermally coupled distillation flowsheet. Thus, a systematic procedure for synthesizing DWCs for multi-component distillation was achieved. With Chapters 2, 3 and 4 put together, a multitude of options are now available for distilling any given mixture in a DWC.

In Chapter 5, we proposed and studied general methods to consolidate distillation columns of a distillation configuration using heat and mass integration. The proposed methodology encompassed all heat and mass integrations known till date, and included many more. Each heat and mass integration eliminates a

distillation column, a condenser, a reboiler and the heat duty associated with a reboiler. Thus, heat and mass integration can potentially offer significant capital and operating cost benefits. Such possible benefits were demonstrated through multiple case-studies.

In Chapter 6, we studied three special cases of column-consolidation in greater detail. This study was important because of the potential widespread application of the special cases during distillation-configuration-synthesis, and a total lack of knowledge in the literature on the subject. After a comprehensive study, it was observed that while one of the special cases of column-consolidation is never useful at all, the other two are useful only for certain kind of feed conditions, the characteristics of which were reported. This chapter is the first such work to better understand and throw light on the special cases of column-consolidation.

In Chapter 7, we compared two approaches: the short-cut approach and the rigorous approach for performance evaluation of distillation configurations. The purpose of the work was to verify whether short-cut approaches, along with their underlying assumptions, can be trusted for relative heat duty comparison and rank-listing of distillation configurations. We verified this by observing that, for a case study to separate four-component mixtures into pure products, there was a close overlap between the ranklists generated from the two approaches among the configurations considered for the study.

Chapter 8 presented a new, alternate formulation to identify, and synthesize thermodynamically equivalent thermally coupled configurations. While a formulation for this task has been presented in the literature, the current formulation has some merits over the known formulation. These merits were discussed briefly. A small example problem was solved to demonstrate the utility of the formulation. The formulation is work in progress. Going forward, equations to quickly identify a more operable thermally coupled configuration can be incorporated into the model. In the long-run, this formulation can be used as a starting point to model thermodynamically equivalent thermally coupled configurations, along with other configurations in the search space, in a mixed integer nonlinear programming formulation for cost evaluation.

In summary, I believe the thesis has shown that, despite distillation being considered an old, mature technology, there is scope for introducing novel concepts and for improving various aspects of the technolgy. In this thesis, the novelties suggested were in the realms of novel processes for distillation, and systematic methods for their synthesis. It is hoped that these novelties will positively impact at least some stage of the “conception to implementation” of distillation processes industrially in the future.

APPENDICES

Appendix A

A proof that establishes the equivalence between a thermal coupling and a liquid-only transfer stream is presented here. Figure A.1(a) shows a thermal coupling at the top of Section ‘a2’, and the converted liquid-only transfer arrangement is shown in Figure A.1(b) with a newly created Section ‘b1’. The fate of the vapor and origin of the liquid at the top of the Sections, ‘b1’ and ‘b3’, are same as that of Section ‘a3’, i.e., if for example, there is a condenser at the top of Section ‘a3’, a condenser is placed at the top of each Section ‘b1’ and ‘b3’.

The notation for the symbols used in the figure is shown above it. We retain the same liquid-vapor traffic of Section ‘a2’ in Section ‘b2’, and likewise, the liquid-vapor traffic of Section ‘a4’ in ‘b4’.The difference therefore in the two arrangements of Figures A.1(a) and A.1(b) arises due to sections ‘a3’, ‘b1’ and ‘b3’. To ensure that the Sections ‘a3’, ‘b1’ and ‘b3’ are all equivalent to each other, they must have the same number of stages and L/V ratio. This implies that:

$$\frac{L_{b1}}{V_{a2}} = \frac{L_{a2} + L_{a4}}{V_{a2} + V_{a4}} \qquad \text{and} \qquad \frac{L_{b3}}{V_{a4}} = \frac{L_{a2} + L_{a4}}{V_{a2} + V_{a4}}$$

$$\Rightarrow L_{b1} = V_{a2}\left(\frac{L_{a2} + L_{a4}}{V_{a2} + V_{a4}}\right) \qquad \text{and} \qquad L_{b3} = V_{a4}\left(\frac{L_{a2} + L_{a4}}{V_{a2} + V_{a4}}\right)$$

Clearly, $L_{b1} + L_{b3} = L_{a2} + L_{a4}$. Further, we know that

$$\text{Net mass flow in Section } 'a3' = V_{a2} + V_{a4} - L_{a2} - L_{a4} > 0 \qquad \text{(A.1)}$$

$$\text{Net mass flow in Section } 'b1' = V_{a2} - L_{b1} = V_{a2}\left(\frac{V_{a2} + V_{a4} - L_{a2} - L_{a4}}{V_{a2} + V_{a4}}\right) > 0 \qquad \text{(A.2)}$$

$$\text{Net mass flow in Section } 'b3' = V_{a4} - L_{b3} = V_{a4}\left(\frac{V_{a2} + V_{a4} - L_{a2} - L_{a4}}{V_{a2} + V_{a4}}\right) > 0 \qquad \text{(A.3)}$$

$$\text{Net mass flow in Section } 'b1' \text{and } 'b3' \text{combined} = V_{a2} + V_{a4} - L_{a2} - L_{a4} \qquad \text{(A.4)}$$

Compare Equations A.1 and A.4, and observe Equations A.2 and A.3. Note that V_{a2} and V_{a4} could be arbitrary vapor flows between 0 and V_{a2} + V_{a4}. This implies that any section (rectifying or stripping, as we have not invoked the nature of the section so far) with vapor flow V_{a2} + V_{a4} can be split/divided into two new equivalent sections, with the vapor flow distributed between the two new sections in any proportion (V_{a2} and V_{a4}). Then, the net mass distilled from each new section is proportional to the vapor flow assigned to the section (V_{a2} (or V_{a4})) ***/*** (V_{a2} + V_{a4}). So, in the case under study, the mass that is distilled in a single Section 'a3' in Figure A.1(a) is divided between two Sections 'b1' and 'b3', as shown in Figure A.1(b). Further, assuming the composition of the liquid/vapor is the same at the level of the thermal coupling (Figure A.1(a)) and the liquid-only transfer stream (Figure A.1(b)), the composition of the liquid/vapor at the top of each of the Sections 'b1' and 'b3' will be equal to that at the top of Section 'a3' because all these three sections have equal stages and (L/V) ratios. Hence, the two arrangements are thermodynamically equivalent irrespective of the equilibrium model that is used or the number of components that are involved.

Now, we only need to show that, in Figure A.1(b), L_{a2}<L_{b1} to guarantee that the liquid transfer happens in the direction shown. To show this, we use the fact that the net mass flow in Section 'b2' is in the upward direction, while that in Section 'b4' is in the downward direction. As a result, observe that:

$$\frac{L_{a2}}{V_{a2}} < 1 < \frac{L_{a4}}{V_{a4}}$$

$$\Rightarrow \frac{V_{a4}}{V_{a2}} < \frac{L_{a4}}{L_{a2}}$$

$$\Rightarrow \frac{V_{a4}}{V_{a2}} + 1 < \frac{L_{a4}}{L_{a2}} + 1$$

$$\Rightarrow \frac{L_{a2}}{V_{a2}} < \frac{L_{a4} + L_{a2}}{V_{a4} + V_{a2}} = \frac{L_{b1}}{V_{a2}}$$

$$\Rightarrow L_{a2} < L_{b1}$$

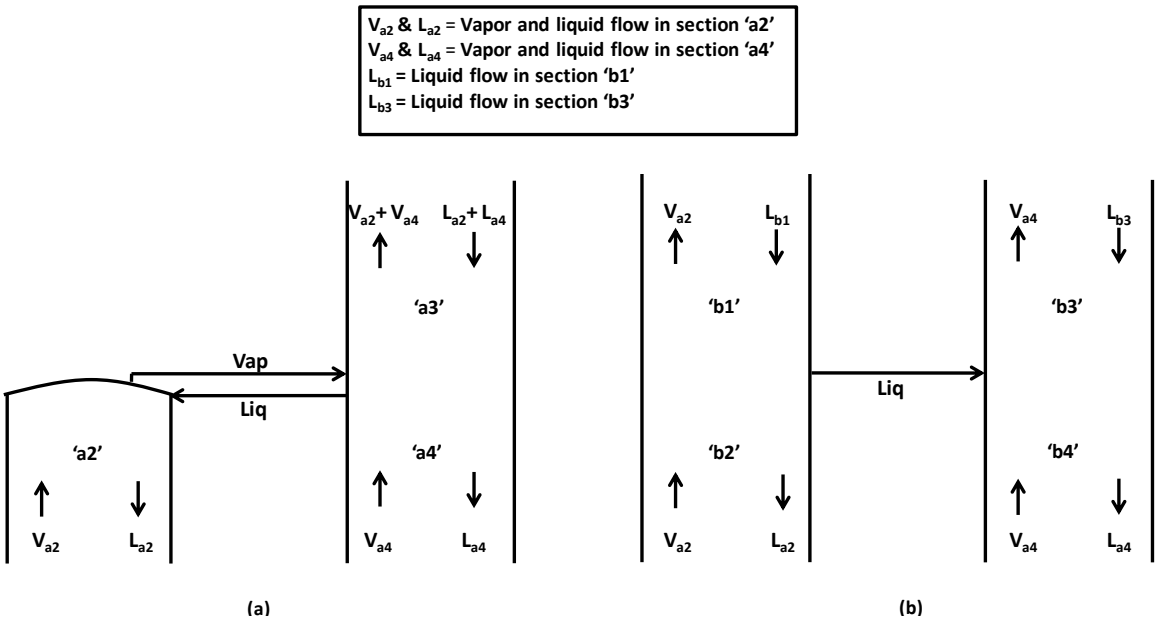

Figure A.1 (a) Any thermally coupled arrangement; (b) the liquid-only transfer arrangement obtained by transforming the thermally coupled arrangement in (a).

Appendix B

Consider the FTC configuration shown in Figure 3.5(e). This configuration is obtained from the FTC configuration in Figure 3.5(d) after converting the thermal coupling at *AB* between Column 1 and 2 to a liquid-only transfer. The resulting Liquid *AB* transfer in Figure 3.5(e) should have been between Columns 1 and 2, but is shown in the figure to be withdrawn from Column 1 and fed directly to Column 3. The guarantee of this liquid transfer from Column 1 to 3 follows from the following reasoning. Consider the FTC configuration of Figure 3.5(a). On converting the *AB* thermal coupling at the top of Column 2 to a liquid-only transfer, the FTC configuration in Figure B.1 is obtained. In the FTC configuration of Figure B.1, when the *AB* thermal coupling at the top of Column 1 is converted to a liquid-only transfer, the FTC configuration of Figure 3.5(e) results, with a direct liquid transfer from Column 1 to 3. Another point worthy of note is that the FTC configurations in Figures 3.5(d) and B.1 differ only in where the thermal coupling *AB* from the top of Column 1 is fed to. To incorporate the FTC configuration of Figure B.1 into a DWC, conventional vertical partitioning cannot be used because vapor transfers occur between each pair of distillation columns, and hence each parallel zone in a DWC must be adjacent to each other. To achieve this in a DWC, unconventional partitioning, as shown in References 15 and 23 (of Chapter 3), will have to be used. In this chapter, we shall not consider such DWCs with unconventional partitioning. Our work in this chapter

focuses on DWCs with conventional partitioning, just like most of the prior literature on DWCs does.

Also note that in a FTC DWC such as the one in Figure 3.6(e), if needed, liquid *AB* from the feed side of the partition could be directly fed to the zone next to it (to the same zone receiving liquid *ABC*). This can be clearly seen by extending the Column 1 in Figure 3.5(d) to *A* and feeding liquid *AB* to Column 2. However, we do not distinguish between such options and when feasible, continue to show the transfer of the liquid submixture to the distillation zone producing product streams.

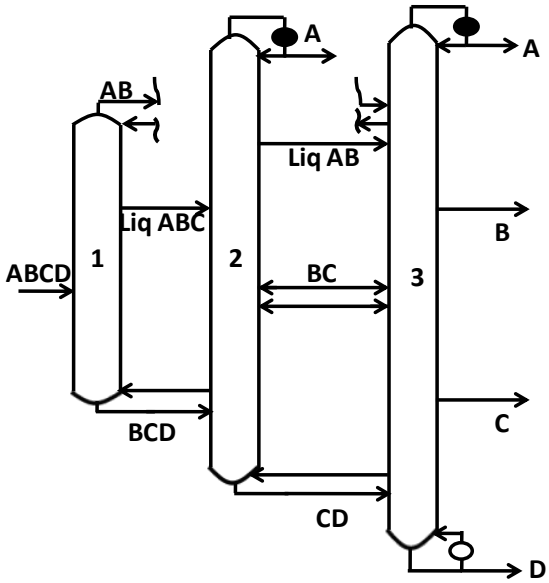

Figure B.1 Configuration obtained from the configuration in Figure 3.5(a) after converting the thermal coupling at *AB* on the top of Column 2 to a liquid-only transfer.

Appendix C

FTC distillation has been known to be very useful for multicomponent separations due to its low heat duty requirements. Agrawal[4] suggested the conversion of a Refer to Figure C.1 for a depiction of the enumeration methodology starting from the four-component FTC DWC of the classic-FTC configuration. When the thermal coupling at the top (bottom) of a partition is converted to a liquid-only transfer, the partition gets extended upwards (downwards). Depending on the extent of usage of the thermal coupling to liquid-only transfer strategy, the circled submixtures at the top/bottom of a partition denote possible termination points for the respective partition at the respective end. The denoted number adjacent to a partition counts the number of possible termination points for the partition at the respective end (top/bottom). Product of the denoted numbers gives the total number of four-component FTC DWCs (36).

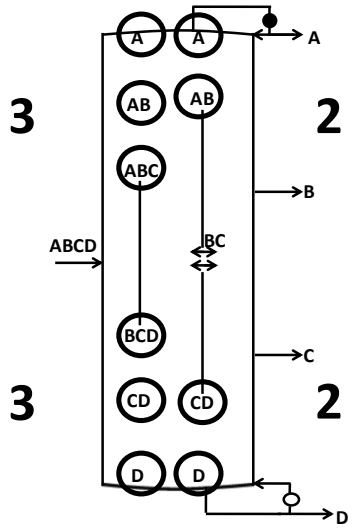

Figure C.1 Depiction of the enumeration methodology (for 4-component case) starting directly from the DWC of the classic-FTC configuration, Figure 3.2(b).

Appendix D

The objective of this appendix is to calculate the total number of possible sub-categories of HMAs that may exist among all distillation configurations for an n-component distillation. A distillation column belongs to a different sub-category than another if at least one of three things happens: (1) the number of components in the top streams is different, (2) the number of components in the bottom streams is different, or (3) the number of overlapping components is different. For convenience, instead of using *A*, *B*, *C*, *D*, etc., to represent the components, as in the main text, we simplify the notation by denoting them using A_1, A_2, A_3, A_4, etc in this appendix. Here, A_1 represents the most volatile component, while A_n is the least volatile component.

In order to form an HMA, the top stream must be the bottom stream of a column and therefore cannot contain A_1. Similarly, the bottom stream is the top stream of a column and therefore does not contain A_n. Since the most volatile elements are in the top stream of the HMA and the least volatile elements are in the bottom stream, it follows that the components in an HMA are a subset of $\{A_2,\ldots,A_{n-1}\}$.

We say that the components of a stream are shifted to more volatile components if, for all k, A_k is replaced by A_{k-1} in the stream. Now, to count different sub-categories, it suffices, by shifting iteratively the components in both the top and bottom streams together to more volatile ones, that A_2 is the most volatile component in the top stream. Similarly, by shifting the components in the

bottom stream alone to more volatile ones, we may eliminate any gap between the most volatile component of the bottom stream of the HMA and the least volatile component of the top stream of the HMA. Observe that the above shifts do not change the number of components in the top or bottom stream and do not change the number of overlapping components in the stream, thereby maintaining the sub-category of the HMA.

We argue that the number of different sub-categories is the same as partitioning the sequence 2,…, *n*-1 into four ordered buckets such that the top stream consists of the components in the first two buckets and the bottom stream consists of the components in the 2nd and 3rd bucket. See Figure D.1 for an illustration. This corresponds to placing three partitions in the sequence 2, …, *n*-1. The location of the last (third) partition governs the total number of components in the two streams. The location of the second partition fixes the number of components in the top stream. Finally, the location of the first partition dictates the number of overlapping components. It is clear from the construction that each location corresponds to a unique way to obtain an HMA sub-category. Nevertheless, we also need to ensure that the first two buckets or the second and third buckets are not simultaneously empty because the streams of an HMA must each have at least one component.

Now, the calculation is straightforward. The number of ways in which the sequence 2, …, *n*-1 can be partitioned into four ordered buckets is given by ${}^{n+1}C_3$, because it is equivalent to permuting *n*-2 dots, one for each number in the sequence, and three partitions.[21] Then, first and second bucket are empty if and

only if the first two partitions are placed before 2, which can be done in $n - 1$ ways. The second and third buckets are empty when the three partitions are together, which after discounting the case where all the partitions are before the first dot, corresponding to the number 2, and has already been deducted, can occur in n – 2 ways. Therefore, the number of ways in which the partitioning can be done is ${}^{n+1}C_3 - (n - 1) - (n - 2)$. Finally, there is no need to create an HMA of a product stream with itself (sub-category represented with A_2 as the top stream and A_2 as the bottom stream). Therefore, the number of unique sub-categories of HMA for n-component distillation is ${}^{n+1}C_3 - (n - 1) - (n - 2) - 1 = (n^3+13n+12)/6$.

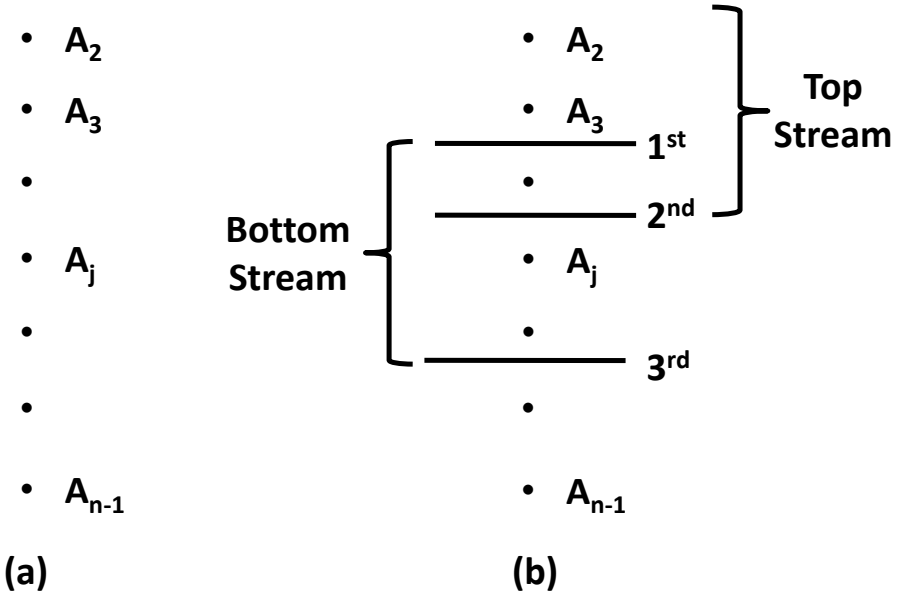

Figure D.1 (a) List of possible components in a top/bottom stream of an HMA; (b) There are n-1 locations available for the 3 partitions.

Appendix E

In this appendix, we calculate all the different possible HMAs. The difference from Appendix D is that HMAs that belong to the same sub-category but involve different components in the top or bottom stream are counted separately. Observe that an HMA is different from another if either the top or the bottom stream is different. Any stream is completely determined by its most volatile and least volatile elements. Therefore, to distinguish different HMAs, we consider four locations partitioning the sequence 2, …, n-1, two before the most volatile components of the top and bottom stream, and two after the least volatile components of these streams. Since there is at least one component in each stream, the two locations that arise from the same stream are always distinct.

Since top and bottom streams of an HMA completely determine the location of the partitions, an HMA column cannot simultaneously correspond to two different ways of locating the four partitions described above. Nevertheless, given the location of the partitions the streams of an HMA are still not fixed. In particular, the first partition fixes the most volatile component of the top stream and the last partition fixes the least volatile component of the bottom stream. However, the least volatile component of the top stream and most volatile component of the bottom stream remain undecided.

Now, we count the ways in which these two remaining components can be obtained using the partition locations. This is more easily done by classifying the locations based on how many of them are distinct. First, assume that all the four

locations are distinct. Such locations can be obtained in $^{n-1}C_4$ ways. With each of these arrangements, there are two distinct ways in which the top and bottom stream of the HMA can be formed as are shown in Figure E.1(a) and E.1(c). If there are three distinct locations, then the top and bottom stream of the HMA can be formed in three ways as shown in Figure E.1(b), E.1(d), and E.1(f). Finally, if

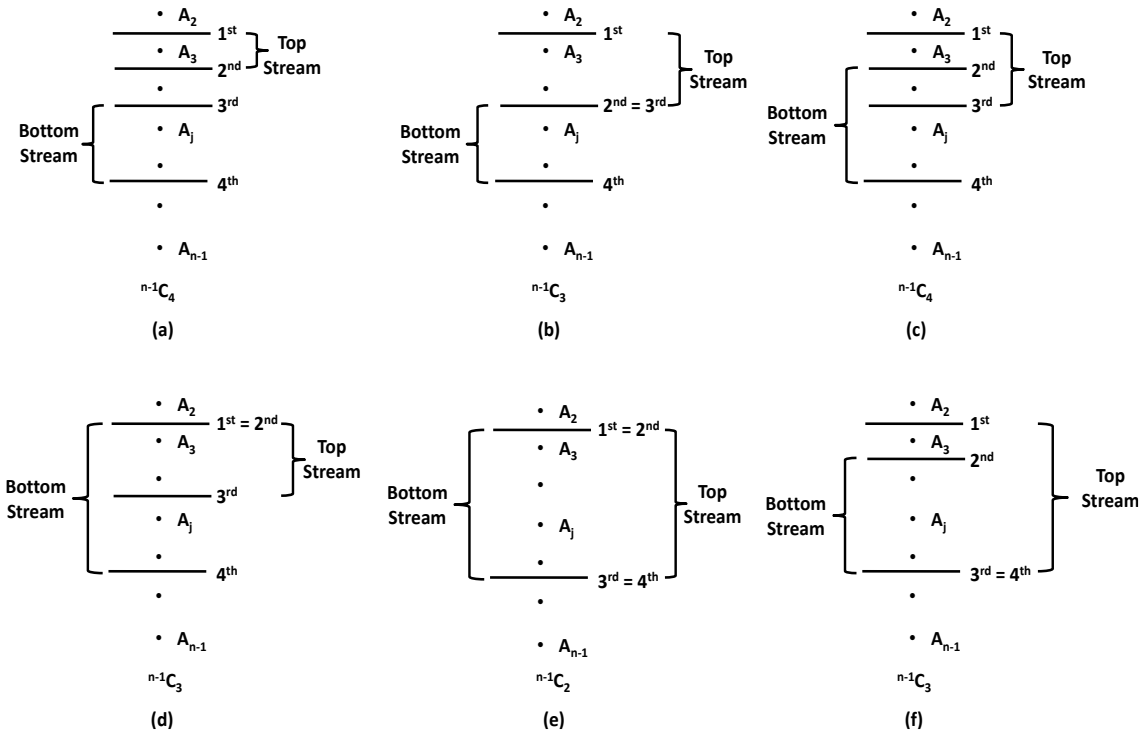

Figure E.1 Various scenarios of partitions used to enumerate the HMAs.

there are only two distinct locations then there is only one way to fix the two remaining components as shown in Figure E.1(e). All together, there are $^{n-1}C_4 \times 2 + {}^{n-1}C_3 \times 3 + {}^{n-1}C_2$ ways in which the HMA top and bottom streams can be obtained. As was also mentioned in Appendix D, there is no reason to form an HMA where a particular product stream forms the top as well as the bottom stream. There are $n - 2$ such HMAs we counted in our enumeration above, one

for each of the products A_2, …, A_{n-1}. Therefore, the number of distinct HMAs is ${}^{n-1}C_4 \times 2 + {}^{n-1}C_3 \times 3 + {}^{n-1}C_2 - (n-2) = \frac{n(n-1)^2(n-2)}{12} - (n-2)$.

Appendix F

A *two-way communication set* comprises of two transfer-streams, one for vapor, and another for liquid, between intermediate locations of two distillation columns. For example, Figure 6.2(c) shows a two-way communication set each for B_1C_1 and B_2C_2. In the two-way communication set, the direction of mass transfer in the vapor stream and the liquid stream individually is not known, and determined usually through an optimization exercise, but the overall mass transfer in the two streams combined is known.

A *one-way communication* is a single transfer-stream, either all liquid or all vapor, whose mass flow direction is known a priori to be from one particular column to another. For example, in Figure 6.1(a), streams for submixtures *ABC* and *BCD* are one-way communications.

A *two-way communication* is a single transfer-stream, either all liquid or all vapor, whose mass flow direction is not known a priori, but the two columns it connects are known. For example, the BC_{TOP} stream in Figure 6.5(b) is a two-way communication. A two-way communication becomes a one-way communication as soon as the direction of mass transfer gets fixed. 2 two-way communications together make a two-way communication set.

Appendix G

α_{BC}	Relative volatility of *B* with respect to *C*
b1 & b2	Net component flow of *B* in B_1C_1 & B_2C_2
c1 & c2	Net component flow of *C* in B_1C_1 & B_2C_2
L_{B1C1} & L_{B2C2}	Total liquid flow in B_1C_1 & B_2C_2
m_{PQ}, m_{OR}, m_{OP}, m_{RQ}	Slope of operating lines PQ, OR, OP, RQ
M_r & M_t	Net mass flow in sections r & t of Figure 6.2
Q_F	Quality of feed F
V_{B1C1} & V_{B2C2}	Total vapor flow in B_1C_1 & B_2C_2
V_r, V_t	Actual vapor flows in the sections r, t of Figure 6.2
$V_{rB1C1pin}$, $V_{tB1C1pin}$	Intermediary variables for vapor flows in the sections r, t of Figure 6.2 when the column is pinched at feed B_1C_1
$V_{rB2C2pin}$, $V_{tB2C2pin}$	Intermediary variables for vapor flows in the sections r, t of Figure 6.2 when the column is pinched at feed B_2C_2
x_J & y_J	Composition of *B* in the liquid & vapor(at Point J on the graph)

.

Appendix H

The *n*-component FTC Petlyuk column has *n*(*n*-1) sections. Each additional section in its parallel-feed counterpart is associated with a feasible submixture that doesn't contain the most volatile and least volatile components of the feed. So, the parallel-feed configuration with the maximum number of sections has all feasible submixtures without the most and least volatile components. The maximum number of such feasible submixtures for an *n*-component feed can be derived by the following logic. For example, *ABCD* has 1 binary (*BC*), *ABCDE* has 1 ternary (*BCD*) + 2 binary (*BC*, *CD*), *ABCDEF* has 1 quaternary (*BCDE*) + 2 ternary (*BCD*, *CDE*) + 3 binary (*BC*, *CD*, *DE*),…..and an *n*-component feed has 1 (*n*-2)-component submixture + 2 (*n*-3)-component submixtures + …. + (*n*-3) binary submixtures to give a total of (*n*-3)(*n*-2)/2 feasible submixtures without the most and least volatile components. Thus, the maximum number of sections a parallel-feed configuration can have is *n*(*n*-1) + (*n*-3)(*n*-2)/2 = (3n^2-7*n*+6)/2. streams.

Appendix I

To establish the equivalence between the parallel-feed and parallel-feed+section arrangements, consider Figure I.1. Figures I.1(a) and I.1(b) are respectively the arrangements of Figures 6.2(a) and 6.2(c) with liquid and vapor flows assigned to each section. 'L' and 'V' in this figure are liquid and vapor flows

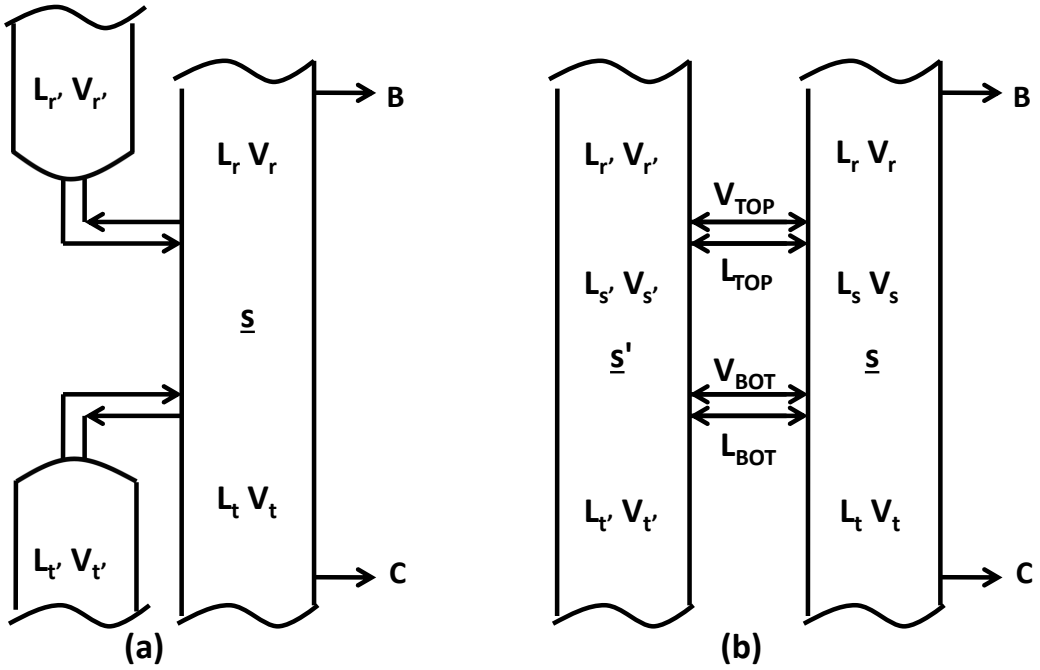

Figure I.1 Sectional liquid and vapor flows in (a) the parallel-feed arrangement of Figure 6.2(a); (b) the parallel-feed+section arrangement of Figure 6.2(c).

in the subscripted sections. Here, we assume that the liquid and vapor flows in the parallel-feed arrangement, Figure I.1(a), are given to us, and derive the liquid and vapor flows in Figure I.1(b) to establish equivalence between the two arrangements. Here, the goal is to establish one-to-one equivalence between the

sections of the parallel-feed and parallel-feed+section arrangements, and equivalence between the two arrangements will then automatically follow.

We use the following sign convention. Any liquid or vapor flow in the direction of net mass flow is positive, otherwise negative. All the following comments are made with reference to Figure I.1(b). Observe that {$V_{BOT} = V_{t'}$, $L_{BOT} = -L_{t'}$, $V_{TOP} = -V_{r'}$, $L_{TOP} = L_{r'}$} is a flow combination that directly simplifies the parallel-feed+section arrangement to the parallel-feed arrangement, making s' a redundant section. Likewise, observe that {$V_{BOT} = -V_t$, $L_{BOT} = L_t$, $V_{TOP} = V_r$, $L_{TOP} = -L_r$} is another solution which achieves the same simplification, making Section s redundant. In fact, these two solutions are two extremes of multiple flow-arrangements/operating-modes in the parallel-feed+section arrangement which are all operationally equivalent to the parallel-feed arrangement. In the following paragraph, we identify all these operating modes.

To start with, though not required, we assume V_{BOT}, L_{BOT}, V_{TOP} and L_{TOP} are in the direction of net mass flow. Under optimal operation, Sections s and s' have equal L/V ratios. For these two sections to operate with the same L/V ratio, the following should hold:

$$\frac{L_{s\prime}}{V_{t\prime}-V_{BOT}} = \frac{L_s}{V_t+V_{BOT}} \tag{I.1}$$

$$\Rightarrow \quad V_{BOT} = \frac{L_s V_{t\prime} - L_{s\prime} V_t}{L_{s\prime}+L_s} \tag{I.2}$$

Substituting Equation (I.2) in (I.1), and using $L_{s\prime} + L_s = L_{r\prime} + L_r$ to determine the L/V ratio in the two sections:

$$\left(\frac{L}{V}\right)_{\text{section s'}} = \left(\frac{L}{V}\right)_{\text{section s}} = \frac{L_{r\prime}+L_r}{V_{t\prime}+V_t} \tag{I.3}$$

which is interestingly the same L/V ratio in Section s of Figure I.1(a). Thus, Section s of Figure I.1(a) is simultaneously equivalent to Sections s and s' of Figure I.1(b) as long as V_{BOT} is given by Equation (I.2). Further, using $L_{s'} = L_{r'} - L_{TOP}$, $L_s = L_r + L_{TOP}$, and simple mass balances, we get

$$V_{BOT} = \frac{L_r V_{t'} - L_{r'} V_t + L_{TOP}(V_t + V_{t'})}{L_r + L_{r'}} \quad (I.4)$$

$$L_{BOT} = L_t - (L_r + L_{TOP}) \quad (I.5)$$

$$V_{TOP} = V_r - (V_t + V_{BOT}) \quad (I.6)$$

Thus, $\{V_{BOT}, L_{BOT}, V_{TOP}, L_{TOP}\}$, where V_{BOT}, L_{BOT} and V_{TOP} are given by Equations (I.4), (I.5) and (I.6) respectively, with a degree of freedom in L_{TOP} which can vary between the extremes of $L_{r'}$ and $-L_r$, represent all the operating modes of the parallel-feed+section arrangement which are equivalent to the parallel-feed arrangement. We observe that $V_{BOT}=0$, $L_{BOT}=0$, $V_{TOP}=0$, and $L_{TOP}=0$ correspond to four unique operating modes when one of these transfer-streams is eliminated, and may be useful from an operational perspective. In the special case when $V_{r'} = V_{t'}$, both vapor transfers in the 2 two-way communications sets, i.e., V_{BOT} and V_{TOP}, can be done away with.

VITA

VITA

GAUTHAM MADENOOR RAMAPRIYA

EDUCATION

Purdue University, West Lafayette, IN
Ph.D. in Chemical Engineering, August 2016

Purdue University, West Lafayette, IN
M.S. in Chemical Engineering, May 2015

Indian Institute of Technology, Madras
Dual Degree (B.Tech. & M. Tech.) in Chemical Engineering, July 2011